Petroleum Research 11 (2026) 641–686

Contents lists available at ScienceDirect

Petroleum Research

journal homepage: http://www.keaipublishing.com/en/journals/petroleum-research/

Review Article

Cellulose bionanomaterial design for enhanced oil recovery: A review of existing, emerging technologies and future outlook

Francis Nyah [a,*], Norida Ridzuan [a], Emmanuel Epelle [b], Mohd Aizudin Bin Abd Aziz [a], Barima Money [a], David Abutu [a], Augustine Agi [a,c,**]

[a] Faculty of Chemical and Process Engineering Technology, Universiti Malaysia Pahang Al-Sultan Abdullah, Lebuhraya Persiaran Tun Khalil Yaakob 26300 Kuantan, Pahang, Malaysia
[b] Institute for Infrastructure and Environment, School of Engineering, The University of Edinburgh, Robert Stevenson Road, Edinburgh, Scotland EH9 3FB, United Kingdom
[c] Centre for Research in Advanced Fluid and Processes (Fluid Centre), Universiti Malaysia Pahang Al-Sultan Abdullah, 26300 Gambang, Pahang, Malaysia

ARTICLE INFO

Article history:
Received 31 March 2025
Received in revised form
28 November 2025
Accepted 22 December 2025
Available online 27 December 2025

Keywords:
Cellulose nanoparticles
Nanofluid
Biomass
Chemical flooding
Mechanisms
Enhanced oil recovery

ABSTRACT

Cellulose nanoparticles are attracting interest in diverse fields because of their availability, low cost, and benign nature. Albeit previous studies have reported excellent experimental results, the application of cellulose nanoparticles in oilfield remains a challenge. Therefore, the objective of this research is to provide vital information on how to design cellulose nanoparticles for oilfield applications. Herein, the sources of cellulose and their derivatives were presented. Subsequently, cellulose pretreatment and extraction methods were elucidated. Likewise, the design of cellulose nanoparticles for oilfield applications were discussed. Also, the enhanced oil recovery (EOR) mechanisms of cellulose nanoparticles for high temperature high pressure (HTHP) reservoirs were identified and their application in EOR was reviewed. The challenges hindering full scale field application of cellulose nanoparticles were presented while concurrently shedding light on diverse methodologies employed to maintain their stability in HTHP oil reservoirs. The results indicate that wettability alteration, asphaltene precipitation, interfacial tension and viscosity reduction are the dominant EOR mechanisms by cellulose bionanomaterials, it also demonstrate that cellulose bionanomaterials can increase the viscosity of injected fluid by 10–100%, improve sweep efficiency by 52–98% and improve oil recovery by 10–35% original oil in place. It can be concluded that bionanomaterial have potential for oil field applications and are economically viable due to their high recovery rate.

1. Introduction

Enhanced oil recovery (EOR) refers to advanced techniques employed to increase oil from reservoirs after primary and secondary recovery methods have become ineffective. Primary oil recovery utilizes natural reservoir pressure to produce oil, whereas secondary recovery involves injecting fluids like water or gas to sustain pressure and enhance oil production efficiency (Agi et al., 2019a; Gbadamosi et al., 2018). After these initial and secondary stages of recovery, approximately 30–35% of the original oil in place (OOIP) is entrapped in the reservoirs. EOR techniques are categorized into thermal EOR, microbial EOR, chemical methods, and gas methods. Each of these techniques is designed to improve oil recovery rates and optimize production from declining reservoirs (Abutu et al., 2026).

Thermal EOR techniques use heat to lower crude oil viscosity, enhancing its flow through pores. Methods such as steam injection and in-situ combustion are especially effective for producing heavy and extra-heavy crude oils. For instance, steam flooding produced over 4 billion barrels of oil in the USA from 1980 to 2002 (Alvarado and Manrique, 2010; Musa et al., 2023; Ngouangna et al., 2023; Yakasai et al., 2023). However, the high energy requirements for generating steam contribute to substantial operating costs

* Corresponding author.
** Corresponding author. Faculty of Chemical and Process Engineering Technology, Universiti Malaysia Pahang Al-Sultan Abdullah, Lebuhraya Persiaran Tun Khalil Yaakob 26300 Kuantan, Pahang, Malaysia.
E-mail addresses: Francis.nyah@yahoo.com (F. Nyah), augustine@umpsa.edu.my (A. Agi).

Peer review under the responsibility of Editorial Office of Petroleum Research.

https://doi.org/10.1016/j.ptlrs.2025.12.002

(Ramesh et al., 2021). Additionally, issues such as preferential flow through high permeability zones and environmental concerns, including greenhouse gas emissions and potential groundwater contamination, pose significant challenges (Mishra et al., 2023). Studies have shown that thermal EOR may not always be economically viable or environmentally sustainable (Jiang et al., 2023; Umunnawuike et al., 2024; Yakasai et al., 2021).

Another EOR technique is microbial enhanced oil recovery (MEOR). MEOR involves injecting microorganisms, like macrobacteria, into oil recovery formations to enhance recovery (Sakthipriya et al., 2017). Known for its low-cost and environmentally friendly operations, MEOR has been implemented in countries such as Malaysia, China, and Saudi Arabia (Abutu et al., 2025). However, this method faces challenges, including low oil recovery rates and complex, time-consuming procedures. Gas injection technique (Secondary recovery method), which involves injecting gases like CO_2 or lean hydrocarbons to achieve miscibility with oil, has been successfully employed in fields such as Canada, the US, Mexico, and Libya (Su et al., 2018; Wu et al., 2016). Despite significant recoveries, issues such as unfavorable mobility ratios and separation problems hinder their effectiveness. Chemical EOR (CEOR) uses chemicals like polymers, surfactants, and alkalis to increase oil recovery by reducing interfacial tension (IFT), altering wettability, and improving sweep efficiency (Afolabi et al., 2022; Gbonhinbor et al., 2023). CEOR has been successfully implemented in various countries, including Bahrain, India, Venezuela, and Russia, demonstrating technical and economic feasibility with reasonable capital costs (Levitt and Pope, 2008). Chemical EOR is a crucial technology in the oil and gas industries aimed at maximizing the production of crude oil from reservoirs that as already undergone primary and secondary recovery methods. As conventional oil reserve depletes, CEOR plays an essential role in meeting global energy demands by releasing additional hydrocarbons that remain trapped in geological formations.

The most widely applied CEOR techniques include alkaline flooding, surfactant flooding, polymer flooding, surfactant-polymer (SP) flooding, and alkaline-surfactant-polymer (ASP) flooding. In polymer flooding, polymers are introduced to increase the viscosity of the injection fluid, thereby stabilizing the displacement front and reducing the mobility ratio, which delays early breakthrough (Zeynalli et al., 2023; Zhong et al., 2022). This enhances macroscopic sweep efficiency and prevents the formation of viscous fingers, which can result in unswept oil zones (Mohsenatabar Firozjaii and Saghafi, 2020). Increasing the elasticity of polymer solutions has also been shown to further improve oil recovery and suppress viscous fingering (Podoprigora et al., 2024; Zhong et al., 2025). For example, Yan et al. (2022) reported that a viscoelastic polymer achieved an oil recovery efficiency of 71.68%, significantly higher than that of conventional water flooding. These findings highlight the critical role of polymer rheology in optimizing CEOR performance. The polymers commonly used in EOR are classified into synthetic polymers and biopolymers (Imuetinyan et al., 2022; Sheng et al., 2015). Biopolymers like Xanthan gum and Guar gum, as well as novel polymers like polyacrylamide (PAM) and hydrolyzed polyacrylamides (HPAM), have been developed recently for EOR applications (Al-Jaber et al., 2023; Gbadamosi et al., 2022). One significant issue with polymer flooding is polymer degradation under high temperatures and high salinity conditions (Nyah et al., 2024).

Consequently, several studies have been conducted to address these limitations. Hence, the use of nanofluid in the EOR process has been reported recently by researchers. In addition to being more resistant to high salinity and high temperatures, nanofluid (base fluid + nanoparticle) also has the advantages of longer stability, less clogging, and better retention in reservoirs. Recent advances in nanotechnology have concentrated on combining polymers and nanoparticles to create nanofluids with unique properties (Al_Ani et al., 2024; Gbonhinbor et al., 2025). For instance, numerous studies have documented the application of silica (SiO_2), alumina (Al_2O_3), zirconia (ZrO_2) (Salem et al., 2024) and graphene oxide (Lashari et al., 2024) nanoparticles to enhance the viscoelastic and rheological properties of HPAM. Salem et al. (2024) revealed that the polymer viscosity was boosted by 110%, 45%, and 12% for HPAM-SiO_2, HPAM-Al_2O_3, and HPAM-ZrO_2 respectively under the investigation range of temperature. Moreover, the polymer viscosity was improved by 73%, 48%, and 12% for HPAM-SiO_2, HPAM-Al_2O_3, and HPAM-ZrO_2 respectively under the investigation range of salinity. Nanocomposites are also found to be a remarkable agent for reducing IFT and changing the contact angle. The flooding experiments confirmed that the EOR by HPAM, HPAM-SiO_2, HPAM-Al_2O_3, and HPAM-ZrO_2, was 8.6%, 17.4%, 15.3%, and 13.6% of OOIP respectively. The improved oil recovery was attributed to the bonding effects, structural integrity, morphological interconnections, and stability of the nanoparticles with polymer. Nonetheless, Gbadamosi et al.(2019) reported that at a prolonged propagation of the polymeric nanofluid under high-temperature reservoir conditions, the bonding effect and structural integrity of the polymeric nanofluid begin to disintegrate leading to increase in IFT and wettability. Hence, researchers have focused their attention on producing nanoparticles from biomass with long chain monomers that can withstand the harsh reservoir condition.

Cellulose derivatives are attracting interest in diverse fields because of their availability, low cost, and benign nature (Nyah et al., 2025). Previous research has reported excellent results with the application of cellulose nanoparticles in EOR. For example, Agi et al. (2019a) reported that cellulose nanofluid was very effective in mobilizing residual oil at high temperature high pressure (HTHP) reservoir conditions. The pressure drop data confirmed the stability of cellulose nanofluid at 120 °C and the formation of oil bank was enough to increase the oil recovery by 20%. This excellent result has not transcended the number of reviews on the subject.

Few reviews exist on the subject mostly focused on the rheological flow behavior of cellulose nanoparticles. Li et al. (2023) highlight the application of cellulose nanoparticles across the oil and gas industry. These nanoparticles are used in upstream activities like nanosensors for well logging and nanofluids for drilling, cementing, fracturing (Money et al., 2025). In midstream, they enhance plastic-based pipelines and storage tanks. In downstream, their role includes oil-water separation, dealkylation, alkylation, desulfurization, and wastewater treatment, demonstrating their wide-ranging impact on industry operations. Rana et al. (2024) focused on recent advancements in utilizing cellulose nanoparticles as an additive in drilling fluid and their role as foam and emulsion stabilizing agent. The existing literature indicates a conspicuous void is apparent in literature regarding in-depth evaluation of EOR mechanisms of cellulose nanoparticles and their application in HTHP reservoirs.

Therefore, this research aspires to furnish a comprehensive review on the mechanisms of cellulose nanoparticles for HTHP reservoirs and the challenges hindering field application. The primary objective is to provide detailed information on how to design cellulose nanoparticles to optimize their EOR mechanisms for oilfield application. However, the information presented can also be used in material science, chemistry, and chemical engineering. Herein, the sources of cellulose and their derivatives were presented. Subsequently, cellulose pretreatment and extraction methods were elucidated. Likewise, the design of cellulose nanoparticles for oilfield applications were discussed. Also, the EOR mechanisms of cellulose nanoparticles for HTHP reservoirs were identified and their application in EOR was reviewed. The challenges hindering full scale field application of cellulose nanoparticles were presented while concurrently shedding light on diverse methodologies employed to maintain their stability in HTHP oil reservoirs.

The remainder of the paper is organized as follows: Section 2 highlights the sources of cellulose and their derivatives. Section 3 discusses the different pretreatment methods of cellulose while Section 4 elaborated on the extraction methods. The review delved into cellulose nanoparticles synthesis methods and functionalization for HTHP reservoirs in Section 4. The EOR mechanisms of cellulose nanoparticles were extensively discussed in Section 5 and their subsequent application in both laboratory and field application was elucidated in Section 6. Finally, Section 7 discussed technical challenges, limitations and perspectives for future research.

2. Cellulose sources and its derivatives

Cellulose is an abundant, water-insoluble polymer composed of repeated β-1,4 linked anhydro-D-glucose monomers, resulting in a high molecular weight, low-cost biodegradable biopolymer that can be extracted from plant cell walls and biomass wastes (Abbas et al., 2024; Huang, 2018; Kedzior et al., 2021). It is abundantly found in materials such as palm kernel shell (PKS), rice husk (RH), oil palm empty fruit bunch (OPEFB), cotton stalk (CS), and others. As illustrated in Table 1, cellulose can be synthesized from various biomass waste sources, ranging from hardwood, agricultural residues and industrial wastes. Cellulose consists of a crystalline region and an amorphous region, which includes both the reducing and non-reducing ends. The global production of cellulose is estimated at approximately 1.5x10E12 tons per year, primarily driven by the wood and cotton industries, which utilize 90% and 98% of pulp, respectively (Dey et al., 2022; Haldar et al., 2022). The crystal packing direction and physical characteristics of cellulose are dictated by the presence of three hydroxyl groups: secondary OH at carbon 2 and carbon 3, and primary hydroxyl ions at carbon 6 positions (Peter, 2021). These hydroxyl groups exhibit varying reactivities and can form hydrogen bonds, as shown in Fig. 1. Cellulose is classified based on the position of the hydroxyl groups on its backbone, with natural cellulose belonging to cellulose I (Aziz et al., 2022). Cellulose I is a crystallized form of cellulose that can exist in either monoclinic unit cell (Iβ) or triclinic unit cell (Iα) forms (Tashiro and Gakhutishvili, 2019). Depending on the treatment of cellulose I, other forms such as cellulose II, III, and IV can be obtained.

Fig. 1 illustrates that 3 hydroxy groups are bearded by each of the glycopyranose units, and they give cellulose some of the remarkable features such as chirality, biodegradability, hydrophilicity which are initiated because of the hydroxy group. Moreover, cellulose can be synthesized from bacteria, yielding the purest form of cellulose. Bacterial sources include *Acetobacter xylinum, Gluconacetobacter xylinum,* and *Acanthamoeba castellani* (Ali et al., 2023). Bacterial cellulose, derived from acetic acid-producing bacterial strains such as *Acetobacter, Gluconobacter, Gluconacetobacter,* and *Komagataeibacter,* is also of interest. These bacteria, commonly found in fermented foods like vinegar and nata de coco, can oxidize alcohol, aldehydes, sugars, or sugar alcohols to acetic acid in the presence of oxygen. Species from the *genera Gluconacetobacter* and *Komagataeibacter* produce a moist extracellular matrix composed of crystalline cellulose (Cannazza et al., 2021; Cielecka et al., 2021; Nóvak et al., 2024; Sumini et al., 2024). Skiba et al. (2020) documented the production of bacterial cellulose from oat hulls, an agricultural residue, on a pilot scale. By utilizing a symbiotic culture of Medusouces gievii and pretreating the oat hulls with 2–6% nitric acid (HNO_3) solutions, which were enzymatically hydrolyzed to yield a sugar-rich solution, the study achieved a production of 80.5 tons of bacterial cellulose per 100 tons of oat hulls. Another unique source of cellulose is tunicates, marine invertebrate animals that produce cellulose in their outer tissue. These sources produce cellulose with high crystallinity, exemplified by species such as *Metandroxarpa uedai, Halocynthia papillosa,* and *Halocynthia roretzi* (Dwivedi et al., 2022; Yadav et al., 2021). Table 1 provides an overview of additional cellulose sources.

2.1. Cellulose pretreatment methods

Pretreatment is the first step taken to eliminate or alter compounds that can obstruct the crystallization process such as lignin, hemicellulose ash, and others, during the production of crystalline cellulose from different biomass sources. Cellulose isolation involves eliminating lignocellulosic components, such as lignin and hemicellulose, from biomass sources (Haji Badri, 2016; Kallel et al., 2016; Wang et al., 2024a). Hemicellulose, characterized by its unstable nature compared to cellulose and lignin, can be readily hydrolyzed into simple sugars using enzymatic or hydrothermal methods (Yang et al., 2019a). In contrast, lignin acts as a complex barrier coating cellulose and hemicellulose, making it more resistant to removal. Studies have demonstrated that lignin can be effectively removed through delignification techniques involving sodium chlorite (NaClO) combined with alkaline solutions (Pramasari et al., 2021; Shi et al., 2014). This process alters the lignin structure within the biomass, leaving behind primarily cellulose (polysaccharides) for subsequent processing. Alkaline treatments or delignification mechanisms involve saponification of intermolecular ester bonds, facilitating easier extraction of cellulose (Lee et al., 2024; Sofla et al., 2016). Lani and Ngadi (2014) focused on isolating cellulose from empty fruit bunch (EFB), reporting a cellulose yield of 93.01% from this biomass source. This finding underscores the efficiency of cellulose isolation methods, particularly from agricultural residues like EFBs, which are rich in cellulose content. These pre-treatment techniques are divided into chemical, physical, and biological, based on cellulose source and preferred properties.

2.1.1. Chemical pretreatment methods

Chemical pretreatment methods, such as the use of acids, bases, or solvents, are essential for cellulose extraction from biomass. These methods break down lignocellulosic components, improving cellulose accessibility while altering the structure of lignin and hemicellulose, thereby facilitating more efficient extraction.

Acid pretreatment entails the application of acids such as hydrochloric acid (HCl) or sulfuric acid (H_2SO_4) to biomass wastes, effectively removing hemicellulose while preserving the cellulose structure (Baksi et al., 2023; Ravindran and Jaiswal, 2016). This method has proven to be highly effective in yielding cellulose from diverse sources including wood chips, corn stover, bamboo, EFB, sugarcane bagasse, rice husk, garlic straw, sugarcane, and cassava peel (Akhtar et al., 2016; Saha and Ghosh, 2019). The application of acid pretreatment has been instrumental in enhancing cellulose accessibility for subsequent processing into various products. For instance, Mankar et al. (2021) investigated the pretreatment of wheat straw at 180 °C for 10 min using 2% dilute H_2SO_4 and 43.1% of cellulose was recovered. Using 700 mL of 6% w/v HNO_3 combined with 70 g of powdered sugarcane bagasse. Evans et al. (2019) investigated the effects of pretreatment for 2 h at 80 °C. The results

Table 1
Biomass waste sources and composition of cellulose, hemicellulose and lignin.

References	Biomass source	Cellulose	Hemicellulose	Lignin
Odejobi et al. (2024)	Sugarcane bagasse	44	28	21
Birlie and Mamay (2024)	Grewia ferruginea	60.4–72.6	18.5	13.5
Gupta and Tiwari (2024)	Agave sisalana			
Randis et al. (2024)	Oil palm frond	55.17	8.52	1.74
Suyambulingam et al. (2024)	Tarmind seed	90.57	1.84	6.77
Vicente-Flores et al. (2024)	Cuajilote	40.45	18.7	32.8
Nyoo Putro et al. (2024)	Jackfruit peel	79.8	5.2	3.7
Vijayakkannan and Rajendran (2024)	Habara Plant Stem	67.9	12.7	11.8
Shibly et al. (2024)	Bark of Rosa hybrida plant	52.99	18.49	17.34
Zheng et al. (2024)	Brewer spent grain	BSG = 20.5 ; BSGC = 88.12	27.12; 2.15	14.93; 1.59
Ebrahimi et al. (2024)	Hazelnut shell (HNS), Treated Hazelnut shell (THNS)	32.1; 70.8	17.9; 8.6	38.7; 11.3
Ogunjobi et al. (2023)	Siam weeds	39.6	27.5	28.7
Soppie et al. (2023)	Cordleaf (Triumfetta cordifolia)	38.8	16.9	6
Sheferaw et al. (2023)	Cyperus papyrus	59.8–63.8	11.4–12.3	2.15–3.4
George et al. (2023)	Water hyacinth	67.5	6.6	22.3
Chavez et al. (2023)	Stipa Obtusa raw	29.4	27.57	23.76
Andoko et al. (2023)	Timoho fiber	63.9	2.57	9.23
Meraj et al. (2023)	Kenaf fiber			
El Amri et al. (2023)	Stems of reed plant large-leaved cattail (Typha latifolia)	59	–	–
Gopinath et al. (2022)	Bauhinia purpurea	67.46	20.1	10.21
Shaikh et al. (2022)	Date palm trunk mesh	33.7	–	22.53
Wahib et al. (2022)	Date pit (DP)	DP = 21.2; AT(DP) = 63.1; BT(DP) = 84	DP = 28.1; AT(DP) = 7.95; BT(DP) = 2.6	DP = 19.9; AT(DP) = 7.02; BT(DP) = 0.51
Islam et al. (2021)	Rice husk	35	30	18
Smriti et al. (2023)	Water hyacinth	25.7	18.4	9.9
Nitzsche et al. (2021)	Beechwood chip	41.6	22.3	25.9
Jiang et al. (2021)	Pepper stalk	77.9	12.1	2.1
Ventura-Cruz and Tecante (2021)	Rose stem	28.6	29.2	24.9
Kassab et al. (2020)	Hemp stalk	72	19	5
Pulido-Barragán et al. (2021)	Euphorbia antisphilitica	45	16	37
Kian et al. (2020)	Oliver fibre	39.4	24.2	14
Abu-Thabit et al. (2020)	Date seeds	24.6	25	30.6
Baruah et al. (2020)	Kans grass	48.2	32	17.1
Fisher et al. (2020)	Milkweed	55	8	19
Chakraborty and Panigrahi (2020)	Cissus Vitiginea	65.43	14.61	10.43
Singh et al. (2020a)	Corn stover	30.92	41.52	7.39
Zhang et al. (2020)	Lemon seeds (Citrus limon)	Ls = 19.16	Ls = 13.16	Ls-9.31
Painuli et al. (2020)	Raw kenaf	45.8	21.2	22.8
Crespo et al. (2020)	Eucalyptus globulus	50	14.1	20.5
Singh et al. (2020b)	Jute	42.5	12.24	31.58
Dilamian and Noroozi (2021)	Rice straw	38.4	25.6	21
Saravana Kumaar et al. (2019)	Carica Papaya	58.71	11.8	14.26
Collazo-Bigliardi et al. (2019)	Coffee husk	61.8	27.2	2.6
Zheng et al. (2019)	Walnut	27.4	31.4	36.3
Trilokesh and Uppuluri (2019)	Jackfruit peel	20.08	24.04	1.85
Li et al. (2018)	Almond shell	38.48	28.82	29.54
Garcia-Garcia et al. (2018)	Pine cone	45.3	5.4	39.7
Manimaran et al. (2018)	Acacia leucophlea	68.09	13.6	17.73
Delicano (2018)	Abaca leaf	56–63	20–25	7.0–13
Collazo-Bigliardi et al. (2018)	Rice husk	91.92	0.72	4.34
Manimaran et al. (2018)	Furcraea foetida	68.35	11.46	12.32
Vergara et al. (2018)	Wheat straw	32.8	29.9	13.8
Cudjoe et al. (2017)	Miscanthus giganteus	50	25	12
Bano and Negi (2017)	Groundnut shells	38.31	21	27.62

demonstrate that the alkaline pretreatment method totally broke down lignin and hemicellulose. To assess the impact of pretreatment on sugarcane bagasse, Vaz et al. (2021) used 1% (w/v) H_2SO_4 at a solid-liquid ratio of (1:10) at a temperature of 121 °C for 20 min. Their findings indicate that hemicellulose and lignin were eliminated from the raw cellulose, and the yield of cellulose increased. Another chemical pretreatment is using alkaline.

Alkaline pretreatment represents another effective chemical method for biomass processing, involving the use of sodium hydroxide (NaOH), ammonia (NH_3), sodium carbonate (Na_2CO_3) and calcium hydroxide ($Ca(OH)_2$) to remove hemicellulose and lignin from biomass materials (Bhutto et al., 2017; Zhang et al., 2022). NaOH is regarded as the most efficient alkali among them for pretreatment of lignocellulose biomass (Melikoğlu et al., 2019). This process improves the crystallinity and purity of cellulose, as demonstrated in studies highlighted in Table 2. Alkaline pretreatment is known for its efficiency in modifying biomass structure, making cellulose more accessible for downstream applications in industries requiring high-quality cellulose fibers or nanocrystals (CNCs). Additionally, solvents like N-

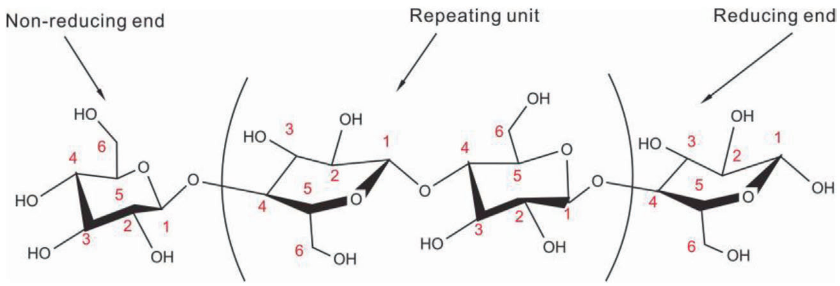

Fig. 1. Cellulose crystalline region and amorphous regions (Reducing and Non-reducing ends) (Kumar et al., 2017; Thakur et al., 2021).

methylmorpholine N-oxide (NMMO) have shown promise in pretreatment processes, particularly for producing high-quality CNCs from biomass sources (Bishnoi et al., 2024; Emenike et al., 2023; Yang et al., 2013). Several studies have confirmed the efficiency of NaOH and other solvents in the pretreatment of cellulose. For instance, Bhandari et al. (2022) isolated cellulose fiber from rice husks to synthesize microcrystalline cellulose (MCC) using NaOH. The milled rice husk was combined with 10% w/v NaOH and stirred continuously for 90 min at 450 rpm and 55 °C. They reported that lignin and hemicellulose were significantly removed from biomass. Using an ionic liquid treatment after a Na_2CO_3 pretreatment, Sankhla et al. (2021) were able to successfully separate cellulose microfibers from sugar bagasse. They concluded that Na_2CO_3 treatment was successful in solubilizing lignin and hemicellulose, as evidenced by a maximum cellulose yield of 84%.

The impact of pretreatment on palm kernel meal (PKM) cellulose extraction was investigated by Chamathka et al. (2024) using 4% w/v NaOH at 50 °C for 180 min. They observed that the treated sample turned dark brown relative to the raw PKM. Their analysis attributed these changes to the breakdown of hemicellulose and depolymerization of lignin, disrupting covalent bonds between lignocellulose components. Similarly, Pratama et al. (2024) used 5 wt% NaOH at 80 °C for 120 min. They reported that alkali treatment degraded hemicellulose and lignin, increasing cellulose crystallinity. Ebrahimi et al. (2024) pretreated Hazelnut shells (HNS) with 3% w/v NaOH (pH 12) at 80 °C for 3 h; Fourier transform infrared (FTIR) spectra revealed a reduction in peak intensity in treated HS due to hemicellulose and lignin removal. Kusmono et al. (2020) applied a 2% NaOH treatment to ramie fiber at 90 °C for 2 h, resulting in hemicellulose and lignin elimination and increased cellulose content. Theivasanthi et al. (2018) investigated the alkaline pretreatment of cotton with 5% NaOH at 25 °C for 4 h, alkaline pretreatment reduced hydrogen bonding due to hydroxyl group removal through NaOH reaction. Kumar et al. (2024) assessed the effect of increasing alkaline concentrations on palm font fibers, observing through microphotography that 10% NaOH caused constricted edges and surface fiber damage. These chemical pretreatment techniques highlight the adaptability of methods enhancing cellulose extraction efficiency and purity, advancing sustainable biorefinery technologies.

Organosolv pretreatment represents a sophisticated technique in biomass processing, particularly valued for its ability to segregate cellulose, hemicellulose, and lignin into distinct streams. This method offers several advantages, including the extraction of highly pure cellulose, the recyclability of organic solvents used, and effective lignin and hemicellulose recovery for possible use in goods with added value (Abolore et al., 2024; Zhang et al., 2020). Organic solvents like ethanol, known for their low boiling points and ease of recovery through simple distillation, are preferred in this process due to their cost-effectiveness, ready availability, and good solubility in water (Rana et al., 2021). During organosolv fractionation, ethanol in an acidic environment facilitates the breakdown of ester-acid bonds in hemicellulose-lignin compounds and ether bonds in lignin, leading to the incomplete hydrolysis of glycosidic linkages in hemicelluloses, as indicated in Fig. 2. The polysaccharides and aromatic rings found in biomass are broken down as a result of this chemical interaction. To enhance the efficiency of delignification and hydrolysis, researchers have employed various catalysts including organic acids, mineral acids, bases, salts, and hydrogen peroxide (Klochko et al., 2020; Zhang et al., 2022). These additives further aid in breaking down complex biomass components and facilitating the extraction process. Additionally, organosolv extraction techniques have been pivotal in isolating CNCs from diverse sources, demonstrating the

Table 2
Pretreatment of biomass waste sources by different techniques.

References	Sources	Solution of NaOH by (%w/v)	Condition	Findings
Xu et al. (2021)	Corncob	16% KOH	70 °C @ 90mins	Most of the cellulose with small portion of Xylan
(Noremylia et al., 2022; Rossi et al., 2021)	Sugarcane bagasse	2% KOH	85 °C @ 2 h	Increases cellulose and hemicellulose content
Kusmono et al. (2020)	Ramie fiber	2	90 °C @ 2 h	Indicated elimination of hemicellulose and lignin
(Czaikoski et al., 2020; Weligama Thuppahige et al., 2023)	Cassava peel	5% KOH	25 °C @ 14 h	Processes were not enough to eliminate all lignin
Zheng et al. (2019)	Walnut	2	100 °C @ 4 h	Cellulose increase to 36.7%
Pinto et al. (2022)	Cocoa pod husk	2	80 °C @ 3 h	Favorable conditions
Ye et al. (2018)	Sugarcane bagasse	6	95 °C @ 2 h, continuous agitation	Short (25 h)
(Garcia-Garcia et al., 2018)	Pinecone	4.5	80 °C @ 2 h	Litter brown appearance
Theivasanthi et al. (2018)	Cotton	5	25 °C @ 4 h	Minimized hydrogen bonding by eliminating hydroxyl group by a reaction with NaOH

versatility and applicability of this approach (Barbash et al., 2023; García et al., 2017; Rana et al., 2021). The extraction of CNCs through organosolv methods underscores the method's effectiveness in leveraging biomass resources for advanced materials applications. During organosolv fractionation, cellulose is typically recovered as a residual solid, while lignin is extracted into the organic solvent phase, and hemicellulose along with other derivatives are washed off in an aqueous solution. This process enables the separation of biomass components with high precision, contributing to the production of purified cellulose suitable for various industrial applications.

Numerous studies have explored and documented the efficacy of organosolv pretreatment techniques in biomass processing (Nair et al., 2023; Zadeh et al., 2020). Ferreira and Taherzadeh (2020) further underscored the importance of controlling biomass particle size and solid-to-liquid ratios in laboratory settings, essential parameters that influence the effectiveness and scalability of organosolv processes. Hermsdorff et al. (2023) examined the impact of organosolv pretreatment on sugarcane bagasse via organic acid and supercritical carbon dioxide (CO_2) and ethanol as solvent. They reported that the optimum delignification of 86%, 60% ethanol in water, was 1 wt% oxalic acid, and 25 g of CO_2. An investigation of the effectiveness of organosolv pretreatment methods on sugarcane bagasse to extract CNC was carried out by Hajiali et al. (2022). They employed a pretreatment condition utilizing 50 v/v% ethanol as the organic solvent, along with 20 wt% H_2SO_4 and 1% 3-*tert*-butyl-4-hydroxyanisole as a surfactant to enhance lignin removal, at a temperature of 160 °C for 30 min. Their findings indicated substantial removal rates of biomass components, with 87% of hemicellulose and 71.2% of lignin was effectively eliminated. resulting in a high cellulose recovery of 84%. In related research, Zhang et al. (2020) explored the impact of organosolv pretreatment using sugarcane as the biomass source. They utilized 60 v/v% ethanol as the organic solvent combined with 8 wt% NaOH, functioning for 30 min at 180 °C. Their study concentrated on improving the removal of lignin and hemicellulose, achieving significant reductions of 82.6% and 11.7% in non-cellulosic components, respectively. This optimized process led to an impressive cellulose recovery rate of 96.3%. Furthermore, they employed 90 v/v% glycerol supplemented with 0.06 mL/L $FeCl_3$ at a temperature of 150 °C for 20 min. Their investigation highlighted effective removal rates of lignin and hemicellulose, with 71.0% and 85.8% elimination. Tang et al. (2024) explored the use of glycerol as an organic solvent for pretreating rice straw to extract cellulose, respectively, resulting in a high cellulose recovery of 96%.

Hernández et al. (2018) conducted comparative research on the impact of three different treatments—organosolv, soda, and sodium chlorite—on the percent yield, degree of polymerization, thermal stability, and size distribution of cellulose extracted from woody and herbaceous agricultural waste. Their results indicated that the organosolv method yielded the highest cellulose content even within a short duration, demonstrating its environmental friendliness. Additionally, the organosolv-treated samples exhibited superior thermal stability compared to the other methods. Similarly, García et al. (2017) applied three treatment methods—autohydrolysis, soda, and organosolv (using 60% acetic acid), followed by bleaching and acid hydrolysis—to extract CNC from pea stalks (PS) and apple tree pruning (ATP). Their findings revealed that the organosolv method produced CNCs with the best size distribution in relationship to length, aspect ratio, and polydispersity index, although autohydrolyzed CNCs showed higher thermal stability.

2.1.2. Solvent pretreatment

Solvent pretreatment techniques such as ionic solvent, deep eutectic solvent (DES), and subcritical methods are all modern techniques in recent times that play integral roles in modifying the properties and structure of cellulose materials (Chen et al., 2022; Tian et al., 2020). DES has attracted much attention lately as a lignocellulosic biomass pretreatment method. DES is a sustainable substitute for ionic liquid in delignification processes. DES is created by combining a certain ratio of hydrogen bond donor (HBD) and hydrogen bond acceptor (HBA). Smith et al. (2014) stated that a eutectic mixture can be created by mixing the two components, HBA and HBD, at a temperature between 70 and 100 °C for a few minutes to many hours. The hydroxyl groups in cellulose and hemicellulose would interact with the DES's HBD component, while the aliphatic hydroxyl and phenolic groups of the lignin interact with the HBA component of the DES. The intermolecular forces that keep the biomass together are weakened by hydrogen bonding contact, which also causes the structure to degrade. Many researchers have reported using DES to extract cellulose from biomass waste (Lee et al., 2022; Lou and Zhang, 2022). For instance, Tian et al. (2020) investigated the effect of liquid hot water (LHW) pretreatment poplar substrate added with DES. About 6 g of LHW pretreated poplar was added with 120 g of acidic DES and stirred continuously at 130 °C for 3 h

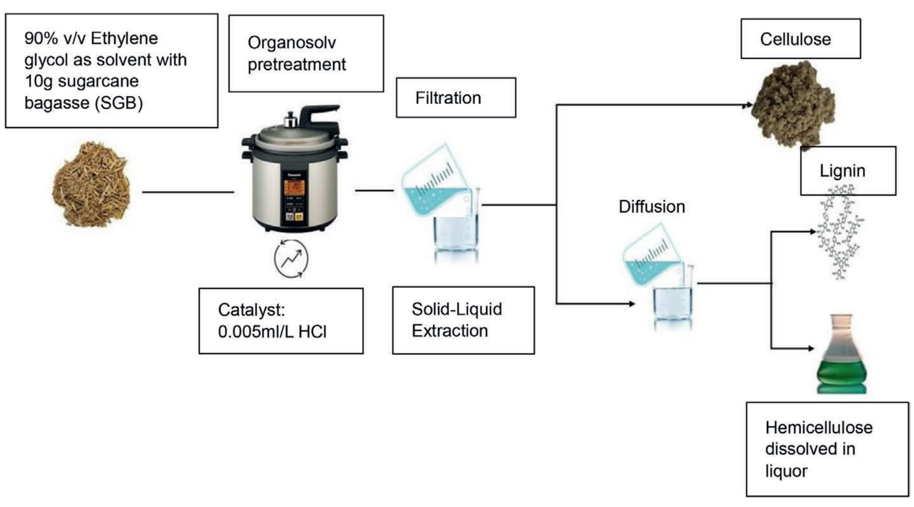

Fig. 2. Organosolv pretreatment for extraction of cellulose from SGB (Wei et al., 2021).

in a flat bottom flask. Their findings show that the cellulose-rich fraction content significantly increased from 61.1 to 79.8–85.4%. Using choline chloride (ChCl) as a hydrogen bond acceptor and three hydrogen bond donors—lactic acid (LA), citric acid (CA), and acetic acid (1:1) (AA), Morán-Aguilar et al. (2022) investigated the impact of DES on sugarcane bagasse. They concluded that ChCl:AA facilitated sugarcane bagasse (SCB) breakdown through morphological and functional group modifications.

Another solvent for pretreatment techniques is high-temperature liquid hot water pretreatment (HTP). HTP, also referred to as autohydrolysis, is a biomass pretreatment method that relies solely on hot water to dissolve hemicellulose and disrupt the lignin-carbohydrate matrix, eliminating the need for external mineral acid catalysts. This technique offers economic advantages with low capital and operational costs. Typically conducted in the range of 150–200 °C under pressures around 30 bars and lasting from 5 to 25 min. HTP aims to modify the structure of lignocellulosic biomass by selectively removing hemicellulose and partially converting lignin into a liquid phase (Pangsang et al., 2019). The primary objective of HTP is to adjust the structural composition of lignocellulosic materials, focusing particularly on the unstable hemicellulose components due to their heterogeneous nature, branched structure, and presence of amorphous polysaccharides. Hemicellulose side chains undergo a breakdown during HTP, involving the release of organic acids and acetyl groups, resulting in the formation of shorter oligomers. This breakdown disrupts the bonding between hemicellulose and lignin, thereby affecting the hydrogen bonds within the cellulose structure (Ng et al., 2021; Patel et al., 2016).

HTP plays a substantial role in biomass conversion processes by facilitating subsequent steps for extracting valuable components like cellulose while enhancing overall biorefinery efficiency and sustainability. HTP effectively removes the lignin from biomass waste, thereby increasing accessibility to cellulose. Numerous studies have investigated HTP in batch reactors, highlighting its efficacy in hemicellulose and lignin removal through the generation of hydronium ions and the release of acetic acid from hemicellulose (Yang et al., 2020). Research by Kumar et al. (2010) further explained that increasing temperatures during HTP weaken the hydrogen bonding network of water, facilitating the dissociation into hydronium ions (H_3O^+) and hydroxide ions (Meng et al., 2022). Based on the analysis presented, it is evident that novel techniques offer enhanced viability and feasibility due to their reduced toxicity rates, minimal chemical usage, and shorter processing times. In contrast, conventional methods often entail high chemical toxicity, significant environmental pollution, and challenges in disposing of the water used in the process.

2.2. Physical pretreatment methods

Physical pretreatment techniques such as mechanical, thermal, and irradiation methods play integral roles in modifying the properties and structure of cellulose materials (Taylor et al., 2019). Mechanical techniques such as ball milling, ultrasonication, and high-pressure homogenization are employed to break down cellulose fibers and enhance their surface area, thereby improving accessibility for subsequent chemical or enzymatic treatments (Zeng et al., 2021). These methods effectively reduce cellulose particle size and increase uniformity, which is crucial for applications requiring fine cellulose fibers or nanocrystals. Thermal pretreatment techniques, such as steam explosion, are employed to alter the structure of the plant cell wall and increase accessibility to cellulose fibers (Ravindran and Jaiswal, 2016). Steam explosion involves exposing biomass to steam under high pressure, then followed by rapid depressurization, which breaks down lignocellulosic bonds and facilitates easier separation of cellulose from lignin and hemicellulose components (Yu et al., 2022). This process is advantageous for enhancing cellulose purity and crystallinity, making it suitable for various industrial applications. Irradiation pretreatment methods utilize gamma or electron beam radiation to induce structural changes in cellulose fibers, thereby increasing their crystallinity and improving material properties (Wang et al., 2018). Irradiation techniques are effective in modifying cellulose at a molecular level, enhancing its thermal stability, biocompatibility and mechanical strength for applications in fields such as biomedical engineering and materials science (Aziz et al., 2022). These pretreatment techniques highlight the versatility and innovation in cellulose processing, contributing to advancements in sustainable biorefinery technologies and the development of high-value cellulose-based products.

2.3. Biological pretreatment methods

Microbial techniques involve the utilization of microbes, like bacteria or fungi, to break down lignin and hemicellulose, increasing the accessibility of cellulose for subsequent processing such as hydrolysis (Bhardwaj et al., 2021; Houfani et al., 2020; Thapa et al., 2020). For example, Kameshwar and Qin (2018) highlighted the use of white-rot fungi to effectively degrade hemicellulose and lignin in plant biomass. This microbial action enhances the accessibility of cellulose fibers by breaking down complex structures that bind cellulose with other components. White-rot fungi are particularly adept at enzymatically degrading lignin, thereby facilitating the isolation of cellulose with improved purity and accessibility for downstream processing in biorefinery applications. In addition to fungi, bacterial strains like *Acetobacter xylinum* have been utilized for their ability to produce cellulose with high purity and crystallinity (Aswini et al., 2020; Florea et al., 2016; Skiba et al., 2022). These bacteria synthesize cellulose through fermentation processes, yielding fibers that exhibit desirable properties for various industrial uses, including biomedical applications where high-quality cellulose is crucial. Microbial degradation of lignocellulosic biomass not only enhances the efficiency of cellulose extraction but also offers a sustainable approach to biomass utilization, aligning with efforts to develop environmentally friendly biotechnological solutions for cellulose-based materials. Sikder et al. (2023) successfully pretreated OPEFB using an enzymatic method. Initially, the OPEFB underwent rigorous washing to eliminate contaminants such as dirt, wax, oil, and sand particles. The fibers were further processed by physical separation and washed with a 1% detergent solution followed by thorough rinsing and drying. After sun-drying, the samples were cut into pieces measuring 0.5 mm in length. Subsequently, the cellulose fibers were subjected to pretreatment using free laccase enzyme in an acetate buffer solution at pH 5.0 and 50 °C for 12 h. This pretreatment step significantly increased the raw cellulose content from 39.19% to 73.55%.

3. Cellulose extraction methods

Extraction of Cellulose from various agricultural wastes, municipal wastes, hardwoods, and softwoods are all significant areas of research (Ali et al., 2023; Chaka, 2022; Gunjan and Manikanika, 2023; Hadou et al., 2024; Harini et al., 2024; Hemida et al., 2023; Parihar et al., 2022; Rovera et al., 2023; Vincent and Kandasubramanian, 2021). This is driven because of the search for sustainable materials that are biodegradable and non-toxic to the environment. These extractions fall into one of several categories, including solvent methods, chemical methods, mechanical and biological approaches, and hybrid procedures

(Mboowa, 2024). Fig. 3 illustrates methods for extracting cellulose and degrading hemicellulose and lignin to increase cellulose crystallinity. Techniques for cellulose extraction from biomass include biological, chemical, mechanical, oxidation, solvent-based, and hybrid methods. Notably, hybrid techniques yield high cellulose output with reduced chemical use, offering an efficient and environmentally friendly approach.

3.1. Microwave-assisted method

Microwave-assisted extraction has emerged as a leading technique for the efficient retrieval of cellulose from various biomass sources (Camani et al., 2020; Destandau and Michel, 2022). Using electromagnetic waves with wavelengths between 1 mm and 1 m and frequency between 300 MHz and 300 GHz, this method harnesses microwave energy to facilitate chemical treatments and solvent extraction processes (Arpia et al., 2021; Mishra et al., 2024). This approach is particularly favored for its environmental friendliness, high thermal efficiency, energy savings, and ability to achieve uniform heating and deep penetration into materials (Zhu et al., 2023). Microwave-assisted techniques are notably advantageous in hemicellulosic extraction, minimizing polymerization and acetyl loss under mild conditions while preserving hemicellulose branch structures effectively (Agi et al., 2023).

Liu et al. (2021a) conducted research focusing on the microwave-assisted extraction of cellulose from wheat straw. They reported achieving a high purity of cellulose at 90.66% and significantly reducing reaction times by 67%. Moreover, their findings indicated that increasing the concentration of NaOH led to a rise in the crystallinity index of the extracted cellulose, demonstrating the method's efficiency in enhancing the structural integrity of the cellulose fibers. Using a bleaching procedure in conjunction with microwave-assisted extraction, Azlan et al. (2022) studied the recovery of cellulose from oil palm mesocarp fiber. Their research revealed a notable average cellulose yield of 64% using γ-valerolactone as a solvent. Similarly, Anwar et al. (2024) extracted cellulosic bioethanol from Pennisetum purpurem using γ-valerolactone and microwave-assisted solvent extraction, yielding a noteworthy 70% alpha-cellulose and 97.9% beta-cellulose/hemicellulose recovery. These studies underscore the versatility and effectiveness of microwave-assisted techniques in extracting cellulose from diverse agricultural residues, offering promising avenues for sustainable biomass utilization.

Louis et al. (2022) explored the application of microwave technology in extracting nanocellulose from rice straws. Their findings highlighted a substantial boost in the crystallinity index of nanocellulose, underscoring the efficiency of microwave techniques in producing cellulose with enhanced structural properties. These studies jointly demonstrate the capacity of microwave-assisted methods in advancing the extraction and utilization of cellulose from agricultural residues, offering efficient and sustainable pathways toward biomass valorization.

3.2. Microfludization

Microfludization is classified as a high-pressure homogenization (HPH) technique. Steam explosion combined with micro fluidization is a notable technique recognized for its efficient reduction in energy consumption, boasting up to a 70% reduction compared to conventional methods such as ball milling, and its minimal or no use of chemicals (Djafari Petroudy et al., 2021). This method leverages steam pressure to induce hydrolysis of cellulose fractions and the formation of degradation products within biomass (Hongrattanavichit and Aht-Ong, 2020). The intensity of shearing forces exerted during the steam explosion discharge correlates inversely with the pressure differential between the reactor and ambient conditions. Liu et al. (2017) successfully applied microfluidization for cellulose extraction from wheat straw, observing a significant increase in cellulose content from 44.1% to 94.23%, accompanied by reductions in hemicellulose and lignin content. They noted that subsequent microwave-assisted hydrolysis further enhanced the crystallinity index from 45.85% to 48.72%, ultimately reaching 62.15%. Despite initially decreasing crystallinity due to intense forces during micro fluidization, sequential treatments facilitated the removal of hemicellulose and

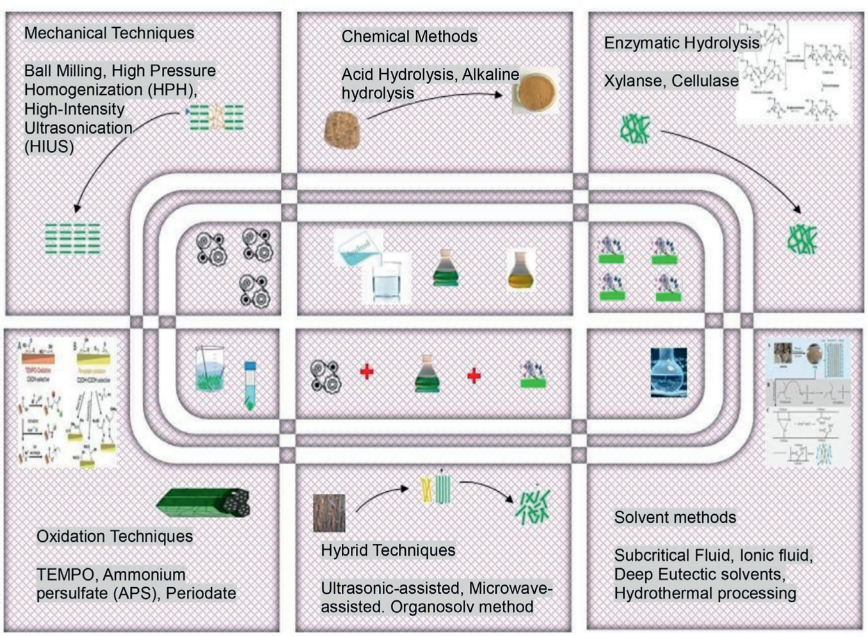

Fig. 3. Conventional and hybrid methods enhance CNC extraction efficiency and purity.

lignin, leading to enhanced cellulose crystallinity (Tong et al., 2023). Additionally, Perez-Palacios et al. (2022) explored the application of micro fluidization in the context of isolating cellulose nanofibrils from agave bagasse. Their study underscores the versatility of micro fluidization in biomass processing, demonstrating its potential to facilitate the extraction of cellulose nanofibrils from agricultural residues. The mechanisms of micro fluidization are based on cellulose pulp preparation, shear force and cellulose formation. The primary principle behind this technique is that shear stress assists in effectively breaking down the cellulose structure without significant thermal degradation, which is essential in maintaining and retaining the properties of cellulose. Factors like pressure, flow rate and even the number of passes through the microfluidizer can be used to adjust the particle sizes of cellulose. Hence, the smaller particles enhance the mechanical properties of materials and their dispersion (Aryasena et al., 2022). During microfluidization, cellulose acquire a negative surface charge due to sulfate ester groups introduced during chemical hydrolysis, even with sulfuric acid. This charge prevents aggregation, providing for stable colloidal dispersion (Chaka, 2022; Kandhola et al., 2020).

3.3. High intensity ultrasonication (HIUS)

Cellulose can be effectively extracted from biomass waste sources using HIUS. HIUS utilizes a transducer with frequencies exceeding 20 kHz to convert mechanical or electrical energy into high-frequency acoustic energy (Agi et al., 2018; Vinatoru et al., 2017). Ultrasonic waves propagate through the medium, creating successive rarefaction and compression cycles that induce acoustic cavitation, as shown in Fig. 4. This phenomenon generates localized temperature and pressure conditions, producing highly reactive free radicals that accelerate chemical processes, such as hydroxyl, hydrogen, and hydrogen peroxide ions which quicken chemical reactions. The ultrasonic waves produce oscillations that cause slurry particles to undergo periodic compression and expansion (Agi et al., 2020b; Gungoren et al., 2024). This process resulted in the formation, expansion, and rapid collapse of microscopic bubbles within the solution, known as cavitation. The benefits of ultrasonic-assisted extraction include reduced treatment times, minimal chemical or enzyme requirements, and environmental friendliness, making it a widely researched technique for extracting and isolating cellulose from various biomass sources (Agi et al., 2022).

Melikoğlu et al. (2019) investigated using ultrasound combined with reflux heating to extract cellulose from apple pomace, a waste product of the food industry. They optimized their pretreatment conditions to include 10.23% NaOH at 69.82 °C for 161.54 min, resulting in a cellulose yield of 27% and an alpha-cellulose content of 85.31%. The cellulose obtained from this process exhibited a high crystallinity index of 78%. Similarly, Wong et al. (2021) successfully extracted cellulose from OPEFB using ultrasonic-assisted alkali treatment. In their study, OPEFB was treated with KOH and subjected to ultrasonication at 80 °C with an ultrasonic amplitude of 30% for 30 min. They achieved an optimal cellulose content of 77.14 wt%, attributing the high crystallinity to the combined effect of alkali and ultrasonic treatment, which effectively damaged the OPEFB cell walls and solubilized hemicellulose present on its surface. Zhang et al. (2023) also utilized ultrasonic-assisted hot water extraction to extract cellulose from *Dictyophora indusiara* fruiting bodies. They employed 5 g of dried *Dictyophora indusiara* powder in 200 mL of deionized water with a solid-liquid ratio of 1:40. Using an ultrasonic microwave combined reaction system at a constant temperature of 80 °C and 600 W for 25 min. After extraction, the cellulose was separated, preliminarily purified, and freeze-dried to obtain the desired cellulose. Saini et al. (2022) carried out research focusing on cellulose extraction from rice straw using homogenization and ultrasonication treatments. Initially, they used 1 M NaOH at 60 °C for 2 h to extract cellulose from dewaxed and bleached rice straw. The extracted cellulose sample was then subjected to homogenization at 12,000 rpm for 10 min, repeated twice. Subsequently, the homogenized suspension underwent ultrasonication at 20 kHz and 600 W for 30 min, followed by centrifugation at 7000 rpm for 30 min to isolate cellulose. The study aimed to enhance the efficiency of cellulose extraction through mechanical and ultrasonic treatments, optimizing conditions to achieve cellulose from rice straw.

3.4. Solvent extraction

Besides the widely recognized method of acid hydrolysis, cellulose extraction can also be achieved through various solvent extraction techniques. These approaches include ionic liquid extraction, supercritical fluid extraction, and DES methods, among others. Each of these techniques presents unique advantages in terms of efficiency, selectivity, and environmental impact, making them valuable alternatives for cellulose isolation and processing.

3.4.1. Ionic liquid extraction

Ionic liquids are promising solvents for cellulose extraction from biomass, offering high dissolving power, enhanced cellulose yield, and environmental benefits, making them an effective and sustainable alternative in biomass processing. Pacheco-Fernández and Pino (2019) highlighted the benefits of ionic liquids, emphasizing their high thermal stability, green solvent properties with low vapor pressure, and versatility in synthetic applications. Glińska et al. (2021) demonstrated the effectiveness of ionic liquids in extracting cellulose fibers from corn stover, achieving a cellulose yield of 84% from the extracted biomass. Similarly, in their study of the use of ionic liquid extraction to sugarcane bagasse, Liu et al. (2021b) discovered that triethylbenzyl ammonium chloride/lactic acid (TEBAC/LA)-based deep eutectic solvents (TEBAC/LA) at 120 °C for 4 h and a solid-to-liquid ratio of 1:15 produced the best results for effective pretreatment and biomass cellulose extraction.

3.4.2. Supercritical fluid

Subcritical and supercritical water hydrolysis represents a significant advancement in the extraction of cellulose from biomass wastes, leveraging the unique properties of water under these conditions (Pattnaik et al., 2021). Water's ability to hydrolyze polysaccharides, facilitated by the presence of hydronium ion (H_3O^+) ions and water molecules, pTElays a crucial role in breaking down hemicellulose in biomass (Cardenas-Toro et al., 2014). Subcritical water conditions, operating below its critical point (critical temperature of water <374 °C under 1–20 MPa for 10–50 min), enhance ionized species concentration, thereby promoting efficient hydrolysis reactions with minimal production of fermentation inhibitors and corrosion issues (Purkayastha et al., 2021). These conditions are particularly advantageous for their high cellulose yields and the preservation of cellulose structure. Subcritical fluid extraction of cellulose has been widely studied. Abaide et al. (2019) explored the use of rice husk to extract cellulose at 220 °C, 2.5 MPa, for 3 min with a 7.5:1 water-to-biomass ratio, achieving hemicellulose and lignin removal. Similarly, Nguyen Thi et al. (2017) examined water hyacinth hydrolysis under laboratory conditions (165 °C, 5 MPa, 30 min, 10:1 water-to-biomass ratio), reporting complete hemicellulose and lignin degradation, enabling cellulose extraction.

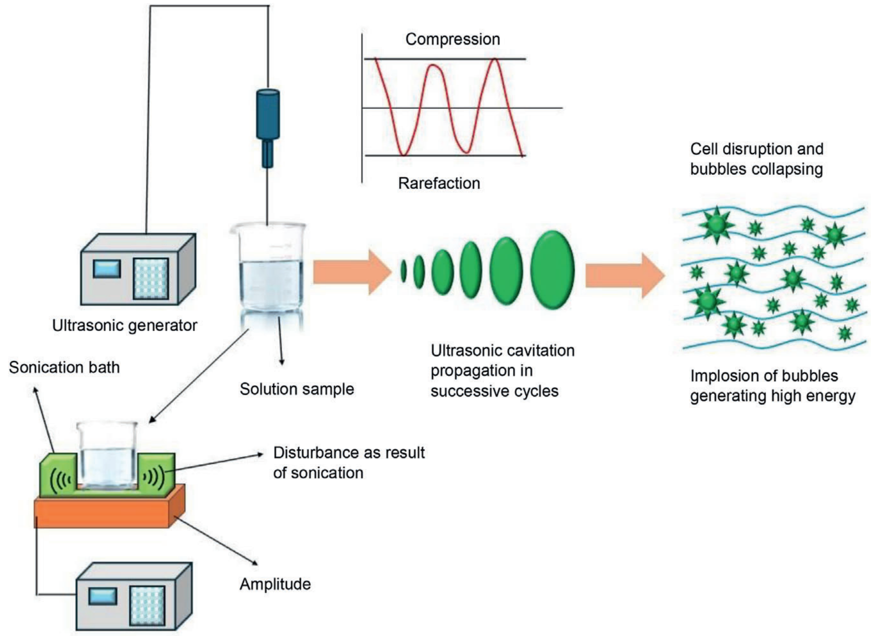

Fig. 4. Ultrasonic-assisted technique for the extraction of cellulose from SGB (Kumar et al., 2023).

3.4.3. DES

DES is a more environmentally friendly version of ionic liquids that are created by combining two or more substances in particular proportions to produce a melting point that is much lower than the sum of their constituent parts (H. Li et al., 2020; Tian et al., 2020). DES have been widely employed in the extraction of biopolymers such as xylan and chitin (Nam et al., 2023). The dissolution of biomass using DES is influenced by various factors, including eutectic composition, viscosity, hydrogen bonding capacity, pH, temperature, reaction time, and solvent-to-biomass ratio. DESs with strong hydrogen bonding interactions and low viscosity effectively dissolve biomass components, and the selection of an appropriate hydrogen bond donor and acceptor depends on the specific biomass composition (Abolore et al., 2024). A well-established example is the eutectic mixture of ChCl and urea in a 1:2 M ratio. Acid-based natural DESs containing ChCl as a hydrogen bond acceptor generally exhibit higher viscosity compared to alcohol-based natural DESs, such as those containing glycol or 1,2-propanediol. Additionally, the incorporation of water reduces the density of DES, which has been attributed to changes in the molecular packing of water molecules within the solvent system (Dai et al., 2013). Consequently, natural DESs with lower molecular weights tend to exhibit lower densities than those with higher molecular weights.

DES have garnered attention for their potential in extracting cellulose from biomass wastes (Chen et al., 2019; Hardiningtyas et al., 2024; Lee et al., 2022; Liu et al., 2023; Meraj et al., 2023; Morais et al., 2020; Morán-Aguilar et al., 2022; Ojala et al., 2018; Scelsi et al., 2021; Wang et al., 2023). For instance, Scelsi et al. (2021) investigated the influence of alcohol as cosolvents in DES systems on the delignification process of various biomass sources. They investigated the effects of alcohol content on lignin fractionation using a DES that contained oxalic acid and ChCl in a 1:1 M ratio. Their findings underscored the critical role of reaction temperature and the DES-alcohol ratio in enhancing biomass delignification efficiency. Notably, butanol exhibited optimal performance, attributed to its effective lignin fractionation and minimal miscibility with water, thereby highlighting the strategic use of cosolvents in DES systems for biomass valorization. Lim et al. (2019) investigated the use of triethylbenzyl ammonium chloride/lactic acid (TEBAC/LA)-based deep eutectic solvents (TEBAC/LA) for extracting cellulose fibers from rice straw. Optimized conditions (140 °C, 100 min, 1:10 straw-to-solvent ratio) enabled partial removal of hemicellulose and lignin, enhancing the crystallinity index and demonstrating the potential of DES in cellulose extraction. Razali et al. (2022) explored an alkaline-DES pulping method using potassium carbonate-glycerol DES, noting an increase in cellulose content to 84.9% during alkaline treatment, albeit with a slight decrease in post-surface modification (Liu et al., 2023). In their study, Gan et al. (2020) demonstrated an effective method for extracting cellulose from EFB using a DES. To create a homogenous DES mixture, they combined potassium carbonate and glycerol in a mole ratio of 1:7 and heated the mixture to 80 °C for 2 h. Subsequently, the EFB was immersed in this DES solution at the same temperature and duration before undergoing a bleaching process. The bleaching process was repeated several times with equal amounts of acetate buffer (made with glacial acetic acid and NaOH), distilled water, and a 1.7% chlorite solution. This meticulous treatment regimen effectively reduced the hemicellulose and lignin content in the EFB from initial levels of 31.9% and 25.9%, respectively, to significantly lower levels of 9.4% and 1% after bleaching with the DES.

4. Cellulose bionanomaterials synthesis

Cellulose can be synthesized into advanced materials for industrial applications such as CNC (Badi et al., 2024; Mohamed et al., 2022; Naseem et al., 2024; Pandi et al., 2021). CNC are rod-shaped particles with diameters ranging from 2 to 5 nm and lengths of around 100 nm. They are good in terms of mechanical strength, stiffness, and thermal stability. CNCs are biodegradable, renewable and non-toxic, making them environmentally friendly (Bangar et al., 2022; Korolovych et al., 2018; Meda et al., 2022; Molnes et al., 2018; Raza et al., 2022). Various techniques have been utilized for the synthetization of cellulose. One of the most common is acid hydrolysis technique which is used to break down the amorphous cellulose chain at an elevated temperature (Akbar et al., 2020; Burhani and Septevani, 2018; Cheng et al., 2017; Espinosa et al., 2013; Gunathilake et al., 2021; Hastuti et al., 2018; Lv et al., 2019a; Neenu et al., 2022; Qu et al., 2020; Xie et al., 2019), as illustrated in Fig. 5. Other methods include enzymatic hydrolysis, ionic hydrolysis, oxidization hydrolysis and mechanical techniques (Campora et al., 2022; Ishak et al., 2018; Zhang et al., 2024a).

4.1. Chemical synthesis methods

Chemical synthesis techniques are among the most widely used methods for producing CNCs. Several types of chemical approaches are employed, including acid hydrolysis, oxidation, and nanoprecipitation. Each method offers unique advantages in terms of yield, particle size control, and crystalline structure, providing diverse options for CNC synthesis (Badi et al., 2024; Bishnoi et al., 2024; Ogunjobi et al., 2023; Pandi et al., 2021; Samsudin et al., 2020; Shaikh et al., 2022; Tuerxun et al., 2019).

4.1.1. Acid hydrolysis

Acid hydrolysis is a well-established technique used to break down amorphous cellulose chains into shorter, more crystalline segments using acids such as H_2SO_4, HCl, nitric acid, or phosphoric acid (Trache et al., 2016). Organic acid hydrolysis, using citric, maleic, formic, or oxalic acid, optimizes cellulose extraction by tailoring conditions and properties. Each acid offers unique advantages and limitations, depending on extraction needs (Bian et al., 2017; Ji et al., 2019; Lv et al., 2019b; Yang et al., 2019c). Mixed acids, combining properties from different acids, are also explored to achieve specific cellulose characteristics (Wang et al., 2020a; Xie et al., 2019). This process cleaves the glycosidic bonds linking glucose units in cellulose, resulting in the formation of shorter chains with a more ordered arrangement. Acid hydrolysis is widely employed for producing crystalline cellulose from numerous plant sources such as wood pulp and cotton fibers due to its cost-effectiveness, efficiency, and relatively short processing time (Dai et al., 2018). Acid hydrolysis is particularly useful for preparing highly purified microcrystalline cellulose, which typically exhibits crystallinity indices ranging from 60% to 80% (Xiong et al., 2012). Nanocrystalline cellulose (NCC) synthesized through acid hydrolysis appears as tough, rod-like particles measuring between 50 and 350 nm in length and 5–20 nm in diameter, depending on the type of acid used, pH conditions, and process parameters, as shown in Fig. 6 (Tuerxun et al., 2019). Acid hydrolysis methods underscore the versatility and adaptability of cellulose processing techniques, catering to diverse industrial and scientific applications that demand precise control over cellulose morphology and properties.

Taflick et al. (2017) synthesized CNCs from Acacia bark using a 70% acetic acid and 80% nitric acid mixture at 20 °C for 15 min. During the alkaline treatment, NaOH facilitated lignin breakdown, while H_2O_2 and H_2SO_4 further purified the cellulose by oxidizing remaining lignin and selectively hydrolyzing amorphous regions, isolating the CNC. The controlled synthesis conditions yielded CNCs with specific properties. Ebrahimi et al. (2024) investigated the effects of chemical treatments on raw and treated hazel seeds (HS and THS) and CNC, noting the compact structure of raw HS with hemicellulose and lignin, which were removed by bleaching and acid hydrolysis. Their study compared chemical synthesis processes, detailing factors such as duration, cost, waste management, and energy efficiency (Table 3). Perumal et al. (2022) used 65% H_2SO_4 at 45 °C for 45 min to create CNCs from areca nut husk, observing uneven fibers (19.3 nm diameter; 195 nm length) with high crystallinity due to amorphous cellulose removal. Moradi and Fathi (2023) synthesized CNC from tomato pomace using 64% H_2SO_4, finding spherical particles (104 nm diameter) and increased crystallinity, indicating successful elimination of non-cellulosic material.

4.1.2. Oxidation hydrolysis

Hydroxyl groups on the surface of cellulose are known to exhibit high reactivity towards oxidative degradation, which renders it susceptible to oxidation by potent oxidizing agents, culminating in the formation of a carboxylic group. This characteristic provides a promising route for the synthesization of CNC through oxidation (Zhang et al., 2024b). Oxidative hydrolysis techniques are categorized into three main systems: the 2,2,6,6-tetramylpiperidol sodium bromide sodium hypochlorite oxygen radical (TEMPO/NaBr/NaClO) alkaline system, TEMPO/NaClO/$NaClO_2$ acidic system, and ammonium persulfate (APS) oxidation system (Zhou et al., 2023). The TEMPO/NaBr/NaClO system is a

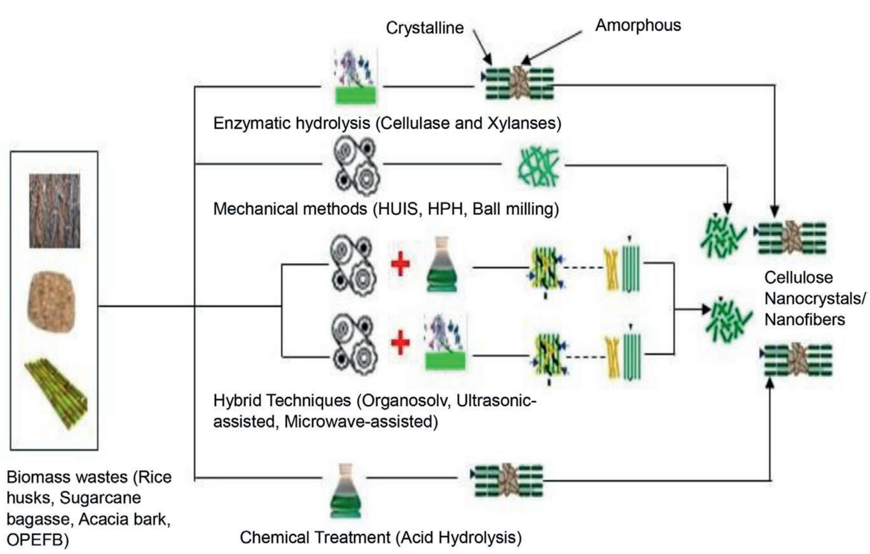

Fig. 5. Novel methods for the synthesis of cellulose, CNCs, CNFs (Chaka, 2022; Yao et al., 2021).

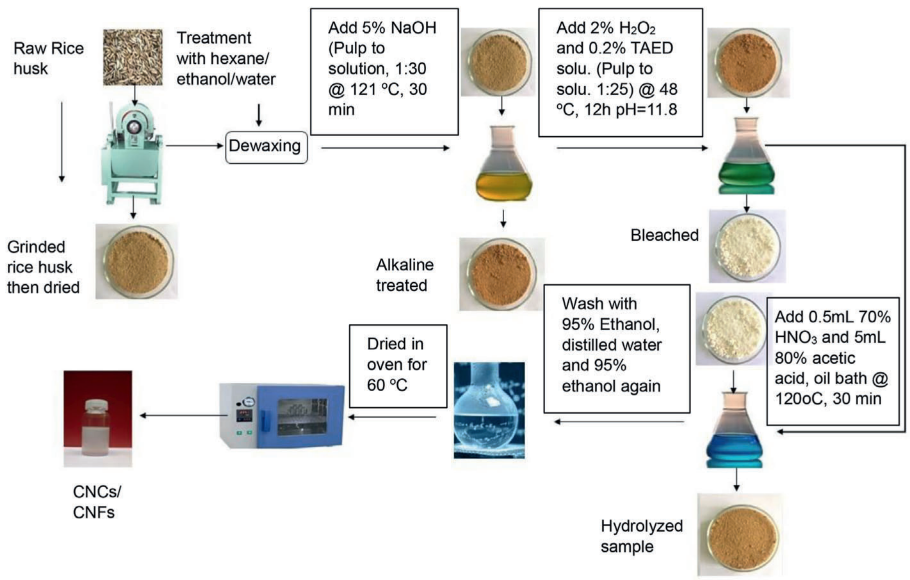

Fig. 6. Synthesis of cellulose nanocrystals from biomass wastes (rice husk) via acid hydrolysis (Taflick et al., 2017).

well-known method for selectively oxidizing polysaccharides, such as cellulose, using TEMPO as a catalyst with NaBr and NaClO in an alkaline medium (pH 10–10.5). By contrast, the TEMPO/NaClO/$NaClO_2$ system operates under acidic conditions (pH 4.6), where the combination of NaClO and $NaClO_2$ enhances oxidation, allowing for effective results under milder conditions, which is particularly advantageous in applications that require controlled oxidation (Filipova et al., 2020).

The TEMPO oxidation system, such as TEMPO/NaBr/NaClO, involves converting the C_6 hydroxyl groups of cellulose into carboxyl groups. However, this method initially oxidizes hydroxyl groups to aldehyde groups, which can lead to aggregation and reduced dispersion of the resultant cellulose (Baron and Coseri, 2020). The TEMPO/NaClO/$NaClO_2$ oxidation system represents a significant advancement in the synthesis of CNC, directly converting hydroxyl groups into carboxylic groups without the intermediate formation of aldehyde groups. This approach enhances the stability and dispersion properties of CNCs derived from cellulose, making them suitable for various industrial applications (Ye et al., 2021). APS is a strong oxidizing agent for various organic substrates, including polysaccharides. Its oxidation mechanism involves free radical generation, which is crucial for initiating polymerization reactions and enabling selective modifications in substrates (Haunreiter et al., 2024). APS oxidation selectively targets the hydroxyl groups on cellulose surfaces, transforming them into carboxylic groups through a reaction involving sulfate ions, peroxide species, and water. This process not only modifies the surface chemistry of cellulose but also enhances its crystallinity by disrupting the amorphous regions. Wang et al. (2020b) demonstrated the effectiveness of APS in synthesizing CNCs from lemon seeds, achieving a high crystallinity index of 74.4% and a remarkable thermal degradation temperature of 346 °C. As shown in Fig. 7, CNCs have been synthesized using a variety of chemical techniques using a variety of agricultural wastes.

4.1.3. Enzymatic hydrolysis

Enzymatic hydrolysis employing cellulase enzymes, such as endoglucanase, exoglucanase, and β-1,4-glucanase, to synthesize CNCs from biomass (Tong et al., 2023; Yarbrough et al., 2017;). This process proceeds through three distinct stages: initially, endoglucanase targets the amorphous regions within cellulose fibers by hydrolyzing glucosidic bonds, thereby generating new chain ends. Subsequently, exoglucanase acts on both the reducing and non-reducing ends of polysaccharide chains, producing cellobiose and tetrasaccharides. Finally, β-glucosidase further degrades cellobiose and tetrasaccharides into glucose, facilitating the synthesis of CNCs (Chin et al., 2018; Shen et al., 2022). CNCs obtained via enzymatic hydrolysis exhibit properties comparable to those derived from acid hydrolysis but offer reduced environmental impact due to the absence of harsh acids (Beltramino et al., 2018; Du et al., 2016). This approach is often integrated with chemical or mechanical techniques to optimize CNC yield and quality. Several studies have been carried out on enzymatic hydrolysis of cellulose to synthesize CNC (Houfani et al., 2020; Tong et al., 2020, Cabrera-Villamizar et al., 2024; Tong et al., 2023).

Nechyporchuk et al. (2015) compared the effectiveness of single endogluacanse against a combination of exoglucanase and endoglucanase and observed that endoglucanase alone improved CNC crystallinity and suspension production. It was also observed that endoglucanase treatment improved crystallinity due to selective degradation of amorphous regions. Tong et al. (2020) utilized a blend of cellulase and xylanase to produce spherical CNC from eucalyptus with an average particle size of 40 nm derived from Eucalyptus pulp, which exhibited thermal stability of about 343 °C. Fig. 8 illustrates the stages involving the complete degradation of the non-cellulosic region and the synthesis of cellulose and CNC. Table 4 illustrates various research works conducted by researchers to synthesize CNC from biomass through pretreatment, alkaline treatment and bleached treatment. Table 5 shows a comparative analysis for the chemical method, mechanical, enzymatic and hybrid techniques used in the synthesis of CNCs.

4.2. Mechanical methods

Nanocellulose, particularly CNC, is increasingly favored in various industries due to its operational simplicity and potential for production on a large scale (Das et al., 2022; Pires et al., 2019). Mechanical techniques are commonly employed to synthesize nanocellulose, involving repetitive cycles to reduce particle size and achieve uniformity in length and fines. Methods such as ball

Table 3
Chemical method treatments of biomass waste sources with their pros and cons.

References	Techniques	Yield (%)	Size	Reaction Duration	Temperature	Conditions	Crystallinity index (%)	Equipment handling	Degradation temp.	Result
(Al-Dulaimi and Wanrosli, 2017; Neenu et al., 2022)	Sulfuric acid hydrolysis	High yield of about 37.1%	CNF: (1–3.5 nm); Length: (50–600 nm)	40–100min	mild operation temp. 40 °C	Requires thorough water washing repeatedly; Centrifugation	High as 80.8%	Requires corrosion-resistant equipment due to highly corrosive conditions	around 200 °C	Requires a control mechanism to stop acid hydrolysis
(Becker et al., 2021; Hastuti et al., 2018; Leboucher et al., 2020)	Hydrochloric acid	Yield cellulose lower about 18–21%	CNF: Width (10–12 nm); Length: 246–301 nm)	Requires about 2 h	Requires a higher reaction temperature at around 80 °C		Moderate around 53–65%		Higher thermal stability; Thermal degradation for CNC around 346–358 °C;	
(Budhi et al., 2018; Meryemoglu, 2021; Qu et al., 2020)	Phosphotungstic acid hydrolysis	CNC can be as high as 44.04%		Long reaction duration (25–35 h)	High operating temperature (80–100 °C)	High concentration of acid (65–85%); Requires dimethyl ether in the process	CNC as high as 84%	Requires expensive mechanical mixing to the limited contact between the acid and pulp		May form aggregates at the end of the process
(Chen et al., 2022; Xu et al., 2020)	Ionic Liquid hydrolysis	High yield of about 52.72%		Longer duration time about 24 h; High temp. time duration shortened to 4 h	Reaction temperature of about 60 °C; High temp. about 140 °C				CNC with moderate thermal stability; Thermal degradation of 325.65 °C	
(Culsum et al., 2021; Indirasetyo and Kusmono, 2022; Madani et al., 2022)	Ammonium Persulfate hydrolysis	High yields	CNC: width (25–31 nm); Length (100–250 nm)	Moderate reaction of about 15 h	about 70 °C	High Concentration of chemicals, around 2 M	CNC as high as 68–78%			Less effective in the removal of hemicellulose and lignin

Fig. 7. Images of biomass sources at the dewaxing stage, alkaline treated, bleached, and acid hydrolysis of (a) Jackfruit peel, (b) Oil palm empty fruit bunch, (c) Rice straw, (d) Corn husk, (e) Sugarcane bagasse, (f) Acacia bark (Chawla et al., 2023; Louis et al., 2022; Rubiyah et al., 2023; Sikder et al., 2023; Taflick et al., 2017; Vu et al., 2024).

milling, HPH, steam explosion, and HIUS are prominent in this regard (Dai et al., 2023; Dey et al., 2022; Pradhan et al., 2022). Among these mechanical techniques, steam explosion stands out as a widely adopted method for producing CNC. This process involves subjecting milled biomass materials to high-pressure steam (14–16 bar) and elevated temperatures (200–270 °C) for a brief period. The rapid pressure release during steam explosion disrupts the biomass structure, effectively decomposing lignocellulosic components like cellulose and lignin while preserving cellulose integrity (Jiang et al., 2021). Besides its ability to enhance crystallinity, steam explosion is advantageous for industrial scalability and integration with other processes such as gasification or fermentation to derive value-added products from cellulose (Sarker et al., 2021).

Another notable mechanical method, HPH, is widely recognized for its effectiveness in reducing particle size and increasing the number of particles produced during homogenization processes (Hongrattanavichit and Aht-Ong, 2020). The key mechanisms included are shear forces, cavitation, and impact force. The high velocity of the fluid creates significant shear forces that break down cellulose fibers into smaller particles. The rapid changes in pressure can lead to cavitation where vapor bubbles collapse violently. This phenomenon further leads to cellulose fiber's fragmentation, whereby enhancing the efficiency of CNC synthesis (Rovera et al., 2023). The principle behind HPH is that HPH depends on the chemical and physical properties of the biomass such as cellulose content, lignin presence, and moisture level. Higher pressures generally lead to smaller particle sizes but in most cases, it may require optimization to avoid excessive energy consumption or degradation of the cellulose (Song et al., 2019). Researchers have applied HPH extensively to synthesize nanocellulose from various sources, showcasing its versatility and efficiency (Chutia and Mahanta, 2021; Lee et al., 2018; Long et al., 2024). For instance, Wang et al. (2020a) synthesized CNC from cotton cellulose using an ionic liquid solution and HPH, highlighting the method's capability to refine cellulose into nanoscale dimensions. Aguado et al. (2022) successfully synthesized CNC from hemp fiber using HPH, achieving a high aspect ratio and significant surface area enhancement through multiple homogenization cycles. The extracted CNC measurement was about 277.76 nm in length and 6.38 nm in diameter, then exhibited a higher aspect ratio of 44.69. Further studies by Chutia and Mahanta (2021) and Long et al. (2024) underscored HPH's capacity to produce CNC with precise morphological characteristics, such as uniform width and length ranges, demonstrating its potential for tailored nanocellulose applications in diverse industrial sectors. Furthermore. HPH does not alter the chemical structure of cellulose. This is evidenced through FTIR analyses which show that functional groups remained intact during post-treatment.

The main mechanism behind HIUS is acoustic cavitation, which involves the creation, expansion, and implosive collapse of microbubbles in a liquid solvent. As ultrasound waves propagate through the liquid, they create high and low-pressure regions. The low-pressure cycles allow gas bubbles to form while high-pressure cycles cause these bubbles to collapse violently. The implosion generates localized extreme conditions, namely high temperatures

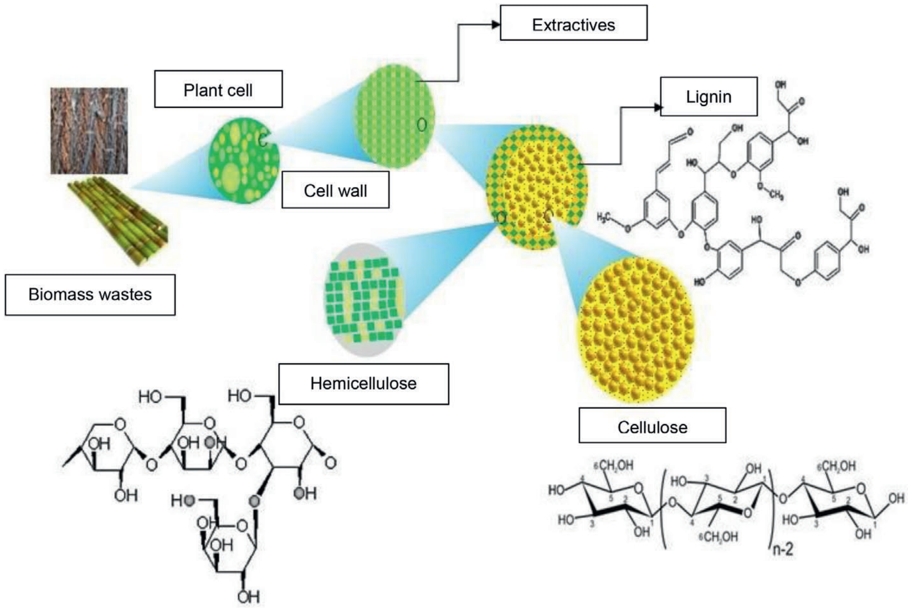

Fig. 8. Extraction of cellulose involving removal of amorphous parts (modified from Moran-Miraba (2013)) The removal of hemicellulose and lignin from amorphous cellulose improves its crystalline structure, raising the material's crystallinity index.

which can disrupt cell walls and facilitate the release of CNCs from biomass (Nugroho et al., 2023). The mechanical forces generated by cavitation lead to the fragmentation of cellulose fibers. Some parameters influence the effectiveness of HIUS synthesis process. For instance, the longer the treatment time the more fragmentation increases and reduces the crystallinity index. Higher amplitudes enhance cavitation intensity, leading to more disruption of the cellulose structures. The total energy delivered during sonication is paramount, as optimal energy maximizes CNC yield while minimizing degradation (Nugroho et al., 2023; Szymańska-Chargot et al., 2022).

Ball milling utilizes mechanical and frictional forces to break down cellulose particles, reducing them to nano-sized dimensions. Zhang et al. (2015) applied ball milling to softwood pulp under ambient conditions, yielding CNC with an average diameter of 100 nm. Despite its effectiveness, ball milling generates frictional heat that can soften cellulose particles, enhance their deformability but also contribute to high energy consumption. This environmental impact and the challenge of achieving good dispersibility have limited the widespread use of ball milling alone for CNC synthesis. However, it remains valuable when combined with other techniques (Sofla et al., 2016), as demonstrated by Hajiali et al. (2022), who successfully integrated ball milling with maleic acid hydrolysis to enhance CNC dispersion stability and achieve higher yields from bamboo fiber. Ultrasonication, another mechanical approach, involves the application of high-frequency sound waves to disrupt cellulose fibers.

4.3. Nanoprecipitation

The synthesis of CNCs via nanoprecipitation is gaining a lot of momentum due to its simplicity and effectiveness. Nanoprecipitation, also known as solvent displacement or interfacial deposition, involves dissolving cellulose in a solvent that is miscible with water (Agi et al., 2019b). This solution is being introduced into an antisolvent which leads to the formation of nanoparticles due to spontaneous diffusion. This method of synthesis allowed for CNCs ranging between 50 and 300 nm in size (Reimer et al., 2023). Various factors may affect nanoprecipitation. The type of solvent used can significantly affect the particle size and morphology of the CNP. For example, Cordt et al. (2020) reported that acetone is noted for its effectiveness in manufacturing stable colloidal suspensions. George and Sabapathi (2015) reported that temperature and pH can alter the stability and solubility of the cellulose solution, hence affecting their final characteristics. The concentration of the cellulose solution can directly affect the size of the resulting CNP as lower concentration normally yields smaller particle sizes of CNP.

Chin et al. (2018) evaluated the impact of cellulose solution concentrations and the volume ratio of solvent (aqueous solution of NaOH/urea/thiourea)/antisolvent (ethanol) in particle formation through nanoprecipitation. They observed that when the cellulose concentration varied from 0.001% to 0.005–0.1% (w/v), the particle size increased from 218 nm to 263–683 nm. However, the variation in solvent/antisolvent ratio from 1:20 to 1:60 decreased the sizes of the particles from 365 nm to 70 nm. Zhang et al. (2019) observed that cellulose concentration can affect particle sizes, resulting in nanoparticles of size (<50 nm). Ho et al. (2020) studied the effect of cellulose fiber obtained from paper waste using a solution of carboxylic citric acid (CA) obtained from TEMPO oxidation and acetylation in ultrapure water and ethanol as an antisolvent. Their findings showed that the nanosphere was reduced to 70–100 nm. Al Hakkak et al. (2019) investigated the effect of MCC solvent dissolved in 1-methyl-3-methylimidazolium acetate ([C_2mim][Ac]) and acetonitrile as an antisolvent. The result shows particles of 100–400 nm nanosphere.

4.4. Surface modification

CNC synthesized from biomass wastes such as EFB, PKS, rice husk, may require surface modification due to their exhibition of large surface areas and high concentrations of hydroxyl groups, which leads to robust hydrogen bonds between the cellulose and the CNCs or cellulose nanofiber (CNFs) structure. Cellulose is also reported to possess excessive hydrophilicity, making it difficult for usage in several applications (Marakana et al., 2021; Missoum

Table 4
Various research on Extraction methods from biomass waste.

References	Biomass waste	Diameter	Length	Treatment	Cellulose (%)
Amirah Badi et al. (2024)	filter paper	16.02	15.09	The paper was cut and washed, then treated with 6% NaOH at 70 °C for 4 h, followed by triple bleaching with 6% $NaClO_2$ at 70 °C for 2 h. Post-neutralization, acid hydrolysis using 64% H_2SO_4 at 45 °C for 60 min selectively removed amorphous regions. The mixture was subsequently diluted, washed, centrifuged, and dialyzed to pH 7 over 4–5 days. After final sonication for 30 min and freeze-drying, cellulose nanocrystals (CNCs) were obtained.	
Moghaddam et al. (2024)	Corn husk (Agricultural residues)	7–30 μm		Corn husk was chopped (100 mm pieces) and treated with NaOH (5–15 g/L) at 120 °C for 120 min (30:1 volume-to-weight ratio) to extract fiber. After washing and neutralization with 5% acetic acid, fibers were bleached with 10% H_2O_2 at 90 °C for 1 h, using NaOH and $NaSiO_2$.	
Suyambulingam et al. (2024)	Lemon grass	5.13		Alkalization, low pyrolysis, acid hydrolysis and bleaching	
Kumar et al. (2024)	Palm grass leaf	2.44		5% NaOH (150 mL of 80% acetic acid +15 mL of nitric acid and anthrone reagent (200 mg of 100 mL H_2SO_4) conc 67%. 10% NaOH	72 82
Chamathka et al. (2024)	Palm Kernel meal	40 = 100 nm		Alkaline treatment extracted cellulose using 4% NaOH (w/v) at 50 °C for 180 min, from 3 to 6 times. The next step was bleaching with 1.7% $NaClO_2$ in distilled water and acetate buffer for 4 h at 80 °C. In order to ensure a neutral pH of 7, acid hydrolysis was carried out using 52% w/v H_2SO_4 at 45 °C for 45 min. Centrifugation was then performed.	42.3
Brahma and Ray (2024)	Jackfruit peel	100–450		Using the Response surface methodology (RSM), best conc 5% NaOH and 2% $NaClO_2$	64–65
Pratama et al. (2024)	Belulang grass		15.46um	Alkalization used 5% NaOH (80 °C, 120 min), bleaching with 3% H_2O_2 and 5% NaOH (80 °C, 90 min), followed by acid hydrolysis with 2.5% HCl (70 °C, 90 min), stopped by adding 5 × distilled water.	34/16
Tengsuthiwat et al. (2024)	Ficus macrocarpa	223.27um		Alkaline treatment (5 wt% NaOH with dissolved 53.77 g of 98% pure pellets) Solution diluted in 1000 mL water	59.7
Birlie and Mamay (2024)	Grewia ferruginea			Stem bark was peel and immersed in 10% (w/v) NaOH (Bark to liquid ratio: 1:20) @ 90 °C for 30–45mins; 15% acetic acid solution for 10min to neutralize the alkalis	60.4–72.6
Ibrahim et al. (2024)	Semantan bamboo (Gigantochloa scortechinii)	BCN_s = 3–17 (w) BCN_b = 3–21 (w)	BCN_s = 33–200, BCN_b = 34-228	Twenty grams of raw bamboo fiber were soaked in 650 mL of water at 95 °C, supplemented with 8 g of NaCl and acetic acid to facilitate lignification. The fibers underwent a 2-h treatment with 10% NaOH, followed by benzoylation in 18% NaOH and benzoyl chloride, then ethanol immersion.	
Shibly et al. (2024)	Bark of Rosa hybrida plant			5% NaOH (w/v) 1:20 @ 100 °C for 4 h. The bark was soaked in fresh water to remove impurities. The 5% helps in breaking down the non-fibrous components such as hemicellulose, lignin, pectin, and others.	57.99
Zheng et al. (2024)	Brewer spent grain (BSG)	90–440		Dried BSG was dispersed in 1.25% H_2SO_4 (1:10 w/v) at 121 °C for 17 min, followed by treatment with 2% NaOH at 90 °C for 2 h (1:20 w/v), repeated four times. Samples were treated in acetate buffer and 2% $NaClO_2$ (1:50 w/v) at 80 °C for 2 h, producing cellulose. Subsequently, 10 g of cellulose was hydrolyzed in 64% H_2SO_4 at 45 °C, followed by sonication to yield CNC.	BSG = 20.5; BSGC = 88.12
Ebrahimi et al. (2024)	Hazelnut shell (HS), Treated Hazelnut shell (THS)			Milled hazelnut shells (HNS) were passed through a 60-mesh sieve and treated with 3% NaOH at pH 12 at 80 °C for 3 h, with continuous stirring at 60 rpm, then washed with distilled water. The bleached samples were treated with a 2.7% $NaClO_2$ buffer solution at pH 4.9 at 80 °C for 1 h and repeatedly washed until a neutral pH was reached. After being milled once again and dried for 12 h at 50 °C, the samples were acid hydrolyzed for 3 h at 90 °C using 3 M HCl (40 mL/g). The resulting CNC was centrifuged, dialyzed to neutral pH, sonicated at 300 W in an ice bath, and freeze-dried.	32.1; 70.8
Zheng et al. (2024)	Black tea residue	5.0–45		The tea residue was pulverized using a 60-mesh filter after being dried at 50 °C. A 2-h alkaline treatment using 10% (w/v) NaOH at 80 °C (solid:liquid ratio of 1:20) was carried out. The residue was bleached	Cellulose I

				using 7.5% w/v $NaClO_2$ at pH 4 and 75 °C for 2 h, followed by a second bleaching with 0.9% w/v H_2O_2 at 55 °C for 1 h. Acid hydrolysis involved 68% H_2SO_4 at varying concentrations (52–67%) and times (5–90 min) with solid-to-liquid ratios ranging from 1:12 to 1:22.	
Nyoo Putro et al. (2024)	Jackfruit peel	5.0–30	100–500	Jackfruit skin was washed, cut into smaller pieces, and dried at 105 °C to achieve 12% moisture content. The dried skins were milled through a 100-mesh sieve before undergoing delignification in 500 mL of 2 N NaOH at 80 °C for 5 h. Following centrifugation, the solid was bleached using a solution of H_2O_2 and NaOH at 50 °C for 5 h. Acid hydrolysis was performed with 100 mL of 56% H_2SO_4 at 45 °C for 2 h, followed by centrifugation at 9500 rpm for 10 min.	79.8
Naseem et al. (2024)	Urtica dioica (Stinging nettle)			Sono-microwave assisted chlorine-free and Ionic Liquid (SMACIL). pre-chemical treatment before starting to bleach them with hydrogen peroxide (HPO) and 1-butyl-3-methylimidazolium acetate (BMIM-Ac) having different mole ratios (5, 7.5, and 10) to expose cellulose	88% more than HPO-10
Bahndral et al. (2024)	Lemon grass			microwave-assisted alkali extraction, followed by characterizing the extracted material. At microwave power of 540 W using 8 % NaOH for 3 min for lignin removal and 540 W for 2 min for bleaching showed the maximum yield of 37.46 %.	
Moradi and Fathi (2023)	Tomatoes pomace	104		Tomato pomace was dried, ground, and sieved through a 60-mesh sieve. Alkaline treatment involved soaking the pomace in 2% w/v NaOH at 95 °C for 4 h with continuous stirring, followed by washing until neutral pH and drying at 40 °C. Bleaching was performed with 1.7% w/v $NaClO_2$, buffer solution (27 g NaOH), 75 mL acetic acid, and 1 L distilled water at 80 °C for 6 h. Acid hydrolysis utilized 15 mL of 64% w/v H_2SO_4 at 45–50 °C for varying durations, followed by dilution, centrifugation, and dialysis to neutral pH. The final suspension underwent ultrasonic treatment for size reduction and was stored at 4 °C with chloroform to prevent microbial deterioration.	
Ren et al. (2023)	Quinoa straw (QS)	20.34w	125.25	Quinoa straw (QS) underwent Soxhlet extraction with toluene/ethanol (2:1) for 24 h to remove wax and oil. The dried fiber was treated with 11 wt% NaOH at 100 °C for 1 h to eliminate hemicellulose, followed by washing. Lignification occurred with 1.5 wt% $NaClO_2$ at pH 3–4 under stirring at 75 °C for 1 h. Acid hydrolysis utilized 2 g of cellulose in 45–65% H_2SO_4 at 70 °C for 150 min, with reactions halted by cold water. The resulting suspension was dialyzed, ultrasonicated (500 W, 5 h), and freeze-dried to obtain GSCNCs powder, stored at 4 °C.	
Hemida et al. (2023)	Nile Roses (*Eichhornia crassipes*)			The pulping process began by mixing 100 g of raw fiber with 1.750 L of deionized water and 20 g of NaOH at 110 °C for 2 h, followed by washing and drying to a constant weight. The pulped fibers were bleached using 10 g of fiber mixed with 400 mL deionized water, 1.5 g $NaClO_2$, and acetic acid in a water bath at 100 °C for 2 h, repeated ten times. Hydrolysis was conducted by treating the bleached fibers with 60% H_2SO_4 at 45 °C for varying durations, and the resulting suspension was neutralized with $NaHCO_3$ before washing and drying.	
El Amri et al. (2023)	Stems of reed plant large-leaved cattail (Typha latifolia)	6–7 μm		The sample was dewaxed (20 g) using Soxhlet reflux in 2:1 (v/v) acetone/ethanol at 63 °C for 7 h, treated with 7% (w/v) NaOH (10:1 solvent-to-solid) at 80 °C for 3 h (3x), filtered, washed to neutral pH, and bleached in H_2O_2 with pH adjusted to 11 (7% w/v NaOH) at 45 °C for 3 h (2x), then filtered and washed.	
Ogunjobi et al. (2023)	Siam weeds	<100		Siam Seeds (SW) were collected, dried, pulverized, and sieved through a 0.8 μm mesh. Soxhlet extraction in ethanol for 8 h removed extractives. Free samples (10 g) were treated with $NaClO_2$ and acetic acid (70 °C, 1 h) in distilled water, repeated until holocellulose formed, then washed (pH 7) and dried (105 °C, 3 h). Bleached samples (15 g) underwent alkali treatment (20% NaOH, 90 °C, 90 min) and acid hydrolysis (9 g CPC, 65 wt% H_2SO_4, 45 °C, 60 min), followed by neutralization, dialysis (2 weeks), sonication (30 min, ice bath), and freeze-drying to yield CNC-SW powder.	39.6

(*continued on next page*)

Table 4 (*continued*)

References	Biomass waste	Diameter	Length	Treatment	Cellulose (%)
Mahur et al. (2023)	Sunn hemp (Crotalaria juncea)	NC-32 = 55; NC-48 = 31; NC-64 = 40		Samples were washed and cleaned to remove impurities, then air-dried and processed into fine powder through pulping milling. Dewaxing was performed using a toluene-ethanol mixture (2:1) at 40 °C for 6 h via Soxhlet extraction, effectively removing wax and polar/non-polar compounds. To delignify, 750 mL of double-distilled water containing 3.4% w/v $NaClO_2$ was used to soak 10 g of Sunn hemp powder, maintaining a temperature of 75 °C and pH of 3–4 through glacial acetic acid addition, resulting in a color change from light brown to white. Alkaline treatment involved boiling with KOH pellets at 85 °C for 4 h. Following neutral washing, fibers were soaked in DMSO to enhance acid susceptibility. Different quantities of H_2SO_4 were used in acid hydrolysis, which produced colloids at a 32% concentration. After neutralization, the samples were sonicated, frozen at −40 °C, and lyophilized to obtain nanocellulose, which was stored at 4 °C for further analysis.	
Chawla et al. (2023)	Corn husk (Agricultural residues)			Ten grams of corn husk powder were treated with deionized water (70 °C, 4 h) to remove soluble, followed by filtration and drying (55 °C). The residue underwent alkali treatment (5% NaOH, 27 °C, 2 h) and bleaching (24% H_2O_2, 4% NaOH, 45 °C, 2 h). Acid hydrolysis (60% H_2SO_4, 1:30 fiber-to-acid ratio) was conducted for 2 h, neutralized, centrifuged (1000 rpm, 10 min), and dried (55 °C, 24 h). The resulting fine powder was stored airtight.	
Abzan et al. (2023)	Leftover celery pulp	Unbleached; 112–123 μm; Bleached NaCl: 11.25; Bleached with $NaClO_2$: 11.5–12.5		The process involves two pathways: Pathway 1—Step 1 (2% NaCl + 3% acetic acid, 60 °C, 3 h), Step 2 (1.5% NaOH + 1% H_2O_2, 60 °C, 1.5 h), Step 3 (1.25% NaCl + 3% acetic acid, 60 °C, 1.5 h); or Pathway 2—Step 1 (2% $NaClO_3$ + 3% acetic acid, 60 °C, 3 h), Step 2 (1.5% NaOH + 1% H_2O_2, 60 °C, 1.5 h), Step 3 (1.25% $NaClO_3$ + 3% acetic acid, 60 °C, 1.5 h).	
Mohamed et al. (2022)	oil palm empty fuit bunch (OPEFB)			Oil palm empty fruit bunches (OPEFB) were washed, treated with 1% detergent until colorless, sun-dried, cut, and ground to 0.5 mm. OPEFB was then pretreated with free laccase in acetate buffer (pH 5.0) at 50 °C for 12 h. Enzymatic hydrolysis used 1.0 g of laccase-pretreated OPEFB in 50 mL buffer with 80 IU cellulase for 96 h at 150 rpm. The hydrolyzed product was centrifuged at 8000 rpm and freeze-dried, yielding a white powder.	
Judith et al. (2022)	Bean forage			Lemon seeds were pulverized, sieved (80 mesh), and delignified with 5% (w/v) $NaClO_2$ (pH 3.8–4.0, 75 °C, 5 h). The residue was then treated with 10% (w/v) NaOH (30 °C, 12 h), washed with distilled water, and dried.	Raw = 45.87, treated = 60.68
Wahib et al. (2022)	Date pit (DP)			The product was washed to neutral pH, delignified with 6% NaOH (70 °C, 4 h, 6x), bleached, acid hydrolyzed with 64% H_2SO_4 (25 °C, 1 h), then centrifuged, ultrasonicated, and dried.	DP = 21.2; AT(DP) = 63.1; BT(DP) = 84
Perumal et al. (2022)	Areca nut husk fibers	19.3	195	The sample was treated with 4% (w/v) NaOH at 80 °C for 3 h (3x), bleached with 1.7% (w/v) $NaClO_2$ in CH_3COOH buffer at 80 °C for 4 h (3x), then hydrolyzed with 65% (w/v) H_2SO_4 at 45 °C for 45 min. After centrifugation (10,000 rpm, 10 min), it was washed, sonicated (2x, 5 min), and stored at 4 °C.	
Ng et al. (2021)	Elaeis guineensis empty fruit bunch	13–30	150–360	The sample was delignified with 2% (w/v) $NaClO_2$ in acetate buffer at 80 °C for 2 h, treated with 4% (w/v) NaOH to degrade hemicellulose, then hydrolyzed with 58 wt% H_2SO_4 at 45 °C for 45 min, followed by centrifugation at 10,000 rpm for 15 min.	13–30
Guo et al. (2021)	Tea stalk	4.0–8.0w		62.2% H_2SO_4 at 45 °C for 123mins	
Sohni et al. (2024)	Orange peel			5% (w/v) NaOH, 17% (w/v) $NaClO_2$	
Pandi et al. (2021)	Cotton	10.0–50/0		Acid hydrolysis assisted with ultrasonication @ 60 °C	
Corrêa et al. (2020)	Curaua	80.0–100.0		Acid hydrolysis and oxidization @ 45 °C	
Kusmono et al. (2020)	Ramie	108.87		Acid hydrolysis at 50 °C	
Belmabrouk et al. (2023)	Calotropis gigantea fruit bunch	8.8w	242.06	Ball milling defibrillation using SO_4^{2-}/SiO_2 nano-solid superacid catalyst	

Table 5
Comparative analyses of chemical, mechanical, enzymatic hydrolysis and hybrid methods.

References	Extraction Methods	Chemical reagents	Formula	Environmental friendliness	Energy Efficiency	Precise Controllability	Product purity	Wastes Management	Cost	Time
(Cheng et al., 2017; Hu et al., 2021; Li et al., 2020b)	Acid Hydrolysis	Inorganic acid Organic acid Mixed acid	H_2SO_4, HCl, H_3PO_4, HBr Formic acid, Citric acid, Oxalic acid HCl/Citric acid, HCl/HNO_3	Very difficult to treat wastes from acids like H_2SO_4 and HCl due to their corrosive nature. They have the potential to damage equipment	Moderate temperature and pressure	Hard to control reaction	Increases cellulose crystallinity; CNCs synthesized via H_2SO_4 produced remarkable suspension stability.	Toxic wastes: produce high amounts of acid waste' Waste generation and disposal, Difficult operate due to chemicals	Less expensive	Conserve time
(Razali et al., 2022; Zheng et al., 2024)	Mechanical techniques	High-pressure homogenization (HPH) High intensity ultrasonication (HIUS) Ball milling		Environmental friendliness	High Energy consumption	Easily control	Low crystalline	Easily operated		Time-consuming
(Tong et al., 2020; Xu et al., 2020)	Enzymatic Hydrolysis		Xylanase and Cellulase	Environmental friendliness	Low efficiency requires	The process can be conducted under mild reaction	Produces CNC with high-surface stability	Non-toxic wastes; Avoid harsh chemicals	High production cost; Higher cost of enzymes	Time consuming; Slow process
(Filipova et al., 2020; Haunreiter et al., 2022; Wang et al., 2020; Yang et al., 2019b)	Oxidation techniques	TEMPO Ammonium persulfate Periodate	TEMPO/NaClO/NaBr (alkaline); TEMPO/NaClO/$NaClO_2$ (acidic) Ammonium persulfate H_5IO_6/NaOH/$NaClO_2$/sodium periodate		High efficiency; High water consumption	Hard to control reaction condition	CNC with good dispersibility	Non-toxic;	High production cost	Slow reaction rates
(Al Hakkak et al., 2019; Glińska et al., 2021; Liu et al., 2023; Meraj et al., 2023)	Solvent methods	Ionic liquid Deep eutectic solvents	[EMIM] [OAc], [BMIM] HSO4, [BMIM]Cl, TBAA/DMAc Lactic acid/Choline chloride, Malic acid/choline chloride, Glutaric acid/Choline chloride	Environmentally friendly	High solvating power, High energy consumption		Low crystalline	Ionic liquids can be recycled. Deep eutectic solvents are recoverable and biodegradable	Ionic liquids is very expensive	

et al., 2013). Hence, surface modification of samples involves the use of various additives to alter or manipulate the surface properties of the hydroxyl group on CNC to enhance properties such as conductivity (Meulendijks et al., 2017), hydrophobicity (Mohanta et al., 2014) and thermal responsiveness (Raza and Abu-Jdayil, 2022; Zoppe et al., 2011). These chemical modifications may include non-covalent bonding, silylation amidation, etherification, sulfation, oxidation, esterification, polymer grafting, in small molecules and the use of large molecules such as graft copolymerization, as illustrated on Fig. 9 (Habibi, 2014). The main purpose of chemical functionalization is to introduce either negative or positive electrostatic charges on the CNC surface, which provides better dispersion in any solvent or polymer.

4.4.1. Amidation

This method involves introducing amine groups to the cellulose surface through a carbodiimide-mediated reaction, specifically by activating the carboxylic acid moieties on crystalline cellulose to create N-hydroxysuccinimidyl ester, which then reacts with a primary amine to produce an amine product (Bangar et al., 2022; Eyley and Thielemans, 2014). During the second phase, amidation occurs between the carboxylate group (-COO) and the amine functionalities (-NH_2), facilitated by a peptidic linkage using N-(3-dimethyl aminopropyl)-N′-ethyl carbodiimide (EDC)/N-hydroxysuccinimide (NHS) catalyst. Filpponen and Argyropoulos (2010) conducted an experiment using propargyl amine and 11-azido-3,6,9-trioxaundecan-1-amine to examine the effects of amidation on oxidized crystalline cellulose, with transmission electron microscopy (TEM) imaging revealing well-structured and coordinated crystals. Gicquel et al. (2019) found that aromatic functions on the CNCs surface significantly enhanced the sorption of aromatic ring-bearing molecules due to π-π interactions between the sorbent and the sorbate. Their study reported various CNCs modification procedures, including silylation, esterification, and grafting using isocyanates, leveraging the hydroxyl groups present on the CNCs surface. Lasseuguette (2008) produced a series of CNFs amidated with benzylamine, hexylamine, dodecylamine, and amine-functionalized poly(ethylene oxide)-*b*-poly(propylene oxide) (PEO-*b*-PPO) copolymers (commercially known as Jeffamines) under pH 7.58 with EDC and NHS. The advantages of amidation via EDC/NHS coupling include minimal chemical usage and the ability to perform the reactions under aqueous conditions.

4.4.2. Esterification

Esterification is one of the easiest ways to introduce new surface functionalities on the nanocellulose hydroxyl group (Kalia et al., 2014; Wang et al., 2018; Zhang et al., 2023). Acid anhydride esterification is commonly used, particularly for surface acetylation, CNC is esterified under dry conditions with acetic and acetic anhydride alongside an acid catalyst (Leszczyńska et al., 2019). This experiment is performed without water because water, a by-product of esterification, can easily hydrolyze the esterification agents. Espino-Pérez et al. (2014) used acetic anhydride to esterify CNCs with citric acid as the catalyst. The images of CNC obtained from the acid hydrolysis procedure showed the typical acicular structure of CNCs with dimensions ranging from 100 to 200 nm in length and 10–20 nm in width. Moreover, the rod-like shape and the nanocrystals' dimensions were not significantly affected by acetylation, suggesting that only the surface of the CNC was modified during the reaction. Transesterification of vinyl acetate in the presence of potassium carbonate has also been used to acetylate CNC surfaces without damaging their crystal structure, although this was highly dependent on reaction time and temperature (Mokhena and John, 2020).

4.4.3. Acetylation

Acetylations can be performed with the additional presence of a nonswelling diluent, such as toluene (Heinze et al., 2018; Rodríguez-Fabià et al., 2022) or pyridine (Martins et al., 2022; Oberlintner et al., 2021), to minimize the solubilization of acetylated chains in the reaction medium or the peeling effect. Dhali et al. (2021) studied the structural aspects of acetylation of cellulose using a mixture of acetic acid and acetic anhydride, employing toluene to stop the swelling and dissolution of cellulose acetate. They found that acetylation proceeds by reducing the diameter of the crystal without significantly affecting its length. It was deduced that in a system allowing the dissolution of the resulting cellulose acetate, chains are stripped from the surface of the crystal into solution. The addition of a non-swelling solvent retains modified chains at the surface of the crystal, resulting in a

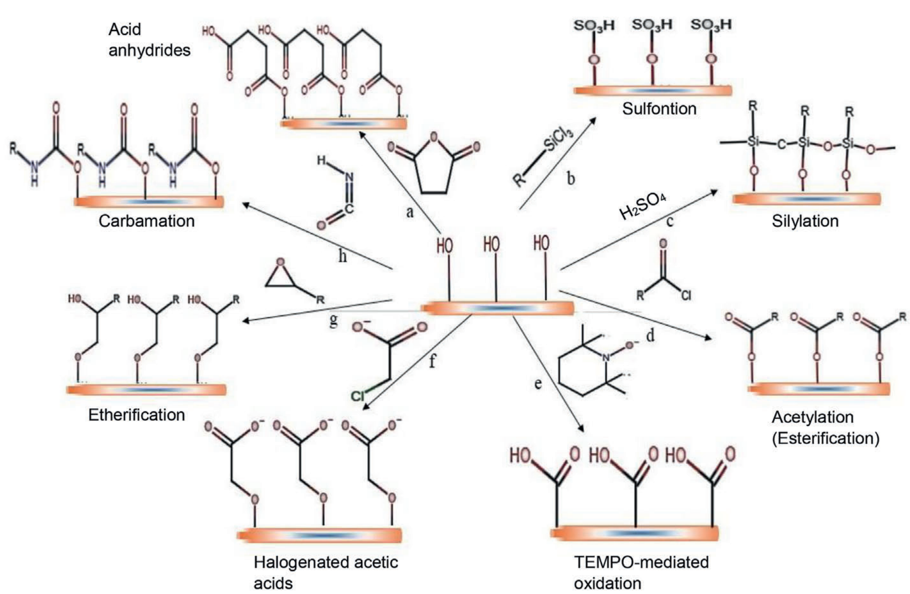

Fig. 9. Common chemical types used for modification of cellulose (a) Acetylation, (b) Sulfonation, (c) Silylation, (d) Esterification (acid halides), (e) Amidation, (f) Carboxymethylation, (g) Etherification, (h) Carbamation (Patel et al., 2019).

core of unmodified cellulose with a cellulose acetate shell (Campora et al., 2022; Wang et al., 2018).

4.4.4. Etherification

Etherification is a prevalent modification technique reported in literature, often conducted in aqueous media (Ge et al., 2022). Fibers are first activated with an alkali hydroxide (NaOH), and then mono-chloroacetic acid or its sodium salt is used for converting the hydroxyl group into carboxymethyl moieties. Examples of etherification processes include carboxymethylation, hydroxyethylation and hydroxypropylation (Ali et al., 2024; Liu et al., 2022). The key difference between etherification and esterification is that in the former, only the hydrogen of the hydroxyl group is detached to form the ether linkage (–*O*–), while in the latter, the entire hydroxyl group is substituted by the ester group (–COOR) which involves glycidyltrimethylammonium chloride (GTMAC) or its derivatives to cationize the cellulose surface. To modify GTMAC, it is mixed with a CNC suspension in a sodium hydroxide solution and heated for several hours. Four different modified product types, non-ionic, cationic, anionic, and amphoteric are often produced as a result of etherification (Aziz et al., 2019). Habibi (2014) reported that surface cationization using epoxypropyltrimethylammonium chloride (EPTMAC) resulted in a stable aqueous suspension of cellulose with thixotropic gelling abilities, as the alkali-activated cellulose hydroxyl group underwent nucleophilic reaction with the epoxy group of the EPTMAC. EPTMAC is a chemical used to modify CNCs. Acting as a cationization agent, it introduces positively charged quaternary ammonium groups to CNC surfaces. This process converts the negatively charged cellulose surface into a cationic one through esterification reactions (Li et al., 2016; Littunen et al., 2016; Sunasee and Hemraz, 2018). However, the resulting crystalline cellulose became more hydrophilic than the initial form, posing limitations. Sun et al. (2014) and Chauhan et al. (2023) used GTMAC as a cationization agent to etherify CNCs by adding a mixed solution of CNCs containing NaOH and heating it to complete the modification. A nucleophilic reaction occurred between the epoxy groups of the GTMAC and the hydroxyl group of the CNC surface. The results showed an increase in the positive charge density on the CNCs, enhancing their dispersion. Recently, the environmentally friendly SolReact process was developed by Gomri et al. (2022), in which CNC surface hydroxyl groups were esterified with phenyl acetic acid and hydrocinnamic acid. These carboxylic acids acted as both reagents and solvents during the esterification reactions. In this unique case, in situ solvent exchange by water evaporation drives the reaction forward without drying CNCs.

4.4.5. Sulfonation

Sulfonation involves partially replacing the hydroxyl groups on the nanocellulose surface with ionic sulfonic acid groups (-SO_3H) to form sulfate half-esters, resulting in stable cellulose colloidal suspensions (Bangar et al., 2022; Eyley and Thielemans, 2014; Habibi et al., 2010; Jaouahar et al., 2024). These sulfate half-ester groups are crucial for the stability of CNC dispersions, with the degree of replacement primarily influenced by the concentration of sulfuric acid, the source of CNC, production methods, and reaction temperature. High temperatures facilitate the easy transfer of anionic charge to the CNC surface (Thomas et al., 2018). Although sulfuric acid-prepared CNCs exhibit poor thermal stability, Mu and Gray (2014) noted that neutralization with NaOH can enhance their stability. Controlling the resultant ester group can be challenging; thus, Habibi (2014) suggested adding regulated sulfate moieties to CNC surfaces via HCl acid hydrolysis (Etale et al., 2023). Thompson et al. (2019) reported that sulfate esters created highly stable colloidal suspensions that, when dried under controlled conditions, formed optically active films. Araki and Nakajima (2023) developed controlled post-modification methods using H_2SO_4 to introduce sulfate-half ester groups on CNCs produced by HCl. Camarero Espinosa et al. (2013) found that surface modification of CNCs by HCl or hydrobromic acid enzymes did not produce surface charges but rather destroyed the amorphous areas holding the crystallites together.

4.4.6. Phosphorylation

The introduction of negative charges on CNC surfaces through the incorporation of phosphate (PO_4^{3-}) ester groups results in the modification of CNC with inorganic esters, producing phosphate and sulfate (Thakur et al., 2021). These esters release phosphoric and H_2SO_4, which accelerate dehydration (P. Li et al., 2020; Thakur et al., 2018). Zoppe et al. (2020) pioneered the use of phosphoric acid to produce phosphorylated CNCs. Camarero Espinosa et al. (2013) experimented with CNC surfaces under optimal conditions using 74 wt% phosphoric acid for 90 min at 100 °C. The results demonstrated homogeneous dispersion with an average dimension of 30 × 320 nm^2 and high thermal stability.

4.5. Characterization of cellulose and nanomaterials

Different characterization techniques are employed to investigate the surface morphology, topography, crystallinity, and thermal properties of cellulose nanocrystals. Morphology and topography samples can be evaluated through transmission electron microscopy (TEM) and field emission scanning electron microscopy (FESEM). Particle size distribution and zeta potential can be determined using dynamic light scattering (DLS). Minerology and thermal stabilities of cellulose nanocrystals can be analyzed using X-ray diffraction spectroscopy (XRD), FTIR, and thermogravimetry (TGA), respectively. Various characteristics techniques and tools are used to investigate the crystalline structure, crystallinity index, morphology and topography, and elemental and thermal properties of CNCs extracted from any of the biomass wastes.

4.5.1. SEM

Morphology and topography of cellulose can be evaluated using SEM. The morphology of each type of cellulose including its dimension, shape, size and other features are affected by factors such as the techniques used in isolation of cellulose and processes, source of cellulose, and treatment applied before and after processing. SEM can scan in real-time and observe morphology with relatively low quality but a comparatively large area. Several studies have shown the effectiveness of SEM through its images (Jaouahar et al., 2024; Kallel et al., 2016). For instance, Kumar et al. (2024) investigated the effect of increasing alkaline concentration during the treatment of Plam grass font (PGF) through the help of a microphotograph. They observed that all four fiber samples (3 chemically extracted and 1 extracted by water retting) were affected due to the concentration of NaOH used during treatment. The result shows that the use of 10% NaOH during treatment leads to constricted edges and damaged surface fiber, as can be seen in Table 5. Chamathka et al. (2024) examined the surface morphological features, and orientation composition of raw PKM cellulose and fibers treated with alkaline treatment, bleaching and acid hydrolysis. They observed that during acid hydrolysis, hydronium ions (H_3O^+) targeted the amorphous region of the cellulose, leading to the facilitation of hydrolytic breaking down of glycosidic linkages. The result of the topographical images of PKM cellulose were homogenous and spherical. Shibly et al. (2024) employed SEM to analyze the surface morphology of raw Rose hybrida plant bark (RHB). They observed that the uneven surface of the fiber was warped by the hemicellulose, lignin and other contaminants which were responsible for poor surface wet-out and inadequate fiber-matrix bonding. Ebrahimi et al. (2024) studied the effect of chemical treatment on raw hazel seeds (HS), treated hazel seed (THS). They observed that the raw material exhibited a compact structure and contained intercellular compounds such as hemicellulose and lignin. Impurities were removal as a result of bleaching and acid hydrolysis treatment. Sikder et al. (2023) successfully cellulose from OPEFB using enzymatic hydrolysis. They observed that the cellulose was largely made up of irregular shaped aggregated long fibrils. They noticed that the original cellulose was segmented and degraded to a large volume after cellulase enzymatic hydrolysis resulting in tiny rodlike forms.

4.5.2. TEM

TEM is usually used to acquire the shape of CNCs at high magnification (Kumar et al., 2014). Due to their small-sized CNCs in nature, consisting of hydrogen bonding and low electron density, it is challenging to image CNCs individually (Li et al., 2015). Normally, TEM with high resolution and magnification is used to investigate the defined shape and distribution of CNCs. Through TEM analysis, the diameter of CNCs can be determined as well as any possible occurrence of agglomeration. Li et al. (2015) investigated the morphological characteristics of CNCs using TEM, the results revealed the appearance of needle-like shape CNC. In a similar analysis, Rohaizu and Wanrosli (2017) conducted tests on CNCs obtained through TEMPO-assisted oxidation of Elaeis guineensis EFB in the presence of sonication treatment. The TEM images result of MCC, TEMPO-oxidized MCC and CNC widths isolated from empty fruit bunches were 31, 15, and 4 nm respectively. TEM provides better and high-resolution images in nanoscales. They can exhibit individual atoms compared to SEM. TEM micrographs are used in CNC characterization to determine the particle size distribution and shape. Many researchers have carried out a lot of research on this. For instance, Burhani and Septevani (2018) conducted an experiment to investigate the morphology of CNCs OPEFB. The result shows that CNCs-OPEFB had a morphology rod with a diameter and length of 43 nm and 147 nm respectively. Junior de Menezes et al. (2009) observed the morphology of ramie NCC with TEM. Findings from the images show that the diameter was about 10.8 nm and the length was around 135 nm. Similarly, Rohaizu and Wanrosli (2017) analyzed CNCs obtained from TEMPO-assisted oxidation of EFB in the presence of sonication treatment. The results show that the TEM images of microcrystalline cellulose (MCC), TEMPO-oxidized microcrystalline cellulose and CNCs extracted from EFB width were measured to be 31 nm, 15 nm and 4 nm respectively. They attributed the size reduction to the presence of TEMPO-oxidation and sonication, which replaced the hydroxyl group with carboxylate groups which leads to the formation of weak inter-fibrillar bonds.

Ibrahim et al. (2024) observed and accessed the Bamboo cellulose nanoparticles (BCN) shape and aggregation from micrograph producing TEM images of BCN treated with NaOH NCNs and BCN treated with benzoylated compound BCN_b. The TEM images revealed that both are nanoscale needle-like. Indicating that acid hydrolysis breaks down the strong hydrogen bonds that hold together the cellulose fibers and reduce the sizes. BCN_s TEM image shows that they are well separated, with a length 33–200 nm and a wide 3–17 nm, whereas BCNb TEM image shows a length 34–228 nm and a wide 3–17 nm. They attributed it to the interfacial hydrogen bonding, where the aggregation tendency of BCNb is denser than BCNs. Wahib et al. (2022) investigated the effect of chemical treatment on cellulose nanocrystals extracted from a date pit, an agricultural solid waste. The result shows that CNC true modification was made through sulfuric acid hydrolysis leading to cellulose microfibrils with a packed structure.

4.5.3. FESEM

FESEM can be used to obtain high-resolution images of cellulose nanoparticles. FESEM can produce low-voltage images with a magnification factor up to 30,000 and can detect and measure samples are small as 1 nm. Hence, FESEM is far better than SEM in terms of resolution because the beam gun in FESEM is electromagnetic while the beam gun used in SEM is thermionic. Unlike optical microscopes, FESEM functions based on electrons rather than light (Chorkendorff and Niemantsverdriet, 2003). The surface morphology of raw, treated and cellulose nanocrystals can be surveyed and analyzed through FESEM. Besides, FESEM can be coupled with DLS technique to further identify and clarify the particle size distribution of cellulose nanocrystals produced. The diameter of cellulose nanocrystals will reduce in size due to the removal of hemicellulose and lignin, after performing hydrolysis and bleaching treatments (Kamelnia et al., 2019). To achieve the adequate size and distribution of CNCs, ultrasound treatments could be introduced. CNCs exist in rod-like shapes or spherical shapes of the nanocrystals. So, this information can be recorded in FESEM. The morphology of the cellulose nanoparticles obtained from PKM was similar to cotton linters' morphological features. It was revealed in the study by Chauhan et al. (2019) that the spherical cellulose nanocrystals obtained from cotton linter powder were 45–75 nm, which is smaller than the size of the CNP obtained in the current study. FESEM is another technique that also evaluates the morphology of CNCs. Unlike other techniques that use optical microscopes. FESEM uses electrons instead of light. Several studies have shown that the larger the diameter of the fibers, the greater the strength. Zhang et al. (2019) conducted a morphological test on CNCs using FESEM. The study's findings show FESEM images of rice straw CNC (CNCS-RS) and poplar wood (CNCS-PS) freeze-dried at 75 °C for 48 h. The average diameter of CNCs-RS and CNCs-PS were 11.6 nm and 13.7 nm, respectively. Using the FESEM images, Vicente-Flores et al. (2024) observed that the raw fiber had a very rough topography and that the longitudinal surface of the fiber presented many impurities such as waxes, the presence of sugars, and remains of hemicellulose (Hernández et al., 2020). They observed that for the alkaline treated fiber, there were less impurities, this fact was proven as the surface cleaner, improving the roughness of the fibers (Ganapathy et al., 2019). For the bleached process fibers, the bleaching process using an oxidizing agent ($NaClO_2$) created an opening in the fiber bundles showing single helical microfibers with more regular shapes and less rough surfaces and a size reduction (Reddy and Yang, 2009). Ng et al. (2021) conducted a morphological study on cellulose nanocrystals isolated through acid hydrolysis process. They observed that the EFB surfaces after alkaline treatment were smoother due to the removal of lignin, hemicellulose, wax and other impurities.

4.5.4. X-ray diffraction (XRD)

XRD is a nondestructive technique for the characterization of cellulose and cellulose nanoparticles. XRD is used to measure the crystallinity of fibers, which can investigate the effect of each preparation step used at the point of obtaining a material. Bunaciu et al. (2015) reported that structure, grain size, phase, texture, crystallinity and crystal defection are all obtained through XRD analysis. Song et al. (2018) observed that the cellulose of raw material and NCC both exhibited cellulose I structure with a diffraction peak of the 2θ at 15.1° and 22.5°, which were assigned to planes (101) and (002) respectively. Hence, the structure of cellulose did not exhibit any change during the extraction process. However, the diffraction peaks of NCC were sharp and intense, indicating a corresponding high crystallinity. Bano and Negi (2017) conducted a study on groundnut shell (GNS) that has been dried and subjected to various treatments using XRD analysis. The diffractogram had three (3) peaks of 2θ at 16.4°, 22.5° and 34.4°. The finding of the result shows that the crystal structure of cellulose did not change significantly during the alkaline and ultrasonication treatments. The 2θ at 16° peaks could be classified as secondary peaks for amorphous regions. Whereas the 22° represents the crystalline area of the cellulose. The crystallinity index obtained from CNC-GNS was 74% which is far better than GNS (58%) and CPC-GNS (65%).

Moghaddam et al. (2024) studied the characteristics of fiber extracted from corn husks using XRD. The result shows that the extraction of fiber using the alkaline method leads to the removal of non-cellulosic materials, hence increasing crystallinity by 63% and 44% using treatments, Segal and curve method. However, the bleaching method had no significant impact on the improvement in the crystallinity of the extracted fibers. Bahndral et al. (2024) studied the results obtained from X-ray data on lemon grass cellulose samples. They observed that many of the ranges with high peak intensity had a high crystallinity index. These crystalline peaks were at 16.08°, 22.04° and 35.06° with planes of (101), (002) and (202) respectively. Their findings show that the higher the crystallinity index, the higher the purity and thermal stability of cellulose materials. The crystallinity index increase as crystalline size decreases and crystalline size of cellulose is dependent on chemical treatment. Chavez et al. (2023) study the effect of different concentrations of oxalic acid obtained as a nanofiber and the raw ichu sample. The diffractogram obtained shows that the two well defined peaks at 2θ between 15 and 16° and 22.0–22.5° which corresponds to the planes (110) and (002). It was observed that the higher the concentration of oxalic acid used, the higher the crystallinity index. The crystallinity index for raw ichu, 6% $(COOH)_2$, 8% $(COOH)_2$, 10% $(COOH)_2$ were 45.63%, 52.37, 52.97 and 56.89% respectively. They attributed the increase to the removal of hemicellulose and lignin through delignification in alkaline pretreatment, bleaching and acid treatment.

Hemida et al. (2023) accessed sample patterns for pulp Nile Rose fibers (NRFs), bleached NRFs, and hydrolyzed NRFs. They observed that the pulped NRFs had weak peaks which identified 2θ at 15° and 22°. While the bleached NRFs had broader defined peaks, indicating the removal of non-cellulosic material. The bleached samples that were hydrolyzed also had the same peaks with the appearance of a new peak of 2θ at 35°. The characteristics of these peaks were that of cellulose I corresponding to planes (101), (200) and (040). They attributed the alteration of crystalline structure to bleaching and acid hydrolysis treatment. Brahma and Ray (2024) investigated the effect of chemical treatment on jackfruit peel. They observed that the peak of cellulose structure of 2θ were 16.1°, 22.3°, and 34.3°. Their findings show that the crystallinity was lower than the cellulose value of 44%. This could be attributed to the presence of hemicellulose and lignin. Due to the presence of high amorphous region, H_3O^+ were observed to break down the β-1,4 -glycosidic connection with the cellulose chain, causing the individual crystallites to be released and increasing the crystallinity of cellulose, as indicated on Fig. 10.

4.5.5. FTIR spectroscopy

FTIR is a tool used to identify the functional groups and characteristics of the changes in chemical functional groups before and after extraction of NCC by comparing the spectrum with the relevant database. The FTIR characterization of CNCs particles aims to determine the functional group indicated by the infrared absorption number. These functional groups detect the presence of lignocellulosic compounds such as cellulose, hemicellulose and lignin extracted from CNCs particles, as a different wavelength indicates each lignocellulosic compound (Dungani et al., 2017; Sofla et al., 2016; Supian et al., 2020). For instance, the FTIR spectra of GNS chemically purified cellulose (CPC-GNS) and CNC-GNS (Bano and Negi, 2017) shows some of the adsorption peaks (1735 cm^{-1}, 1512 cm^{-1} and 1264 cm^{-1}) in the GNS particles were lost in the CPC-GNS and CNC-GNS. The loss of the adsorption peak indicates that the extraction of GNS leads to the removal of hemicellulose, lignin and other compounds. This also shows that the CPS-GNS particle synthesis process using NaOH can remove non cellulose compounds. Then the absorption peak of 3410 cm^{-1} on the CNC-GNS spectrum has a higher density, which proves that the non cellulose content in the CNCs-GNS particles has been removed (Van-Pham et al., 2020). Chamathka et al. (2024) studied the functional group present in PKM cellulose nanoparticles and the changes caused by various treatments using FTIR analysis. The treatment involved alkaline-treated raw PKM, bleached PKM and acid hydrolysis PKM cellulose nanoparticles. They observed that the peaks at 3421 cm^{-1} for all spectra corresponded to the O – H stretching which reflects the tendency to be hydrophilic. The alkaline substance reduces the hydrogen bonding within the hydroxyl groups and non-cellulose material. The peaks at 2896 cm^{-1} show that the spectrums correspond to C – H stretching. This indicated the disappearance of peaks of lignin and hemicellulose in PKM after alkaline and bleaching processes. Pratama et al. (2024) studied the effect of various chemical treatments on belulang grass using FTIR spectroscopy. Samples were initial grass fiber, spectra obtained after alkalization, bleaching and acid hydrolysis. They observed that the absorption band at 3300 cm^{-1} became sharper with each treatment compared to the initial grass. They attributed to the O–H stretching in the carboxyl group of the lignin. They also observed that the absorption band around 2860 cm^{-1} weakened and disappeared after alkalization and subsequent treatments. They associated this band with the stretching vibration of C–H groups in hemicellulose and noted that the disappearance indicated decreases in hemicellulose content. Further, they noticed that Belulang grass alkaline treated samples had a peak around 1740 cm^{-1}, corresponding to ketone, aldehyde or carboxylic acid groups in hemicellulose molecules. The intensity of the absorption band at 1440 cm^{-1} increased after bleaching and acid hydrolysis. This corresponds with the high crystallinity index. They concluded that various treatments, particularly alkalization and acid hydrolysis effectively reduced the content of hemicellulose and lignin and increased the crystallinity index of the fiber, as clearly seen in Fig. 11.

4.5.6. TGA

TGA is used to determine the thermal stability of CNCs. Trilokesh and Uppuluri (2019) conducted a study on CNCs extracted from jackfruit using TGA. In the result findings, there are 3 levels of thermal degradation observed in the form of mass loss. Stable conditions were obtained at 150 °C, cellulose thermal properties were observed at 312–350 °C and mass loss at 200–380 °C due to cellulose depolymerization. The mass loss was about 85% because of drying at a temperature of 300–350 °C. Zhao et al. (2015) conducted a comparative analysis on CNCs-RS and CNCs-PS. The TGA result shows that CNCs-PS has a higher peak than CNCs-RS while the CNC-PS has a higher degree of polymerization and hydrogen bonding energy, resulting in better thermal stability. Moghaddam et al. (2024) conducted a study on the effect of temperature on the weight of corn husk lignocellulose fibers using TG analysis. They observed that an increase in temperature led to a continuous decrease in the weight of the fibers. This weight loss was due to the decomposition of high volatile compounds below 160 °C and loss of moisture and the decomposition of cellulose, hemicellulose and lignin at about 200–400 °C. The result shows that during alkaline and bleaching, the percentage of

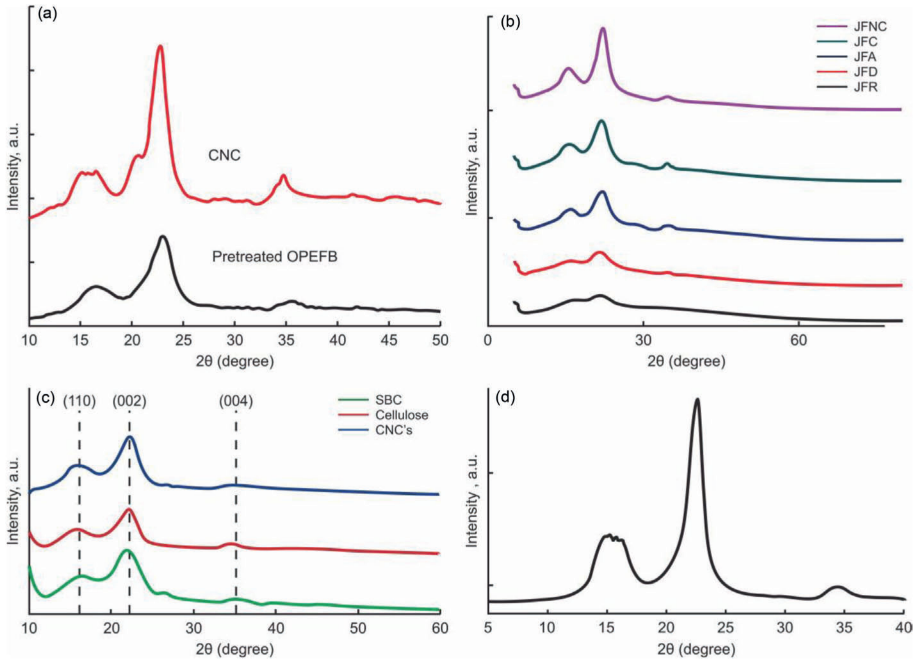

Fig. 10. XRD pattern for cellulose extraction at various stages (a) enzyme pretreated OPEB. (b) Jackfruit (c) sugarcane bagasse (SCB) (d) acacia bark (Evans et al., 2019; Rubiyah et al., 2023; Sikder et al., 2023; Taflick et al., 2017).

cellulose increases as that of hemicellulose and lignin were removed. This led to cellulose being more structured and regular and increases thermal stability. Hence, bleached fiber samples have higher thermal stability than other samples.

Taflick et al. (2017) studied the effect of residue on samples without Soxhlet Extraction (SE)-cellulose and With Soxhlet Extraction (WSE)-cellulose based on the results obtained from TGA data for thermal degradation. They observed that the T_{max} of SE-cellulose was the lowest compared to that of WSE. They attributed the increase of the degradation temperatures of WSE-cellulose to a higher mass of residue (9%), compared to SE-cellulose (4%). To the presence of some compound that extracted by solvent at the commencement of the process. on SE samples and WSE samples. Rubiyah et al. (2023) evaluated the heat stability of both untreated and chemically treated jackfruit peel via TGA. The fiber went through several stages of thermal degradation, weight loss initially at a temperature of 100 °C eliminating water. They observed the breakdown of the C–*O*–C glycosidic bond between the glucose unit of cellulose and depolymerization of the hemicellulose of jackfruit at 287 °C. They also observed that after alkaline treatment and bleaching, hemicellulose was eliminated. Degradation of cellulose is responsible for the peak at about 324–340 °C in all samples. The degradation of lignin was at a peak of 568 °C in the raw samples. From their findings, as indicated in Fig. 12, they concluded that the absence of a high-temperature peak suggests that lignin was removed throughout the subsequent chemical processes.

Kumari et al. (2023) studied the cellulose and CNC that were extracted from lemon via TGA to observe the degradation properties. They observed that each sample had an initial weight loss from 50 to 80 °C, as a result of evaporation of absorbed water. They observed that the thermal decomposition of cellulose onset occurred at 232.84 °C followed by a raid weight loss at 250 °C, which was attributed to hemicellulose degradation. Their results show that CNC was stable to temperature, which was a result of an increase in the crystallinity index. Debnath et al. (2023) investigated the effect of chemical treatment and heat on tea wastes and cellulose extracted from it. They observed that the thermal degradation of the sample resulted in an initial weight loss between 45 and 110 °C, which is due to the elimination of water present in cellulose. The primary decomposition occurred between 200 and 335 °C, which is attributed to the breakdown of cellulose and hemicellulose components. The decomposition of raw tea waste and Tea waste microcrystalline cellulose (TWMCC) started at 240 °C while delignified tea waste started to degrade at temperatures 220 °C and 234 °C, respectively.

4.5.7. DLS

DLS is a technique that can be used to conveniently determine the average size distribution of particles in a sample. This technique is based on the light scattered by diffusing particles. DLS incorporates Rayleigh scattered light and Doppler broadening resulting from the particle Brownian motion or translational diffusion. Similarly, some DLS measurements can also provide zeta potential data for cellulose nanocrystal dispersion in the presence of an electrical potential. DLS technique assists in obtaining size information of particles within a few minutes with diameter running from few nanoscales in measurement to 5um. Very essential to be applied on CNC for size verification while assisting in determining the occurrence of agglomeration between CNCs particles. Foo et al. (2019) studied the effect of size distribution of particle and zeta potential on CNC synthesized from EFB. They recorded an average distribution size of 75 nm and a zeta potential value of less than - 10 mV. Through surface modification with tannic acid and decylamine, they were able to successfully increase the zeta potential value to CNC extracted from EFB to around −65mV.

Similarly, Al-Dulaimi and Wanrosli (2017) successfully increased the zeta potential from −36.2 mV to −69.8 mV by increasing the reaction time from 40 min to 100 min during acid hydrolysis using H_2SO_4 at 58% and 45°C. Ogunjobi et al. (2023) studied the size distribution of particles and zeta potential on CNCs extracted from Siam weeds. They reported that the hydrodynamic diameter average size of 213 nm while the nanocellulose

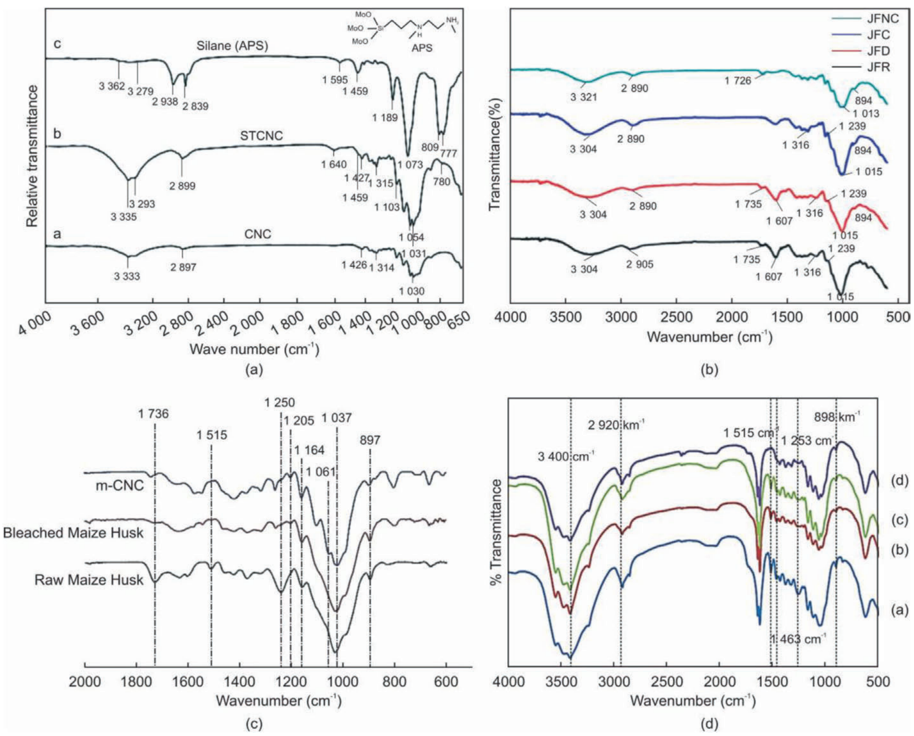

Fig. 11. FTIR spectra of alkaline treatment, bleaching and hydrolysis for (a) OPEFB. (b) Jackfruit peel (c) Corn husk (d) Sugarcane bagasse (SCB), steam exploded SCB with xylanase treated and bleached fiber (Ng et al., 2021; Rubiyah et al., 2023; Smyth et al., 2017; Yee et al., 2024).

had an overall negatively charged with a zeta potential of −9.57 mV. Nang Vu et al. (2024) evaluated the effect of size distribution from CNCs extracted from sugarcane bagasse using formic/peroxy formic acid. They show a hydrodynamic distribution size of about 300.1 nm. Their DLS analysis revealed a sharp profile distribution, indicating uniformity in particle size. Similarly, Pandi et al. (2021) recorded an average hydrodynamic size of CNC of 221 nm from CNC that was synthesized from cotton via ultrasound-assisted acid hydrolysis. Midhun Dominic et al. (2022) synthesized CNFs from millet husk waste via chlorine-free extraction. They observed that the hydrodynamic size of the nanofiber obtained from DLS analysis exhibited an average size of 51.1 nm. Even though DLS analysis may not be accurate for fibrils and rodlike molecules, it can give a nanoscale dimension for fiber preparation. This goes a long way to show the importance of DLS analysis in verifying the surface modification.

Zeta Potential gets an insight into the physical stability of nanosuspensions by estimating the surface charge of nanocrystals. The stability of synthesized cellulose nanocrystals can be determined by measuring the zeta potential of charged particles. CNCs with significant positive and negative zeta potential have adequate intra-molecular repulsion to improve colloidal stability. However, a low zeta potential value might lead to particle flocculation and aggregation because of the van der Waals force of attraction between them (Singh et al., 2023). It helps determine the electrostatic charge on CNCs that they carry during synthesis and causes repulsion between charged particles. Consequently, these repulsive forces help keep distance, resist the combination, and make them more stable in suspension (Samsudin et al., 2020). Naseem et al. (2024) studied the effect of zeta potential on cellulose nanocrystals extracted from Hamelia patens leftover via hydrolysis of microwave-assisted ionic liquid technique. They observed the presence of sulfate ions in acid hydrolysis treatment while ionic liquid hydrolysis (ILH) had the presence of acetate ions leading to the development of a net negative charge on CNC particles. The CNC-ILH had a higher zeta potential value (−35 mV) than CNC-ILH (−30 mV), which makes it more stable due to more repulsion. Their findings show that the suspension of CNC-ILH remains stable after 48 h due to the repulsive force existing between charged particles, while CNC-acid hydrolysis had some sedimented particles due to agglomeration (Wang et al., 2020c).

Ogunjobi et al. (2023) study on DLS revealed that the nanocellulose prepared are uniformly distributed spherically shaped nanocrystals with an average hydrodynamic size of 213 nm and are negatively charged at −9.57 mV. Meda et al. (2022) reported that CNCs was extracted from non-wood, such as Lagenaria siceraria peels, a food-industry waste. They observed the development of charge on the surface of CNC, which was because of sulfate group (-*O*–SO_3–) from acid hydrolysis inducing the particle with a negative electrostatic layer. Their result shows that the zeta potential value of *Lagenaria siceraria* cellulose nanocrystals bottle guord (CNC-BG) was −28.77 mV with an average hydrodynamic diameter of 228.7 nm. They concluded that the repulsive electrostatic force was the most dominant, implying less aggregation of crystals with high entropy and suspension stability. Nang Vu et al. (2024) investigated the effect of various treatments on CNC extracted from sugarcane bagasse. As indicated in Fig. 13, the finding shows that the zeta potential of the CNCs suspension was −62.6 mV. The negative charge was due to the addition of sulfate groups to the surface of the CNCs during H_2SO_4 hydrolysis. Wang et al. (2024b) reportedly studied the effect of stability of CNC extracted from tea residues. They observed that the negative charge on the surface was caused by the fact that during acid hydrolysis, a small part of sulfate groups is attached to the cellulose surface and undergoes esterification with the hydroxyl groups, resulting in residual sulfate groups in the black tea cellulose

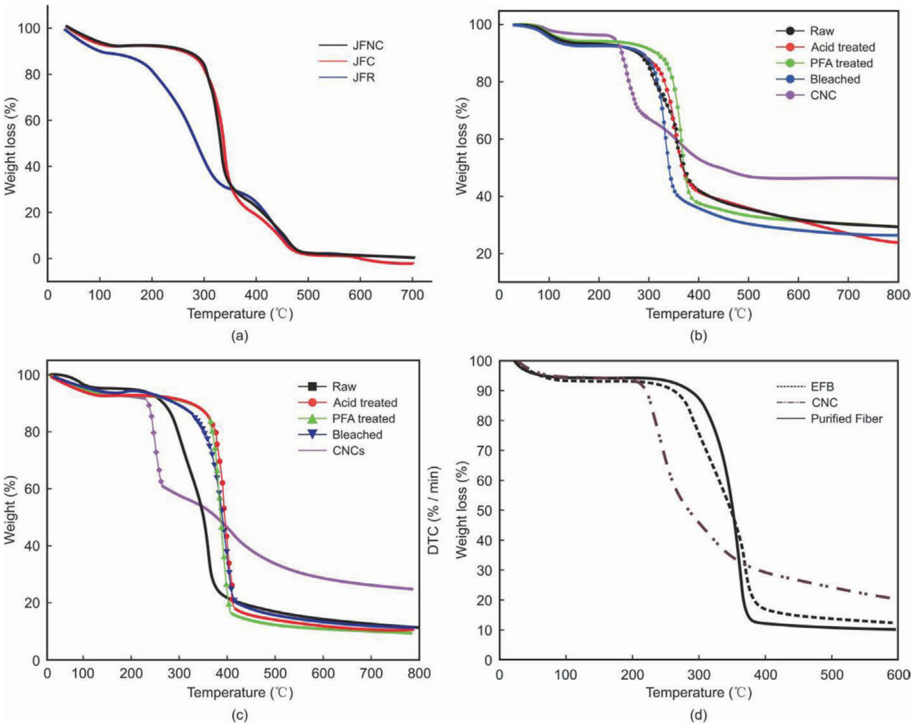

Fig. 12. Thermogravimetric analysis curves at various stages of extraction (a) jackfruit, (b) sugarcane bagasse, (c) rice husk (SGB), (d) empty fruit bunch (EFB) (Moghaddam et al., 2024; Ng et al., 2021; Rubiyah et al., 2023; Nang Vu et al., 2024).

nanocrystals (BT-CNCs). Their result shows that the average zeta potential value of BT-CNC was 31.0 mV. Lima et al. (2023) did a comparative analysis on acid treatment and enzymatic treatment to study the effect of isolation of cellulose nanofiber from *Salicornia ramosissima*, an agro-industrial. They recorded a zeta potential −42.5 mV for CNF (acid treatment) and 52.2 mV for CNF (enzymatic treatment). They observed that both nanofibers had a negative charge. They attributed the higher negative charges of CNF(ET) to good electrical stability.

5. EOR mechanisms of cellulose bionanomaterials

Cellulose nanomaterials have garnered attention and are promising in multidisciplinary fields ranging from drug delivery to applied as environment remediators and EOR due to their green properties (Arif et al., 2024; Jing et al., 2024; Keshu et al., 2021; Khan et al., 2024; Selvaraj et al., 2024; Shahzad et al., 2023; Wang et al., 2022). However, the EOR mechanisms of cellulose nanomaterials include IFT reduction, wettability alteration, viscosity reduction, sweep efficiency, asphaltene precipitation, emulsion formation and stability.

5.1. IFT reduction

The phenomenon of IFT results from the energy differential between water molecules and oil at the fluid interface. IFT quantifies the energy necessary to create a unit area between two immiscible fluids, expressed in Joules per square meter or Newton per meter (Berry et al., 2015). The reduction of IFT plays a crucial role in enhancing oil recovery, as it deforms the trapped oil droplets, facilitating their movement through pore throats and promoting the formation of in-situ emulsions that mobilize and transport oil (Sheng et al., 2015). Several studies have examined the impact of nanoparticle concentration and external conditions like salinity and temperature on IFT. Fig. 14a illustrates a clear trend where IFT decreases as the concentration of CNF increases. This finding aligns with existing research demonstrating that higher nanoparticle concentrations generally result in greater IFT reduction (Nowrouzi et al., 2022). The IFT reduction trend observed with CNPs at an optimal concentration of 0.1 wt% further supports the hypothesis that IFT reduction can be optimized by controlling nanoparticles concentration. However, while the benefits of IFT reduction are widely acknowledged, the extent of the effect of nanoparticles remains controversial. Some studies argue that nanoparticles exert little or no influence on IFT reduction, instead simply interacting with water molecules and oil without impacting the interface (Biswal et al., 2016). In contrast, others report substantial IFT changes when nanoparticles are introduced (Agi et al., 2020a; Gbadamosi et al., 2019; Ngouangna et al., 2020; Pereira et al., 2020). This contradiction suggests a gap in understanding the exact mechanisms by which NPs interact with the contact between water and oil. The addition of CNPs has effectively reduced the IFT between oil and water, acting similarly to natural emulsifiers at the oil-water interface. This reduction in IFT is attributed to the molecular interactions at the interface where CNP adsorbs, lowering the energy barrier. Several studies have demonstrated this phenomenon, with notable effects observed at low concentrations of CNPs (0.1–0.5%), where a significant reduction in IFT occurs. As the concentration increases, the reduction continues but diminishing returns are often observed at higher concentrations. For instance, Hu et al. (2022) reported that IFT decreases linearly with increasing CNC concentration up to a certain level, after which the reduction rate slows. Numerous studies have corroborated these findings; for example, Tiong et al. (2020) observed that at 500 ppm of CNC, the IFT dropped to 16.3 mN/m, while Agi et al. (2019a) demonstrated a concentration-dependent decrease in IFT for CNCs between 0.05 and 0.2 wt% w/v, in agreement with previous studies. Fig. 15a illustrates the effect of

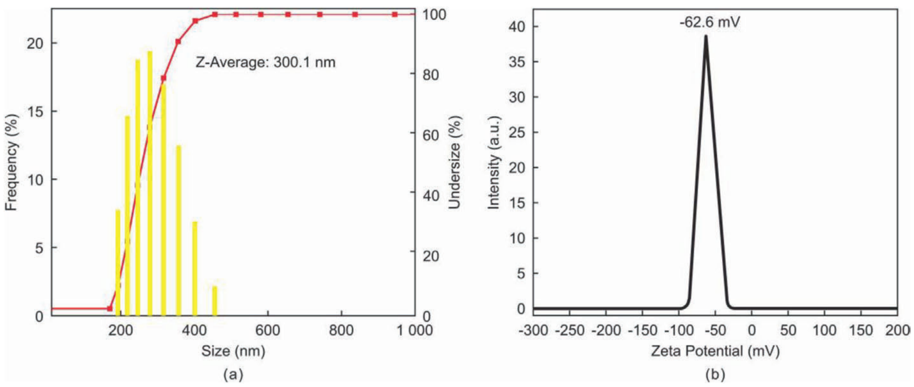

Fig. 13. Hydrodynamic size analysis (a) of CNCs by DLS and zeta potential (b) of CNCs (Nang Vu et al., 2024).

IFT on CNC with time. This shows that the IFT decreases as time increases, leading to more oil recovery over time. The application of CNFs has similarly demonstrated a 20% increase in oil recovery, attributed to the formation of an oil bank. This increase in recovery is ascribed to CNF's effective reduction of IFT, as shown in Fig. 15b. Furthermore, CNFs have demonstrated stability at high temperatures (up to 120 °C), which makes them suitable for usage in reservoirs with high temperatures (Aadland et al., 2019).

5.2. Wettability alteration

Wettability, the tendency of a fluid to adhere to a solid surface in the presence of two immiscible liquids, plays a critical role in oil recovery due to its impact on capillary pressure and relative permeability. Reducing capillary forces and improving oil mobility can greatly enhance oil recovery by altering the wettability of reservoir rocks from oil-wet to water-wet conditions. The high surface area, high surface energy, and unrestricted mobility of nanoparticles within rock pore spaces have made them promising wettability modifiers (Sun et al., 2023; Yao et al., 2021). Various studies have investigated the mechanisms by which nanoparticles alter wettability, as well as their synergistic effects when used with traditional wetting agents such as foams, alkaline solutions, surfactants, and polymers. The ability of nanoparticles to alter wettability hinges on their capacity to adsorb onto the rock surface and influence interactions between ions and the solid matrix. As nanoparticles are introduced into the reservoir, they modify the wettability by forming a layer on the rock surface, shifting it from oil-wet to neutral or water-wet conditions. This adsorption process, combined with the creation of a pressure gradient, has been identified as one of the prime mechanisms for wettability alteration (Druetta and Picchioni, 2019; Natalya et al., 2022). The formation of emulsions by CNPs also aids in altering wettability, further promoting oil displacement and recovery. The application of CNCs or CNPs in EOR has drawn a lot of interest because of their capacity to alter the wettability of rocks found in reservoirs, improving oil recovery rates. CNPs have demonstrated the potential to shift the wettability of reservoir surfaces from oil-wet to water-wet conditions, which is crucial for better displacement of trapped oil. Numerous studies have confirmed that nanoparticles can notably reduce the contact angle, indicating a transition toward a more water-wet state, thus improving oil recovery (Al-Asadi et al., 2022; Ngouangna et al., 2022). The contact angle, a measure of wettability, plays a critical role in oil recovery within porous media. According to Aadland et al. (2020), a lower contact angle reflects a more water-wet condition, facilitating improved oil displacement. Fig. 16 illustrates the effect of wettability alteration on the porous media. With an increase in CNC concentration, the contact angle decreases, changing the wettability of the rock, from an oil-wet to a water-wet state. Furthermore, the concentration of CNPs has a significant impact on the contact angle; higher concentrations lead to a decrease in the contact angle, subsequently improving oil recovery. Wang et al. (2023a) found that the contact angle decreased when the concentration of CNPs was increased from 20 mg/L to 100 mg/, which corresponded with an enhancement in oil recovery from 4.53% to 15.26%. However, the results of Tiong et al. (2020) suggest that CNCs were unsuccessful in altering the wettability of Edwards White rock samples, as shown by the high oil-wet contact angle of 155°, as indicated in Fig. 17. Conversely, Li et al. (2017) observed a significant decrease in contact angle from 127° to 62° when using a modified nanocellulose (SF–CNC) in combination with the surfactant APG1214, indicating a shift in the rock's wettability towards water-wet. Similarly, Li et al. (2016) synthesized nanocellulose grafted with 2-acrylamido-2-methylpropane sulfonic acid (AMPS) and hydrophobic groups, demonstrating superior salt tolerance and salt-thickening properties, which were attributed to the incorporation of hydrophobic groups. These findings underline the promising role of CNCs in EOR applications, especially in enhancing rock wettability.

5.3. Sweep efficiency improvement

A key component of EOR, sweep efficiency, is heavily impacted by the mobility ratio (M), which contrasts the movement of the displaced fluid (oil) with that of the displacing fluid (such as CNCs). In terms of mathematics, the mobility ratio is represented as follows:

$$\text{Mobility ratio} = \frac{\lambda_n}{\lambda o} = \frac{K_{rn}/\mu_n}{K_{ro}/\mu_o} \tag{1}$$

Where λ, K and μ, are mobility ratio, relative permeability and viscosity, respectively. The subscript ‘n’ stands for displacing fluid, CNCs and ‘o’ stands for displaced fluid, oil. When M is more than 1, it means that the displacement of the fluid is greater than that of the displaced fluid, oil. This causes early water breakthroughs because of viscous fingering, which leads to poor oil recovery. To avoid viscous fingering phenomena, the mobility ratio, *M* must be less than or equal to 1 ($M \leq 1$) as illustrated in Fig. 18. One way this

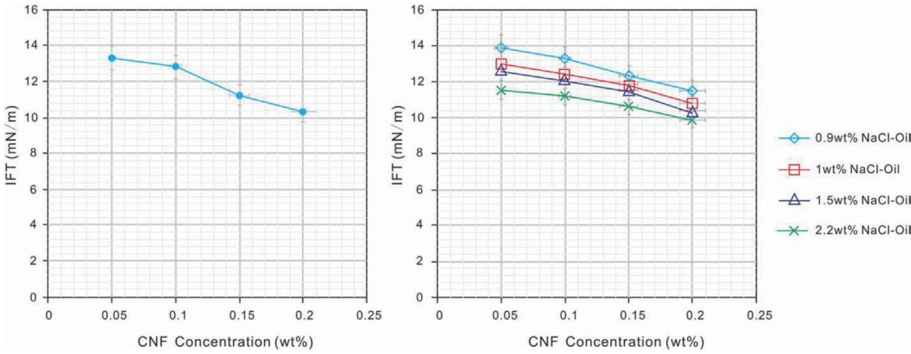

Fig. 14. (a) Effect of CNF concentration on IFT (b) Effect of 0.9, 1, 1.5, 2.2 wt% NaCl concentration on IFT (Agi et al., 2019a).

can be favorable is by improving the displacing fluid's rheology (that is, increasing viscosity). Increasing water mobility causes viscous fingering in the case of a higher mobility ratio (Omidi et al., 2020). CNPs have proven to be effective additives in EOR due to their distinctive characteristics, such as increased surface area and the ability to modify fluid rheology. The integration of CNPs into polymer systems has been shown to significantly impact the mobility ratio, an essential factor in the efficiency of oil displacement (Wang et al., 2023b). Fig. 19 illustrates the effect of good sweep efficiency as a result of a mobility ratio less than or equal to 1. CNPs decrease the mobility ratio by increasing the viscosity of the displacing fluid, bringing it to a level just below unity, which is highly favorable for effective oil displacement. This favorable mobility ratio contributes to greater volumetric sweep efficiency, as demonstrated by Aadland et al. (2020), who investigated the effects of CNPs on mobility ratio and observed that CNPs effectively achieved a favorable mobility ratio, leading to improved oil recovery outcomes.

5.4. Emulsion formation and stability

Emulsions are a proven method for increasing the viscosity of the injected fluid, promoting pore blockage, and rerouting fluid flow toward bypassed areas in EOR. This process aids in oil intrusion into the moving fluid, ultimately leading to improved oil recovery rates (Kumar et al., 2020). The formation of stable emulsions is a key factor in this process. Amphiphilic emulsifiers that are strongly absorbed at the oil-water interface reduce the IFT between the two phases and produce stable emulsions. Droplet coalescence and phase separation are resisted by the protective layer that is formed around the emulsion droplets as a result of this adsorption. Common emulsifiers used in EOR include various surfactants (Kumar et al., 2020; Massarweh and Abushaikha, 2020; Umar et al., 2018). A crucial factor in the stability of emulsions is the role of nanofluids, whose stability is influenced by the type and concentration of salts present in the solution. CNPs have been widely recognized for their ability to stabilize emulsions at the water-oil interface by maintaining a stable dispersion of oil droplets in water, which contributes to a reduction in IFT and, ultimately, the mobility of oil within reservoirs (Ledyastuti et al., 2021; Manikumar et al., 2024). These emulsions, stabilized by CNPs, are particularly resistant to coalescence, a crucial factor in enhancing their stability over time, as seen in Fig. 16. Functionalized CNFs have been reported to perform better in stabilizing emulsions compared to non-functionalized variants, as the latter are often more hydrophobic and less effective in preventing coalescence.

The surface charge of CNPs also plays a significant function in the stability of emulsions. Ojala et al. (2018) reported that a lower surface charge density enhances the packing of particles at the oil-water interface, leading to improved emulsion stability. This effect is seen in their study, where both CNCs and CNFs were employed to stabilize emulsions of oil and water, after pre-treatment with a DES, as seen in Fig. 20. The results showed a substantial reduction in oil droplet size, from 22.5 μm to 8.9 μm, indicating the effectiveness of CNCs and CNFs in stabilizing emulsions by reducing droplet coalescence and ensuring a more uniform dispersion. This underscores the potential of CNPs, particularly when functionalized or pre-treated, to improve the stability and performance of emulsions in various applications. Functionalized CNFs are reported to enhance emulsion stability because of their modified surface properties, which improve interaction with the oil-water interface, whereas non-functionalized CNFs, being more hydrophobic, are less effective and often lead to coalescence. This

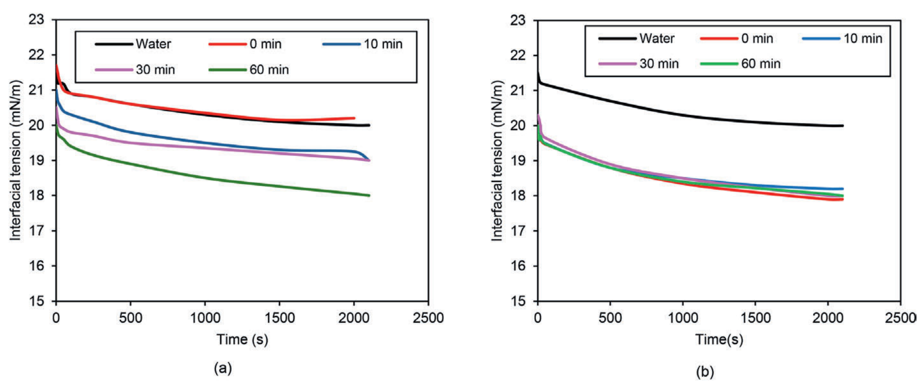

Fig. 15. The effect of IFT over concentration and time duration on (a) CNC and (s (Ni et al., 2021).

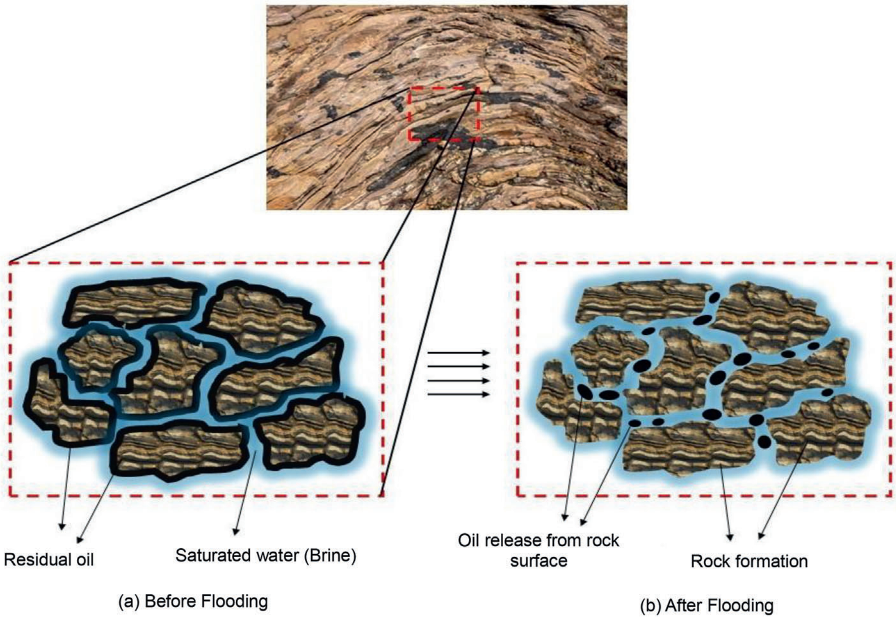

Fig. 16. (a) Water flooding, residual oil is entrapped in the reservoir (b) cellulose nanofluid flooding, oil initially trapped is released from the reservoir rocks (Salem et al., 2024).

highlights a key finding that surface modification is critical in the performance of CNPs as stabilizing agents. Additionally, the versatility of CNPs is demonstrated in functional emulsions, such as curcumin emulsions, where CNPs not only stabilize the emulsion but also provide beneficial properties like high encapsulation efficiency and antioxidant activity.

5.5. Viscosity improvement and control

CNPs have demonstrated significant potential in enhancing the viscosity of injected fluids, particularly in EOR applications, by improving the sweep efficiency of fluids in porous media (Aadland et al., 2019; Agi et al., 2019a). One of the key characteristics of CNP dispersions is their shear-thinning behavior, where viscosity decreases with an increase in shear rate, which allows the fluid to adapt to varying flow conditions. This increase in viscosity is attributed to the interaction between CNPs and the fluid matrix, wherein the unique properties of CNPs enhance overall fluid performance. Studies have shown that aqueous CNC dispersions can experience substantial viscosity increases when subjected to temperatures above 90 °C. For example, Molnes et al. (2017) reported a significant increase in the viscosity of Cellulose nanocrystals in low-salinity brine (CNC-LS) solutions during long-term temperature aging. However, contradictory results were observed in a subsequent study by Ojala et al. (2018), where no increase in viscosity was noted for CNC-LS effluent, highlighting the variability in CNP behavior under different conditions. Earlier research on CNC-LS permeability in core samples typically showed reductions in permeability, attributed to CNC particle entrapment within porous media. More recent work indicated an increase in permeability at 90 °C, likely due to the degradation of residual CNC particles trapped in porous media as a result of prolonged high-temperature exposure, altering the CNC surface chemistry. Concentration and salinity also play pivotal roles in influencing the viciousness of CNP dispersions. A sharp increase in viscosity was observed when CNC dispersions reached a critical concentration of 6000 ppm, marking the transition from biphasic to liquid crystalline regimes, where CNC rods become restricted in their ability to flow freely. Bashir Wani et al. (2020) studied the effects of salinity on CNC dispersions and found that even at low salinity levels, significant agglomeration of CNC particles occurred, causing a dramatic rise in viscosity from 1.70 cP at a shear rate of 11.2 s^{-1} to 11 cP at a salinity of 5 g/L. Additionally, CNCs improve the viscosity and viscoelastic properties of aqueous media due to electrostatic interactions between their whisker structures, which facilitates a better mobility ratio during EOR. Similar to CNC, Agi et al. (2019a) found that the apparent viscosity of CNF solutions shows shear-thinning behavior, which is a feature of pseudoplastic fluids, decreasing with increasing shear rate. At 25 °C, the apparent viscosity varied with shear rate across different concentrations (Fig. 21a). Higher CNF concentrations corresponded to increased apparent viscosity. In region I, viscosity steadily

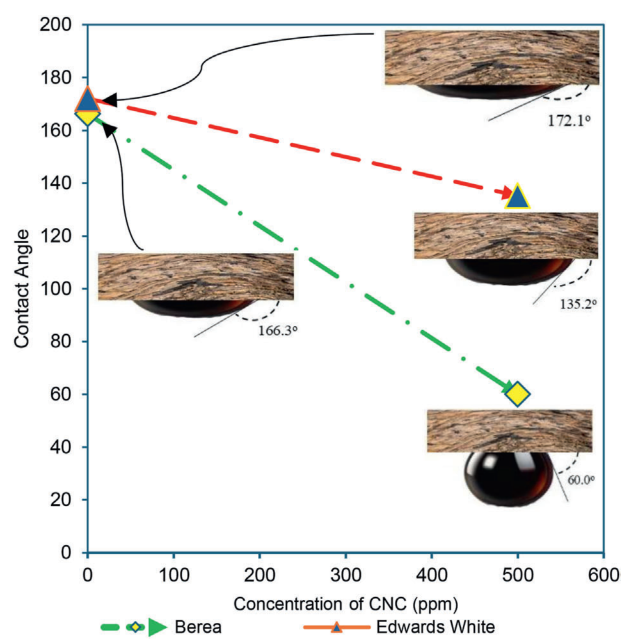

Fig. 17. Contact angle for Berea sandstones and Edward white sandstones as wettability turns towards water-wet conditions (Tiong et al., 2020).

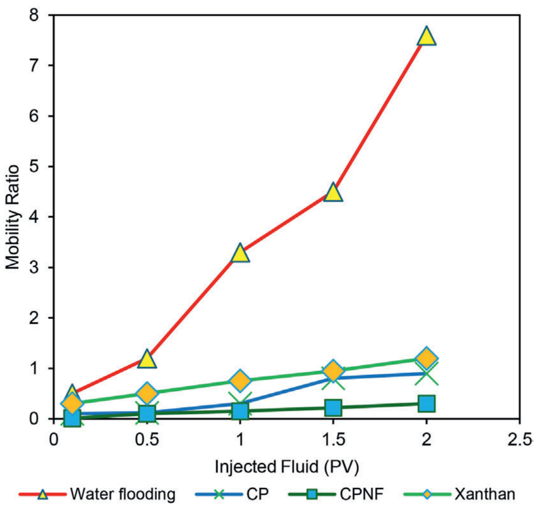

Fig. 18. (a) Mobility ratio of injected fluids (water flooding, CP, CPNF, Xanthan) increases as the pore volume increases (Agi et al., 2020a).

decreased as the shear rate increased, attributed to CNP alignment. A similar trend was observed in region II, where the gradual drop in viscosity resulted from the breakdown of the entangled network at intermediate shear rates. In region III, a plateau formed, with a slight decrease in viscosity due to further disruption of the entangled network at high shear rates, leading to a well-oriented structure (Fig. 21a).

This behavior was further supported by Moon et al. (2011), who attributed the decrease in viscosity at high shear rates to particle alignment that reduces flow resistance. Qiao et al. (2016) also noted that increased NaCl concentration weakens CNC interactions by shielding electrostatic repulsion. In contrast, Agoda-Tandjawa et al. (2010) found that the removal of hemicellulose and lignin from okra-derived CNF resulted in higher viscosity due to strong hydration interactions. Moreover, Raza and Gates (2021) emphasized the environmental benefits of CNPs, highlighting their biodegradability and sustainability as alternatives to synthetic nanoparticles commonly used in EOR processes.

Similarly, Agi et al. (2019a) compared the apparent viscosity of CNF at varying salinity (0.9–2.2%) with that of okra and xanthan at the same concentration (0.2%), as shown in Fig. 21b. They observed a decrease in apparent viscosity for all three samples with increasing salt concentration. The flow behavior of CNF and okra, both anionic polyelectrolytes, was attributed to intra-molecular electrostatic repulsion in water. Salt addition screened this repulsion, causing the polymer coils to contract into compact conformations, leading to reduced viscosity.

Molnes et al. (2017) reported that CNC-LS solutions experience significant viscosity increase during long-term temperature aging, a result supported by the broader understanding that CNPs react to thermal stress by forming stronger networks in the fluid matrix. However, this trend is contradicted by Molnes' later findings Molnes et al. (2018), where no viscosity increase was observed in CNC-LS effluent under similar conditions. This contradiction raises questions about the consistency of CNP behavior in different environments and underscores the complexity of CNP-fluid interactions, which may be influenced by aging conditions, degradation, or surface chemistry changes at high temperatures.

The relationship between concentration and viscosity is not uniform across all conditions. For example, Bashir Wani et al. (2020) observed that salinity significantly impacts CNC behavior, with even low salinity levels (5 g/L) causing particle agglomeration and sharp viscosity increases. While these findings align with general observations of CNPs increasing internal fluid viscosity, they also point to the sensitivity of CNPs to ionic conditions, as Qiao et al. (2016) found that higher NaCl concentrations shield electrostatic repulsion between CNC particles, weakening their interactions and reducing suspension stability. Despite these consistencies, contradictions arise regarding the role of surface functionalization and electrostatic interactions. Molnes et al. (2017) suggested that CNC whiskers improve viscosity through electrostatic interactions, whereas Agoda-Tandjawa et al. (2010) emphasized that removing hemicellulose and lignin from okra-derived CNF increases viscosity due to strong hydration interactions rather than electrostatic forces. This discrepancy points to understanding how surface modifications impact viscosity, depending on the source and synthesis methods of the nanoparticles. Furthermore, the findings from Raza and Gates (2021) highlight the environmental benefits of CNPs in EOR, noting their biodegradability and sustainability as a key advantage over synthetic alternatives. This focus on sustainability is an emerging trend in literature, positioning CNPs as a potential solution to the environmental concerns associated with conventional EOR materials.

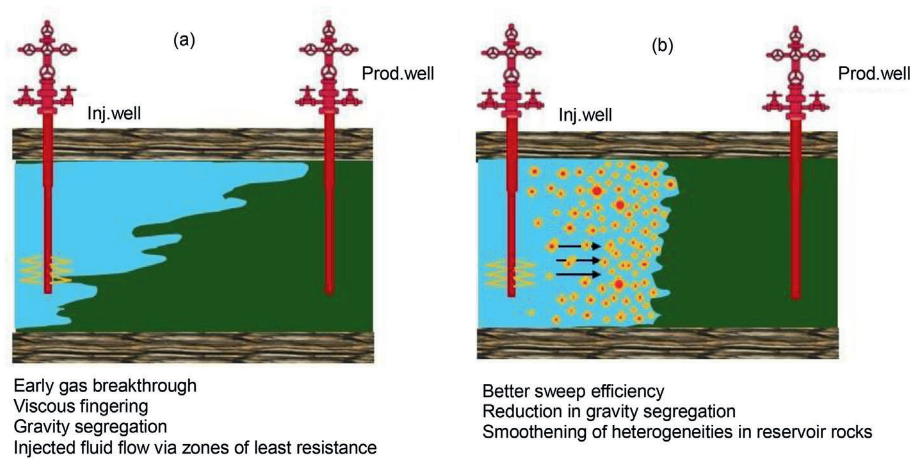

Fig. 19. (a) Early breakthrough due to Mobility ratio, M being >1, (b) addition of CNP increases the viscosity of the displacement, gives better sweep and increases oil recovery (Putra and Temizel, 2018; Zeynalli et al., 2023).

5.6. Asphaltene precipitation

The largest molecular weight component of crude oil is known as asphaltenes. Their fractions are insoluble in pentane and heptane and contribute directly to the viscosity of crude oil. Hence, one of the effective ways to reduce oil viscosity is by removing the heavier component of crude oil (asphaltenes) (Zuo et al., 2019). The more asphaltenes are removed from heavy oil, the greater the viscosity reduction. Natural emulsifiers such as asphaltenes in oil reservoirs are anticipated to have a crucial role in the production of crude oil emulsion. Asphaltene precipitation and deposition can be reduced through nanofluid flooding by the adsorption of the molecules. Nanoparticles operate as inhibitors preventing the precipitation of asphaltenes by encircling and degrading asphaltenes molecules, lowering viscosity, and inhibiting deposition. Numerous research has been conducted to demonstrate that surface modification can improve the adsorption capacities of nanoparticles. As pressure increases, the extent of the asphaltenes precipitation increases up to the saturation pressure and then decreases upon further increases in pressure beyond the saturation pressure. Increasing nanoparticles concentration results in decreasing asphaltene precipitation.

The use of CNPs as inhibitors has emerged as a promising approach for mitigating asphaltene precipitation, a challenge in the petroleum industry. Asphaltenes are complex molecules prone to self-aggregation due to acid-base interactions and hydrogen bonding. CNPs possess distinctive properties that enhance their ability to prevent asphaltene precipitation. According to Zhang et al. (2024c), CNPs can form hydrogen bonds with asphaltene molecules, keeping them suspended within the crude oil. This interaction helps maintain the stability of asphaltenes in a dispersed state, preventing the formation of large aggregates. The presence of CNPs contributes to smaller particle sizes of asphaltene aggregates, improving their overall dispersion within the crude oil system (Yang et al., 2024).

Furthermore, several studies highlight the role of CNCs in mitigating asphaltene precipitation through an adsorption mechanism. CNCs have been found to adsorb asphaltene molecules, thereby reducing their tendency to flocculate and precipitate. This adsorption process limits the aggregation of asphaltenes, improving the stability of crude oil by preventing the formation of large deposits (Aadland et al., 2019). The adsorption mechanism exhibited by CNCs offers a promising avenue for controlling asphaltene behavior, underscoring their potential as effective inhibitors in the petroleum industry. Fig. 22 illustrates the effect of CNCs on asphaltene precipitation, as the CNCs assist in lowering the viscosity of the heavy oil and reduce the aggravation of asphaltenes to smaller sizes, hence recovery-improving oil. In addition to improving sweep efficiency, nanoparticles play a key role in reducing heavy oil viscosity. Heavy oils contain high concentrations of asphaltenes, complex molecules that contribute to the oil's high viscosity by forming viscoelastic networks. Asphaltene precipitation and deposition during oil recovery present challenges such as pore plugging, reduced permeability, and altered rock wettability, all of which hinder oil recovery (Fakher et al., 2019; Shen and Sheng, 2018).

6. Application of cellulose bionanomaterials in EOR

Cellulose nanomaterials have gained attention for their availability, biodegradability, high crystallinity, elastic modulus, and nanoscale dimensions, making them suitable for oil and gas applications (Agi et al., 2020a, 2021). Cellulose nanomaterials, particularly CNCs, show promise in EOR as flooding agents in water-based nanofluid techniques (Ali et al., 2020; Mariyate and Bera, 2023). Their unique properties, including IFT reduction, high surface area, and viscosity modification, enhance oil displacement efficiency, positioning them as effective tools for EOR. Several studies show that CNPs can enhance fluid flow behavior in porous media, resulting in an increase in oil recovery, as seen in Table 6. For example, Abdullah et al. (2019) demonstrated the high effectiveness of CNC nanofluids for displacing crude oil in a Hele-Shaw cell, achieving an impressive sweep efficiency of up to 98% with a 2 wt% concentration. This remarkable efficiency is attributed to the formation of stable interfaces by CNCs, which penetrate the oil phase and generate microemulsions that reduce IFT between the water and oil phases. The improved mobility of the oil phase, aided by the high viscosity of CNC nanofluids, underscores the potential of cellulose nanomaterials to improve oil recovery processes by leveraging their unique structural and functional properties (Li et al., 2021). The viscosity characteristics of CNC nanofluids play a pivotal role in addressing challenges such as viscous fingering and flow diversion within reservoirs, enhancing sweep efficiency in oil recovery (Aadland et al., 2019). It has been observed that the aging time and temperature of CNC nanofluids significantly increase their viscosity, which is advantageous for reservoir engineering applications.

Additionally, CNCs have demonstrated effectiveness in high-salinity, high-temperature reservoir conditions (Durán-Valencia et al., 2014). Aadland et al. (2020) reported a 3–17% increase in oil recovery over water flooding when using surface-functionalized CNFs, noting that grafting hydrophilic and hydrophobic groups improved both interfacial activity and salt tolerance. They attributed the improved oil recovery to wettability alteration, dragging, and emulsification mechanisms. Valencia et al. (2022) reported that CNCs perform well in high-salinity, high-temperature reservoirs. This suggests that while CNPs have a promising role in EOR, their effectiveness may depend heavily on surface modifications and the specific conditions of the reservoir. Similarly, Aadland et al. (2019) observed incremental oil recovery

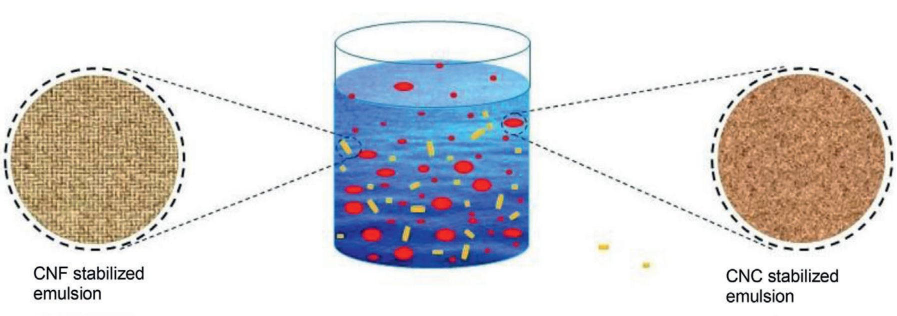

Fig. 20. CNC helps in stabilization of emulsion during oil recovery (Mikulcová et al., 2023).

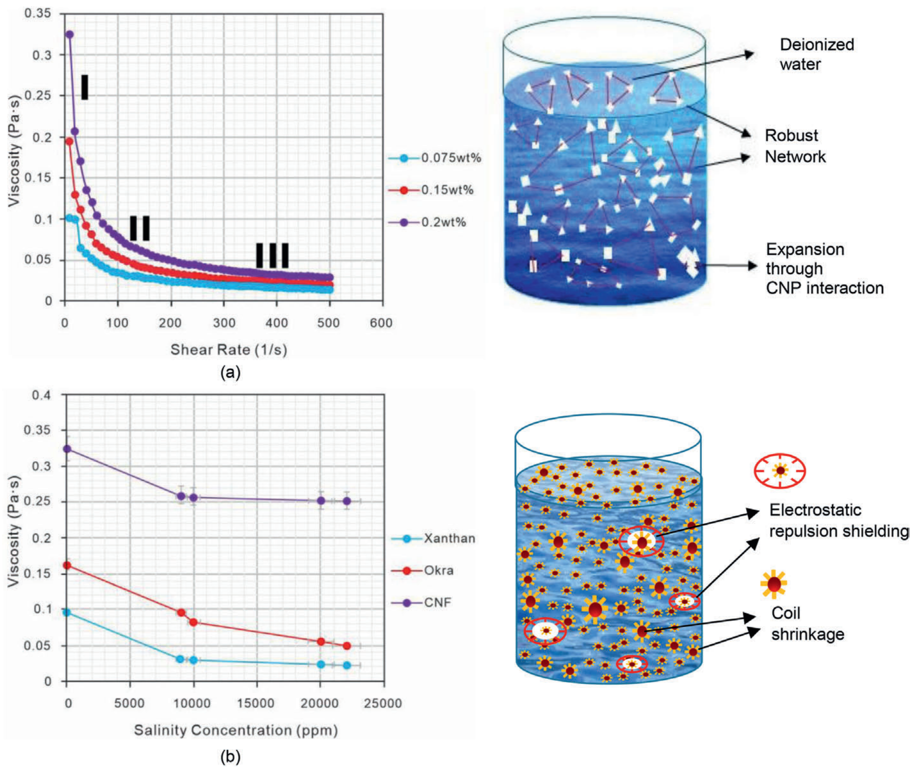

Fig. 21. (a) Effect of Viscosity on shear force (b) Effect of Viscosity on salinity (Agi et al., 2019a).

following the introduction of CNC after initial water flooding, further affirming CNC's efficiency as an EOR agent. Additionally, their study indicated that CNCs act as viscous liquids during core flooding, contributing to favorable mobility ratios during oil recovery. Molnes et al. (2017) explored the injectivity of CNC into highly permeable sandstone cores, finding that CNC demonstrated excellent injectivity at all concentrations tested. This was attributed to the small particle size and good colloidal stability of CNC in low-salinity conditions, which allowed the particles to travel through the sandstone core with minimal obstruction. Li et al. (2017) supported these findings, reporting a 6% incremental oil recovery using CNC dispersion in a visual micromodel experiment. They attributed the enhanced recovery to in-situ emulsification and the viscoelastic properties of CNC, which facilitated oil displacement.

Similarly, Agi et al. (2019c) observed that IFT decreased as the concentration and temperature of CNF increased, resulting in a 20% increase in oil recovery. They attributed this behavior to the shear-thinning and pseudoplastic nature of CNF, which improved oil mobilization in high-temperature, high-pressure reservoirs. Similarly, Tiong et al. (2023) observed significant oil recovery in Berea sandstone and Edwards White formations after the injection of CNC dispersions, with 18.62% and 9.8% additional recovery, respectively, as illustrated in Fig. 23a and b respectively. However,

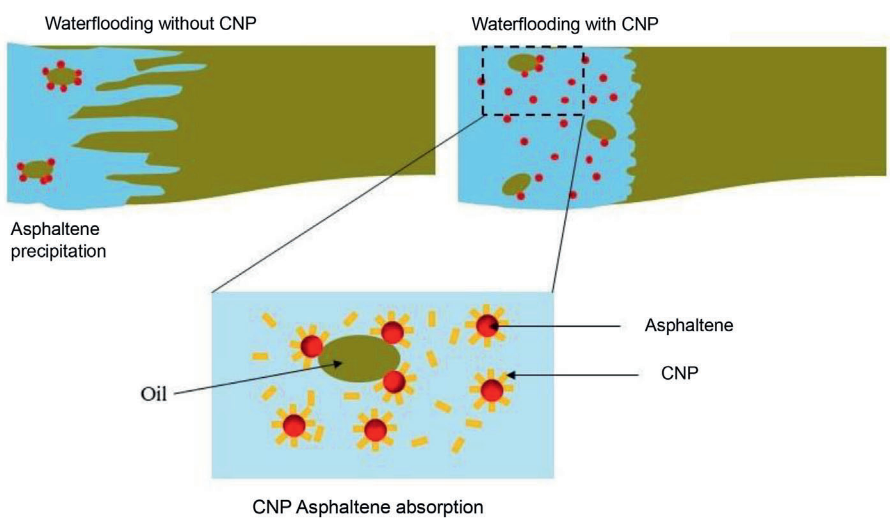

Fig. 22. Effect of CNP on asphaltene precipitation and decomposition (Yakasai et al., 2021).

Table 6
Prior studies on the application of CNC and CNF in EOR.

References	Dia.	length	Functional group	Formulation	Sweep efficiency
Raza and Gates (2021)	–	–	Hydroxyl group (-OH)	0.2 wt% CNCs	98
(Chen et al., 2024; Rajput et al., 2021)	–	–	Sulfonated group ($-SO_3^-$)	3.0 wt% CNCs + 0–70 mL NaCl	60.81–71.58
Aadland et al. (2020)	15	>1000	(-OH group Carboxylate group ($-COO^-$)	0.1 wt% CNCs + 0.1 wt% NaCl	88.7
Wei et al. (2019)	2–5	800	Carboxylate group ($-COO^-$) AMPS ASA	0.3 wt% SCNFs + 1.0 wt% NaCl	61.14–67.63
Wei et al. (2019)	2–5	800–1000	Carboxylate group ($-COO^-$)	0.3 wt% CNFs	
Aadland et al. (2019)	<20	<200	Hydroxyl group (-OH) Sulfated group ($-SO_3^-$)	0.2 wt% CNCs + 0.1 wt% NaCl	66.2
Jakobsen et al. (2018)	<20	>1000	Hydroxyl group and Carboxylate ($-COO^-$) group	0.5 wt% CNCs combined with 0.1 wt% NaCl	–
Ma et al. (2018)	2–5	800	Carboxylate group ($-COO^-$) in AMPS (2-Acrylamido-2-methylpropane sulfonic acid) and ASA (alkenyl succinic anhydride)	0.3 wt% CNFs-KYSS combined with 1.0 wt% NaCl	53–67
Pandey et al. (2018)	15	100–200	Hydroxyl (-OH) group and Sulfonated group ($-SO_3^-$)	3.0 wt% CNCs	86.5
Li et al. (2017)	2–3	800	Carboxylate group ($-COO^-$) in AMPS (2-Acrylamido-2-methylpropane sulfonic acid)	0.3 wt% CNFs (KY/CNFs-KYSS) with 1.0 wt% NaCl	51.9

they noted that permeability differences between the two formations influenced recovery, with CNC particles effectively blocking higher permeability zones in Berea sandstone, while the heterogeneity of Edwards White left some zones unreached by oil, resulting in disconnected flow paths. This suggests that the efficiency of CNC in EOR applications is highly dependent on both rock properties and fluid modification techniques. The findings from Li et al. (2017) and Agi et al. (2019a) point to CNC's shear-thinning and pseudoplastic behavior, which facilitates oil displacement even in challenging high-temperature, high-pressure reservoir conditions. Similarly, Wei et al. (2017) highlighted CNC's capacity to improve the thermal stability and viscoelasticity of EOR fluids, further strengthening its utility in oil recovery. These trends suggest that CNC-based nanofluids can provide a stable and efficient approach to EOR, particularly when used in reservoirs with varying salinity and temperature. However, several contradictions and disagreements emerge when analyzing the efficiency of CNC in different reservoir conditions. Molnes et al. (2017) noted that CNC exhibits good injectivity in high-permeability sandstone cores, a finding echoed by Tiong et al. (2020), who reported significant oil recovery in Berea sandstone after CNC injection. Yet, Tiong et al. (2020) also observed reduced recovery in Edwards White formations due to pore heterogeneity, which resulted in disconnected oil pathways. This highlights the potential limitation of CNC in reservoirs with complex pore structures. Additionally, the mechanisms behind CNC's effect on permeability remain debated. Molnes et al. (2017) attributed CNC's impact on permeability reduction to particle entrapment in the rock matrix, whereas Bashir Wani et al. (2020) reported that CNC particles formed stable micron-sized agglomerates that permanently reduced permeability. Furthermore, there are discrepancies regarding the effect of temperature on CNC's performance. While Agi et al. (2019a) found that CNC's viscosity and oil recovery efficiency increased at elevated temperatures, other studies, such as Wei et al. (2017), suggest that CNC performance is highly sensitive to surfactant interaction and reservoir conditions. These contradictions underscore the need for further research into how CNC's performance varies across different reservoir environments and fluid conditions. Thermal stability is another essential attribute of CNCs in EOR applications. Heggset et al. (2017) reported superior thermal resilience of CNCs relative to traditional agents such as xanthan and guar gum, while Molnes et al. (2017) observed significant viscosity retention after 24 h at 120 °C, underscoring CNC's potential as a stable agent in high-temperature reservoirs. Table 7 illustrates the importance of and essence of using CNC as it helps meet SDG in using biodegradable and eco-friendly materials, which help to reduce toxicity in the environment.

7. Challenges and perspectives

7.1. Challenges

There are several challenges associated with the extraction, modification, and characterization of CNCs from various biomass sources. These are as follows.

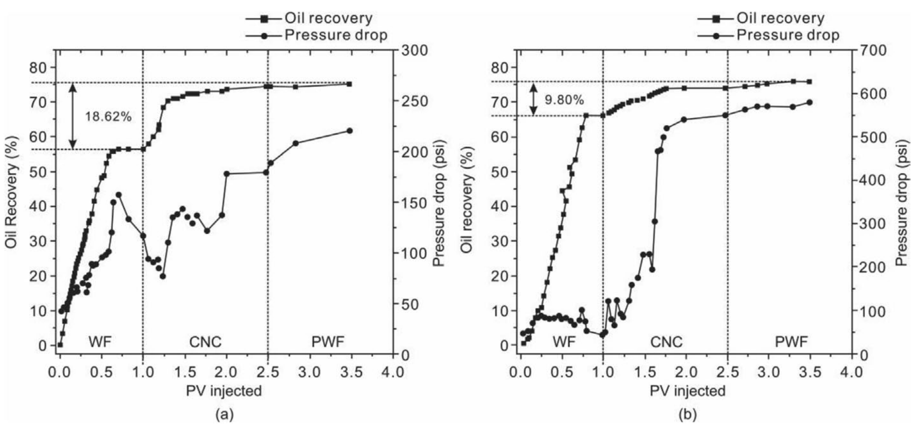

Fig. 23. Oil recovery as a result of CNCs core flooding on (a) Berea sandstones and (b) Edward White formations (Tiong et al., 2023).

Table 7
Top nanoparticles used to enhance oil recovery with their mechanisms.

References	Class of Nanoparticles	Mechanisms	Ultimate Oil Recovery	Environmental Issues
(Aadland et al., 2019; Li et al., 2023)	Cellulose nanocrystals (CNCs)	Modifies wettability, reduces IFT, stabilizes emulsions	Around 20.2% increase in OOIP	Biodegradable and eco-friendly
(Emmanuel, 2024; Sun et al., 2023)	Polymer-Nanoparticles	Improved viscosity, stability and reduces IFT	Around 35% increase in OOIP	It depends wholly on the polymer used
Gholinezhad et al. (2022)	Silica Nanoparticles	Reduces IFT significantly, alters wettability	Around 236% increase in OOIP	Potentially non-biodegradable
(Negi et al., 2021; Tian et al., 2023)	Titanium Dioxide	Alter wettability enhances rheological properties	Around 21% increase in OOIP	Non-biodegradable but non-toxic
(Che Mohamed Hussein et al., 2024; Zhu et al., 2018)	Iron Nanoparticles	Enhances oil displacement, modifies surface properties	Varies mainly around 10–15%	Major metal pollution is a concern

(1) **Acid Hydrolysis:** One major drawback of acid hydrolysis, especially in extracting CNCs from OPEFB, is its low yield and the significant volume of water required for washing to neutralize and remove residual acid. Excessive water consumption poses environmental concerns, particularly in regions with limited water resources. Additionally, acid is highly corrosive, which limits the recyclability of the washing water unless specialized membranes, for recycling (Lanjewar et al., 2021). However, these membranes must be durable enough to withstand acidic conditions, and membrane fouling could further complicate the process.
(2) **Time and Energy Consumption:** ILH is a promising eco-friendly method for biomass processing, yielding CNCs with higher crystallinity and purity than acid hydrolysis. However, it requires prolonged reaction times (up to 24 h) and elevated temperatures (60 °C), leading to high energy consumption and long cycles that limit industrial scalability. Additionally, the recycling of ionic liquids is costly and complex, posing further challenges to commercial viability (Ovejero et al., 2021). Mechanical-enzymatic hydrolysis, utilizing methods like HPH and HIUS, is energy-intensive, costly, and limited by enzyme sensitivity to temperature and pH, resulting in lower yields (Lee et al., 2014).
(3) **Compatibility of CNP with Other Materials:** When incorporated with composite materials, CNP can face compatibility challenges. This is because the interaction between CNP and hydrophobic materials can be very weak, leading to poor mechanical performance in composite (Mariano et al., 2014; Masek and Kosmalska, 2022). To improve this computability and performance, CNP may require chemical modification (Ma et al., 2023). The use of CNPs and its hybrid nanofluids has shown promising results in laboratory-scale studies for improving oil recovery, as these materials can enhance the viscosity and displace residual oil more effectively than conventional fluids.
(4) **High Costs of Nanoparticles:** The economic feasibility of using nanomaterials in EOR projects remains uncertain, as the production of nanoparticles often involves energy-intensive processes and high material costs. Maintaining the nanoscale size of particles is crucial for effective fluid performance, but the associated costs are significant. Researchers have employed advanced synthesis techniques to produce cost-effective CNP from biomass waste, significantly reducing the expense of nanoparticle production (Pereira et al., 2022).
(5) **Solvent Recovery Issues:** DES and microwave-assisted extraction show promise for cellulose extraction but face challenges, including high viscosity, solvent recovery issues, and the need for specialized equipment, hindering scalability (Scelsi et al., 2021). Biomass fractionation methods like organosolv and HTP are similarly limited by high energy demands and recovery difficulties. Although organosolv effectively purifies cellulose, it involves toxic solvents, while HTP's water-based reactions lead to corrosion issues, restricting industrial applications (Zhang et al., 2015). Sustainable fractionation methods with reduced operational complexity are thus essential.
(6) **Reagent Toxicity and Environmental Impact:** Traditional oxidation processes for CNC synthesis often involve toxic reagents, raising environmental and health concerns (Lin et al., 2022). Although alternatives like APS oxidation have gained attention for their lower toxicity, they still face limitations such as longer reaction times and reduced CNC yields. Hybrid approaches, such as APS combined with ultraviolet light, have shown improved particle uniformity (13–20 nm) but still require refinement to mitigate environmental impacts effectively (Wang et al., 2020b). The drive towards eco-friendly materials is reshaping the field of nanomaterial synthesis, particularly in the development of CNPs synthesized from biomass wastes. These bio-nanomaterials hold potential for reducing the environmental footprint of nanomaterial production, as they rely on renewable resources and could lower the energy consumption and waste associated with traditional synthesis methods.
(7) **Efficiency Constraints and Technical Challenges:** Efficiency limitations affect alternative methods like subcritical and supercritical water hydrolysis, which, despite being eco-friendly, require high-cost equipment and rigorous safety protocols (Montesantos and Maschietti, 2020; Novo et al., 2016). CNC nanofluids face salinity-induced viscosity reductions. Surface modifications with polymers like Poly[2-(methacryloyloxy)ethyl]trimethylammonium chloride (PAMPS) have demonstrated increased stability, as seen with CNFs-KYSS, which achieved a 6% rise in oil recovery (Park et al., 2023). CNFs-KYSS refers to cellulose nanofibers (CNFs) that have been surface modified with AMPS (2-acrylamido-2-methylpropane sulfonic acid) and hydrophobic groups. Addressing these technical barriers is essential for optimizing CNC applications in biomass valorization and EOR.
(8) **Temperature and Viscosity inconsistencies:** CNCs have shown viscosity inconsistencies in core flooding applications, with temperature and aging impacting their performance (Aadland et al., 2019). These findings suggest further research is needed on CNC behavior under varying conditions. While CPNs are valued for biodegradability (Agi et al., 2021), practical issues like production costs and scalability for industrial EOR applications remain underexplored, highlighting both the promise and challenges of CNP integration.
(9) **High Energy Consumption and Toxicity:** The combination of organosolv treatment with other chemical methods can enhance cellulose extraction efficiency, yet high energy

demands and solvent recovery issues raise economic and environmental concerns. For example, Chin et al. (2021) achieved a 90% wt cellulose yield from OPEFB, while Aggarwal et al. (2021) obtained microcrystalline cellulose from rice straw. Additionally, Zhang et al. (2016) noted toxicity risks with some solvents, complicating waste disposal.

7.2. Existing research gaps

(1) Inadequate understanding of CNC rheological behavior under harsh reservoir conditions (temperature, salinity, shear).
(2) Lack of scalable, green, and low-cost extraction methods that balance yield, energy efficiency, and environmental safety.
(3) Limited integration of computational modeling for process optimization and fluid dynamics simulations in porous media.
(4) Insufficient lifecycle and techno-economic analysis for nanoparticle-assisted EOR systems.
(5) Scarcity of studies on long-term environmental impacts and degradation pathways of nanomaterials in subsurface environments.
(6) Few industrial-scale demonstrations and pilot trials validating lab-scale successes.

7.3. Future research directions

(1) Green Synthesis and Hybrid Extraction Techniques
- Development of hybrid systems (like DES–microwave, APS–UV) for faster, more eco-friendly CNC production with improved yields and particle control.
- Emphasis on bio-based solvents and recyclable systems to reduce environmental footprint and operational complexity.

(2) **Surface Functionalization and Compatibility Enhancement**
- Designing multi-functional surface treatments for CNCs to improve interaction with polymer matrices and reservoir fluids.
- Exploring stimuli-responsive CNCs (like pH- or temperature-sensitive systems) for controlled behavior in subsurface environments.

(3) Cost Reduction via Biomass Valorization
- Utilizing low-cost agricultural waste (such as OPEFB, rice straw) and optimizing reaction parameters to lower production costs.
- Innovating continuous-flow processing systems for CNC production at large scale.

(4) Nanofluid Stability and Performance Optimization
- Investigating polymer-coated CNCs, hybrid nanofluids, and surfactant blends to improve EOR fluid performance under field conditions.
- Addressing viscosity retention, dispersion stability, and adsorption behavior in heterogeneous reservoirs.

7.4. Potential future developments in research methodologies

(1) Experimental Advances
- Adoption of high-throughput screening tools for rapid CNC synthesis optimization.
- Use of advanced characterization techniques (such as SAXS, AFM, cryo-TEM) for better insight into CNC structure–function relationships.
- Integration of core-flooding simulation units and microfluidic devices for real-time EOR performance testing.

(2) Computational and Modeling Innovations
- Application of molecular dynamics (MD) and density functional theory (DFT) to study CNC–fluid and CNC–rock interactions.
- Development of reservoir-scale computational fluid dynamics (CFD) models incorporating CNC fluid rheology and transport behavior.
- Implementation of machine learning algorithms to predict CNC properties, optimize synthesis parameters, and simulate EOR outcomes.

8. Conclusions

This review depicts critical information on pretreatment, extraction, synthesis, EOR mechanisms, and application of cellulose nanomaterials in oil recovery. The synthesis methods and EOR mechanisms were comprehensively reviewed. The study highlights the potential for field implementation while identifying limitations that open avenues for further research and innovation. The conclusions that followed were drawn from the review's results.

(1) Acid pretreatment is highly effective in yielding cellulose from diverse sources. However, to improve the crystallinity and purity of cellulose for industrial applicability, alkaline pretreatment is preferred.
(2) Nanoprecipitation is very common for small-scale applications while HPH synthesis method is widely recognized for its effectiveness in reducing particle size and increasing the number of particles produced during homogenization processes but for industrial scalability and integration with other processes steam explosion is preferable.
(3) Experimental results indicate that wettability alteration and IFT reduction are the major EOR mechanisms by cellulose bionanomaterial. Nevertheless, for heavy oil, viscosity reduction and inhibiting asphaltene precipitation are the dominant mechanisms.
(4) The literature reviewed demonstrated that cellulose bionanomaterials can increase the viscosity of injected fluid by 10–100%, improve sweep efficiency by 52–98% and improve oil recovery by 10–35% OOIP.
(5) This study shows that bionanomaterials have potential for oil field applications and are economically viable due to their high recovery rate.

In conclusion, while the challenges associated with CNC extraction and nanoparticle stability remain significant, ongoing research into greener synthesis methods, improved dispersion techniques, and the hybridization of materials offer promising prospects for the future of EOR applications using bionanomaterials.

CRediT authorship contribution statement

Francis Nyah: Writing – original draft, Visualization, Methodology, Investigation, Formal analysis, Data curation, Conceptualization. **Norida Ridzuan:** Visualization, Validation, Supervision. **Emmanuel Epelle:** Project administration, Formal analysis. **Mohd Aizudin Bin Abd Aziz:** Software. **Barima Money:** Resources, Investigation. **David Abutu:** Software, Resources. **Augustine Agi:** Writing – original draft, Validation, Supervision, Resources, Funding acquisition, Conceptualization.

Declaration of competing interest

The authors declare that they have no known competing financial interests or personal relationships that could have appeared to influence the work reported in this paper.

Acknowledgment

This work was funded by Universiti Malaysia Pahang Al-Sultan Abdullah through research grants RDU 233305 and PGRS 230309.

References

Aadland, R.C., Jakobsen, T.D., Heggset, E.B., Long-Sanouiller, H., Simon, S., Paso, K.G., Syverud, K., Torsæter, O., 2019. High-temperature core flood investigation of nanocellulose as a green additive for enhanced oil recovery. Nanomaterials 9 (5), 665. https://doi.org/10.3390/nano9050665.

Aadland, R.C., Akarri, S., Heggset, E.B., Syverud, K., Torsæter, O., 2020. A core flood and microfluidics investigation of nanocellulose as a chemical additive to water flooding for EOR. Nanomaterials 10 (7), 1296. https://doi.org/10.3390/nano10071296.

Abaide, E.R., Ugalde, G., Di Luccio, M., Moreira, R. de F.P. M., Tres, M.V., Zabot, G.L., Mazutti, M.A., 2019. Obtaining fermentable sugars and bioproducts from rice husks by subcritical water hydrolysis in a semi-continuous mode. Bioresour. Technol. 272, 510–520. https://doi.org/10.1016/j.biortech.2018.10.075.

Abbas, A.H., Zhuniskenov, Y., Serikov, G., Nyah, F., Ridzuan, N., Gbonhinbor, J., Agi, A., 2024. Navigating the future: a numerical study of natural polymers and CO2 in offshore applications. In: SPE Nigeria Annual International Conference and Exhibition. https://doi.org/10.2118/221614-MS.

Abdullah, M.A., Nazir, M.S., Tahir, Z., Abbas, Y., Akhtar, M.N., Raza, M.R., Hussein, H.A., 2019. Processing aspects and biomedical and environmental applications of sustainable nanocomposites containing nanofillers. In: Thomas, S., Mishra, S., Asiri, A. (Eds.), Sustainable Polymer Composites and Nanocomposites. Springer International Publishing, pp. 727–757. https://doi.org/10.1007/978-3-030-05399-4_25.

Abolore, R.S., Jaiswal, S., Jaiswal, A.K., 2024. Green and sustainable pretreatment methods for cellulose extraction from lignocellulosic biomass and its applications: a review. Carbohydrate Polymer Technologies and Applications 7, 100396. https://doi.org/10.1016/j.carpta.2023.100396.

Abu-Thabit, N.Y., Judeh, A.A., Hakeem, A.S., Ul-Hamid, A., Umar, Y., Ahmad, A., 2020. Isolation and characterization of microcrystalline cellulose from date seeds (phoenix dactylifera L.). Int. J. Biol. Macromol. 155, 730–739. https://doi.org/10.1016/j.ijbiomac.2020.03.255.

Abutu, D., Nwaichi, P.I., Umunnawuike, C., Nyah, F., Money, B., Yussof, H.W., Agi, A., 2025. Numerical simulation of microbial biohydrogen production under high-pressure, high-temperature conditions for enhanced recovery from depleted reservoirs. Petroleum Research. https://doi.org/10.1016/j.ptlrs.2025.07.006.

Abutu, D., Yussof, H.W., Nwaichi, P.I., Umunnawuike, C., Nyah, F., Money, B., gi, A., 2022. Utilizing depleted oil reservoirs for in-situ biohydrogen production: addressing knowledge gaps, sustainable pathways and future research directions. Fuel 406, 136710. https://doi.org/10.1016/j.fuel.2025.136710.

Abzan, N., Abbasian, A., Jonoobi, M., Ghasemi, I., 2023. Cellulose microfiber extraction from leftover celery pulp: chemomechanical treatments, structural, morphological, and thermal characterization. Int. J. Biol. Macromol. 253, 126834. https://doi.org/10.1016/j.ijbiomac.2023.126834.

Afolabi, F., Mahmood, S.M., Yekeen, N., Akbari, S., Sharifigaliuk, H., 2022. Polymeric surfactants for enhanced oil recovery: a review of recent progress. J. Petrol. Sci. Eng. 208, 109358. https://doi.org/10.1016/j.petrol.2021.109358.

Aggarwal, N., Pal, P., Sharma, N., Saravanamurugan, S., 2021. Consecutive organosolv and alkaline pretreatment: an efficient approach toward the production of cellulose from rice straw. ACS Omega 6 (41), 27247–27258. https://doi.org/10.1021/acsomega.1c04030.

Agi, A., Junin, R., Chong, A.S., 2018. Intermittent ultrasonic wave to improve oil recovery. J. Petrol. Sci. Eng. 166, 577–591. https://doi.org/10.1016/j.petrol.2018.03.097.

Agi, A., Junin, R., Arsad, A., Abbas, A., Gbadamosi, A., Azli, N.B., Oseh, J., 2019a. Synergy of the flow behaviour and disperse phase of cellulose nanoparticles in enhancing oil recovery at reservoir condition. PLoS One 14 (9), e0220778. https://doi.org/10.1371/journal.pone.0220778.

Agi, A., Junin, R., Gbadamosi, A., Abbas, A., Azli, N.B., Oseh, J., 2019b. Influence of nanoprecipitation on crystalline starch nanoparticle formed by ultrasonic assisted weak-acid hydrolysis of cassava starch and the rheology of their solutions. Chem. Eng. Process. Process Intensif. 142, 107556. https://doi.org/10.1016/j.cep.2019.107556.

Agi, A., Junin, R., Syamsul, M.F., Chong, A.S., Gbadamosi, A., 2019c. Intermittent and short duration ultrasound in a simulated porous medium. Petroleum 5 (1), 42–51. https://doi.org/10.1016/j.petlm.2018.03.012.

Agi, A., Junin, R., Abdullah, M.O., Jaafar, M.Z., Arsad, A., Sulaiman, W.R.W., Norddin, M.N.A.M., Abdurrahman, M., Abbas, A., Gbadamosi, A., Azli, N.B., 2020a. Application of polymeric nanofluid in enhancing oil recovery at reservoir condition. J. Petrol. Sci. Eng. 194, 107476. https://doi.org/10.1016/j.petrol.2020.107476.

Agi, A., Junin, R., Arsad, A., Abbas, A., Gbadamosi, A., Azli, N.B., Oseh, J., 2020b. Ultrasound-assisted weak-acid hydrolysis of crystalline starch nanoparticles for chemical enhanced oil recovery. Int. J. Biol. Macromol. 148, 1251–1271. https://doi.org/10.1016/j.ijbiomac.2019.10.099.

Agi, A., Junin, R., Jaafar, M.Z., Sidek, M.A., Yakasai, F., Gbadamosi, A., Oseh, J., 2021. Formulation of bionanomaterials: a review of particle design towards oil recovery applications. J. Ind. Eng. Chem. 98, 82–102. https://doi.org/10.1016/j.jiec.2021.03.032.

Agi, A., Junin, R., Jaafar, M.Z., Sidek, M.A., Yakasai, F., Gbadamosi, A., Oseh, J., 2022. Laboratory evaluation to field application of ultrasound: a state-of-the-art review on the effect of ultrasonication on enhanced oil recovery mechanisms. J. Ind. Eng. Chem. 110, 100–119. https://doi.org/10.1016/j.jiec.2022.03.030.

Agi, A., Junin, R., Shakuam, M., Gbadamosi, A., Ridzuan, N., Mahat, S.Q.A., Gbonhinbor, J., Oseh, J., 2023. Microwave assisted technique for oil recovery from oily sludge shale drilled cuttings. Day 3 Wed. https://doi.org/10.2118/217140-MS. August 02, 2023.

Agoda-Tandjawa, G., Durand, S., Berot, S., Blassel, C., Gaillard, C., Garnier, C., Doublier, J.-L., 2010. Rheological characterization of microfibrillated cellulose suspensions after freezing. Carbohydr. Polym. 80 (3), 677–686. https://doi.org/10.1016/j.carbpol.2009.11.045.

Aguado, R., Tarrés, Q., Pèlach, M.À., Mutjé, P., de la Fuente, E., Sanchez-Salvador, J.L., Negro, C., Delgado-Aguilar, M., 2022. Micro- and nanofibrillated cellulose from annual plant-sourced fibers: Comparison between enzymatic hydrolysis and mechanical refining. Nanomaterials 12 (9), 1612. https://doi.org/10.3390/nano12091612.

Akbar, D.A., Kusmono, K., Wildan, M.W., Ilman, M.N., 2020. Extraction and characterization of nanocrystalline cellulose (NCC) from Ramie fiber by hydrochloric acid hydrolysis. Key Eng. Mater. 867, 109–116. https://doi.org/10.4028/www.scientific.net/KEM.867.109.

Akhtar, N., Gupta, K., Goyal, D., Goyal, A., 2016. Recent advances in pretreatment technologies for efficient hydrolysis of lignocellulosic biomass. Environ. Prog. Sustain. Energy 35 (2), 489–511. https://doi.org/10.1002/ep.12257.

Al Hakkak, J., Grigsby, W.J., Kathirgamanathan, K., Edmonds, N.R., 2019. Generation of spherical cellulose nanoparticles from ionic liquid processing via novel nonsolvent addition and drying. Adv. Mater. Sci. Eng. 2019, 1–6. https://doi.org/10.1155/2019/2081027.

Al-Asadi, A., Rodil, E., Soto, A., 2022. Nanoparticles in chemical EOR: a review on flooding tests. Nanomaterials 12 (23), 4142. https://doi.org/10.3390/nano12234142.

Al-Dulaimi, A.A., Wanrosli, W.D., 2017. Isolation and characterization of nanocrystalline cellulose from totally chlorine free oil palm empty fruit bunch pulp. J. Polym. Environ. 25 (2), 192–202. https://doi.org/10.1007/s10924-016-0798-z.

Al_Ani, M., Panis, N.I., Manikumar, Y., Sidek, M.A., Jaafar, M.Z., Ridzuan, N., Gbonhinbor, J., Umunnawuike, C., Money, B., Agi, A., 2024. Optimization of polymeric nanofluid oil recovery mechanisms at reservoir condition. In: SPE Nigeria Annual International Conference and Exhibition. https://doi.org/10.2118/221597-MS.

Ali, J.A., Manshad, A.K., Imani, I., Sajadi, S.M., Keshavarz, A., 2020. Correction to: Greenly Synthesized Magnetite@ {SiO}_{2}@Xanthan Nanocomposites and Its Application in Enhanced Oil Recovery: IFT Reduction and Wettability Alteration. Arabian J. Sci. Eng. 45 (9), 7863. https://doi.org/10.1007/s13369-020-04405-w.

Ali, S.Z., Nahian, M.K., Hoque, M.E., 2023. Extraction of cellulose from agro-industrial wastes. In: Bhawani, S.A., Khan, A., Ahmad, F.B. (Eds.), Extraction of Natural Products from Agro-Industrial Wastes. Elsevier, pp. 319–348. https://doi.org/10.1016/B978-0-12-823349-8.00013-7.

Ali, T.M., Haider, S., Shaikh, M., Butt, N.A., Zehra, N., 2024. Chemical cross-linking, acid hydrolysis, oxidation, esterification, and etherification of starch. In: Mazumder, N., Rahman, M.H. (Eds.), Advanced Research in Starch. Springer Nature Singapore, pp. 47–94. https://doi.org/10.1007/978-981-99-9527-1_2.

Al-Jaber, H.A., Arsad, A., Tahir, M., Nuhma, M.J., Bandyopadhyay, S., Abdulmunem, A.R., Rahman, A.F.A., binti Harun, Z., Agi, A., 2023. Enhancing oil recovery by polymeric flooding with Purple Yam and Cassava nanoparticles. Molecules 28 (12), 4614. https://doi.org/10.3390/molecules28124614.

Alvarado, V., Manrique, E., 2010. Enhanced oil recovery: an update review. Energies 3 (9), 1529–1575. https://doi.org/10.3390/en3091529.

Amirah Badi, N.S., Zul Hilmey Makmud, M., Se Mun, C., Jamain, Z., Asik, J., Mohd Amin, K.N., 2024. Synthesis and characterization of cellulose nanocrystal derived from paper as nanofiller for polymer insulation materials. Mater. Today Proc. 97, 69–74. https://doi.org/10.1016/j.matpr.2023.12.059.

Andoko, A., Gapsari, F., Diharjo, K., M R, S., Siengchin, S., 2023. Isolation of microcellulose from timoho fiber using the process of delinigfication and maceration: evaluation of physical, chemical, structural, and thermal properties. Int. J. Biol. Macromol. 224, 48–54. https://doi.org/10.1016/j.ijbiomac.2022.10.225.

Anwar, A., Zhao, T., Ghaffar, S., Nie, K., Xia, W., Wang, L., Cao, Z., Yang, X., Zhou, C., Zhang, Y., Han, G., Jiang, W., Ben, H., 2024. A novel microwave-assisted

γ-valerolactone and glycolic acid pretreatment for green and sustainable production of hemp fibres. Ind. Crop. Prod. 222, 119625. https://doi.org/10.1016/j.indcrop.2024.119625.
Araki, J., Nakajima, M., 2023. Determination of surface sulfate groups of cellulose nanowhiskers obtained by various desulfation procedures: usefulness of different methods for sulfate group quantification. Cellulose 30 (2), 849–855. https://doi.org/10.1007/s10570-022-04926-7.
Arif, M.D., Hoque, M.E., Rahman, M.Z., Shafoyat, M.U., 2024. Emerging directions in green nanomaterials: synthesis, physicochemical properties and applications. Mater. Today Commun. 40, 109335. https://doi.org/10.1016/j.mtcomm.2024.109335.
Arpia, A.A., Chen, W.-H., Lam, S.S., Rousset, P., de Luna, M.D.G., 2021. Sustainable biofuel and bioenergy production from biomass waste residues using microwave-assisted heating: a comprehensive review. Chem. Eng. J. 403, 126233. https://doi.org/10.1016/j.cej.2020.126233.
Aryasena, R., Kusmono, Umami, N., 2022. Production of cellulose nanocrystals extracted from Pennisetum purpureum fibers and its application as a lubricating additive in engine oil. Heliyon 8 (11), e11315. https://doi.org/10.1016/j.heliyon.2022.e11315.
Aswini, K., Gopal, N.O., Uthandi, S., 2020. Optimized culture conditions for bacterial cellulose production by Acetobacter senegalensis MA1. BMC Biotechnol. 20 (1), 46. https://doi.org/10.1186/s12896-020-00639-6.
Aziz, R., Joekar-Niasar, V., Martínez-Ferrer, P.J., Godinez-Brizuela, O.E., Theodoropoulos, C., Mahani, H., 2019. Novel insights into pore-scale dynamics of wettability alteration during low salinity waterflooding. Sci. Rep. 9 (1), 9257. https://doi.org/10.1038/s41598-019-45434-2.
Aziz, T., Farid, A., Haq, F., Kiran, M., Ullah, A., Zhang, K., Li, C., Ghazanfar, S., Sun, H., Ullah, R., Ali, A., Muzammal, M., Shah, M., Akhtar, N., Selim, S., Hagagy, N., Samy, M., Al Jaouni, S.K., 2022. A review on the modification of cellulose and its applications. Polymers 14 (15), 3206. https://doi.org/10.3390/polym14153206.
Azlan, N.S.M., Yap, C.L., Gan, S., Rahman, M.B.A., 2022. Effectiveness of various solvents in the microwave-assisted extraction of cellulose from oil palm mesocarp fiber. Mater. Today Proc. 59, 583–590. https://doi.org/10.1016/j.matpr.2021.12.086.
Badi, N.S.A., Makmud, M.Z.H., Mun, C.S., Jamain, Z., Asik, J., Amin, K.N.M., 2024. Synthesis and characterization of cellulose nanocrystal derived from paper as nanofiller for polymer insulation materials. Mater. Today Proc. 97, 69–74. https://doi.org/10.1016/j.matpr.2023.12.059.
Bahndral, A., Shams, R., Dash, K.K., Ali, N.A., Shaikh, A.M., Kovács, B., 2024. Microwave assisted extraction of cellulose from lemon grass: effect on techno-functional and microstructural properties. J. Agric. Food Res. 16, 101170. https://doi.org/10.1016/j.jafr.2024.101170.
Baksi, S., Saha, D., Saha, S., Sarkar, U., Basu, D., Kuniyal, J.C., 2023. Pre-treatment of lignocellulosic biomass: review of various physico-chemical and biological methods influencing the extent of biomass depolymerization. Int. J. Environ. Sci. Technol. 20 (12), 13895–13922. https://doi.org/10.1007/s13762-023-04838-4.
Bangar, S.P., Harussani, M.M., Ilyas, R.A., Ashogbon, A.O., Singh, A., Trif, M., Jafari, S.M., 2022. Surface modifications of cellulose nanocrystals: processes, properties, and applications. Food Hydrocoll. 130, 107689. https://doi.org/10.1016/j.foodhyd.2022.107689.
Bano, S., Negi, Y.S., 2017. Studies on cellulose nanocrystals isolated from groundnut shells. Carbohydr. Polym. 157, 1041–1049. https://doi.org/10.1016/j.carbpol.2016.10.069.
Barbash, V.A., Yashchenko, O.V., Yakymenko, O.S., Myshak, V.D., 2023. Extraction of organosolv pulp and nanocellulose from harvested corn residues. In: Proceedings of the 8th International Conference Nanotechnology and Nanomaterials (NANO2020), pp. 3–17. https://doi.org/10.1007/978-3-031-42708-4_1.
Baron, R.I., Coseri, S., 2020. Preparation of water-soluble cellulose derivatives using TEMPO radical-mediated oxidation at extended reaction time. React. Funct. Polym. 157, 104768. https://doi.org/10.1016/j.reactfunctpolym.2020.104768.
Baruah, J., Deka, R.C., Kalita, E., 2020. Greener production of microcrystalline cellulose (MCC) from Saccharum spontaneum (Kans grass): statistical optimization. Int. J. Biol. Macromol. 154, 672–682. https://doi.org/10.1016/j.ijbiomac.2020.03.158.
Bashir Wani, O., Shoaib, M., Al Sumaiti, A., Bobicki, E.R., Alhassan, S.M., 2020. Application of green additives for enhanced oil recovery: cellulosic nanocrystals as fluid diversion agents in carbonate reservoirs. Colloids Surf. A Physicochem. Eng. Asp. 589, 124422. https://doi.org/10.1016/j.colsurfa.2020.124422.
Becker, M., Ahn, K., Bacher, M., Xu, C., Sundberg, A., Willför, S., Rosenau, T., Potthast, A., 2021. Comparative hydrolysis analysis of cellulose samples and aspects of its application in conservation science. Cellulose 28 (13), 8719–8734. https://doi.org/10.1007/s10570-021-04048-6.
Belmabrouk, H., Brahem, R.A., Jabli, M., El-Ghoul, Y., Alminderej, F.M., Alharbi, T., 2023. Characterization of raw and treated Calotropis gigantea fibers: application to the adsorption of methylene blue dye. J. Nat. Fibers 20 (1). https://doi.org/10.1080/15440478.2022.2160401.
Beltramino, F., Roncero, M.B., Vidal, T., Valls, C., 2018. A novel enzymatic approach to nanocrystalline cellulose preparation. Carbohydr. Polym. 189, 39–47. https://doi.org/10.1016/j.carbpol.2018.02.015.
Berry, J.D., Neeson, M.J., Dagastine, R.R., Chan, D.Y.C., Tabor, R.F., 2015. Measurement of surface and interfacial tension using pendant drop tensiometry. J. Colloid Interface Sci. 454, 226–237. https://doi.org/10.1016/j.jcis.2015.05.012.
Bhandari, K., Adaval, A., Bhattacharyya, A.R., Maulik, S.R., 2022. Synthesis of microcrystalline cellulose from carpenter waste and its characterizations. J. Nat. Fibers 19 (6), 1975–1989. https://doi.org/10.1080/15440478.2020.1788688.
Bhardwaj, N., Kumar, B., Agrawal, K., Verma, P., 2021. Current perspective on production and applications of microbial cellulases: a review. Bioresources and Bioprocessing 8 (1), 95. https://doi.org/10.1186/s40643-021-00447-6.
Bhutto, A.W., Qureshi, K., Harijan, K., Abro, R., Abbas, T., Bazmi, A.A., Karim, S., Yu, G., 2017. Insight into progress in pre-treatment of lignocellulosic biomass. Energy 122, 724–745. https://doi.org/10.1016/j.energy.2017.01.005.
Bian, H., Chen, L., Dai, H., Zhu, J.Y., 2017. Integrated production of lignin containing cellulose nanocrystals (LCNC) and nanofibrils (LCNF) using an easily recyclable di-carboxylic acid. Carbohydr. Polym. 167, 167–176. https://doi.org/10.1016/j.carbpol.2017.03.050.
Birlie, B., Mamay, T., 2024. Characterization of natural cellulosic fiber extracted from Grewia ferruginea plant stem. Int. J. Biol. Macromol. 271, 132858. https://doi.org/10.1016/j.ijbiomac.2024.132858.
Bishnoi, P., Siwal, S.S., Kumar, V., Thakur, V.K., 2024. Cellulose-based smart materials: novel synthesis techniques, properties, and applications in energy storage and conversion devices. Electron 2 (2). https://doi.org/10.1002/elt2.42.
Biswal, N.R., Rangera, N., Singh, J.K., 2016. Effect of different surfactants on the interfacial behavior of the *n* -Hexane–Water system in the presence of silica nanoparticles. J. Phys. Chem. B 120 (29), 7265–7274. https://doi.org/10.1021/acs.jpcb.6b03763.
Brahma, R., Ray, S., 2024. Optimization of extraction conditions for cellulose from jackfruit peel using RSM, its characterization and comparative studies to commercial cellulose. Measurement: Food 13, 100130. https://doi.org/10.1016/j.meafoo.2023.100130.
Budhi, Y.W., Fakhrudin, M., Culsum, N.T.U., Suendo, V., Iskandar, F., 2018. Preparation of cellulose nanocrystals from empty fruit bunch of palm oil by using phosphotungstic acid. IOP Conf. Ser. Earth Environ. Sci. 105, 012063. https://doi.org/10.1088/1755-1315/105/1/012063.
Bunaciu, A.A., Aboul-Enein, H.Y., Hoang, V.D., 2015. Vibrational spectroscopy used in polymorphic analysis. TrAC, Trends Anal. Chem. 69, 14–22. https://doi.org/10.1016/j.trac.2015.02.006.
Burhani, D., Septevani, A.A., 2018. Isolation of nanocellulose from oil palm empty fruit bunches using strong acid hydrolysis. AIP Conf. Proc. 2024 (1), 020005. https://doi.org/10.1063/1.5064291.
Cabrera-Villamizar, L.A., Ebrahimi, M., Martínez-Abad, A., Talens-Perales, D., López-Rubio, A., Fabra, M.J., 2024. Order matters: Methods for extracting cellulose from rice straw by coupling alkaline, ozone and enzymatic treatments. Carbohydr. Polym. 328, 121746. https://doi.org/10.1016/j.carbpol.2023.121746.
Camani, P.H., Anholon, B.F., Toder, R.R., Rosa, D.S., 2020. Microwave-assisted pretreatment of eucalyptus waste to obtain cellulose fibers. Cellulose 27 (7), 3591–3609. https://doi.org/10.1007/s10570-020-03019-7.
Camarero Espinosa, S., Kuhnt, T., Foster, E.J., Weder, C., 2013. Isolation of thermally stable cellulose nanocrystals by phosphoric acid hydrolysis. Biomacromolecules 14 (4), 1223–1230. https://doi.org/10.1021/bm400219u.
Campora, L.D., Metzger, C., Dähnhardt-Pfeiffer, S., Drexel, R., Meier, F., Fürtauer, S., 2022. Fluorescence labeling of cellulose nanocrystals—A facile and green synthesis route. Polymers 14 (9), 1820. https://doi.org/10.3390/polym14091820.
Cannazza, P., Rissanen, A.J., Guizelini, D., Losoi, P., Sarlin, E., Romano, D., Santala, V., Mangayil, R., 2021. Characterization of komagataeibacter isolate reveals new prospects in waste stream valorization for bacterial cellulose production. Microorganisms 9 (11), 2230. https://doi.org/10.3390/microorganisms9112230.
Cardenas-Toro, F.P., Forster-Carneiro, T., Rostagno, M.A., Petenate, A.J., Maugeri Filho, F., Meireles, M.A.A., 2014. Integrated supercritical fluid extraction and subcritical water hydrolysis for the recovery of bisoactive compounds from pressed palm fiber. J. Supercrit. Fluids 93, 42–48. https://doi.org/10.1016/j.supflu.2014.02.009.
Chaka, K.T., 2022. Extraction of cellulose nanocrystals from agricultural by-products: a review. Green Chem. Lett. Rev. 15 (3), 582–597. https://doi.org/10.1080/17518253.2022.2121183.
Chakraborty, S., Panigrahi, P.K., 2020. Stability of nanofluid: a review. Appl. Therm. Eng. 174, 115259. https://doi.org/10.1016/j.applthermaleng.2020.115259.
Chamathka, W.W.D.R., Chai, T.-T., Phuah, E.T., Wong, J.X., Chen, S.N., Yassoralipour, A., 2024. Extraction and characterization of cellulose nanoparticles from palm kernel meal for potential application in active food packaging. Int. J. Biol. Macromol. 260, 129637. https://doi.org/10.1016/j.ijbiomac.2024.129637.
Chauhan, I., Aggrawal, S., Muhammad, R., Mohanty, P., 2019. Immobilization of α-Fe2O3 nanoparticles on the cellulose surface: role of cellulose in tuning the microstructure and crystallographic phase. Cellulose 26 (3), 1757–1767. https://doi.org/10.1007/s10570-018-2186-4.
Chauhan, S., Kumari, B., Chauhan, G.S., Chauhan, K., Ranote, S., Kumar, R., Kumar, K., 2023. A highly efficient and green adsorbent for anionic dyes synthesized from whole pine needles modified with glycidyltrimethylammonium chloride: synthesis, kinetic, and thermodynamic investigation. Biomass Convers. Biorefinery. https://doi.org/10.1007/s13399-023-04776-8.
Chavez, B.K., Garces-Porras, K., Parada, D.C., Flores, E., 2023. Thermochemical isolation and characterization of nanofibrillated cellulose from Stipa obtusa fibers. Carbohydrate Polymer Technologies and Applications 6, 100344. https://doi.org/10.1016/j.carpta.2023.100344.

Chawla, P., Sridhar, K., Kumar, A., Sarangi, P.K., Bains, A., Sharma, M., 2023. Production of nanocellulose from corn husk for the development of antimicrobial biodegradable packaging film. Int. J. Biol. Macromol. 242, 124805. https://doi.org/10.1016/j.ijbiomac.2023.124805.
Che Mohamed Hussein, S.N., Jan, B.M., Khalil, M., Amir, Z., Azizi, A., 2024. Surface modification of superparamagnetic nanoparticles for enhanced oil recovery: a review. J. Mol. Liq. 397, 124146. https://doi.org/10.1016/j.molliq.2024.124146.
Chen, Y.-L., Zhang, X., You, T.-T., Xu, F., 2019. Deep eutectic solvents (DESs) for cellulose dissolution: a mini-review. Cellulose 26 (1), 205–213. https://doi.org/10.1007/s10570-018-2130-7.
Chen, X., Shen, M., Yu, Q., Chen, Y., Xie, J., 2024. Recent advance in chemistry modified methods of natural polysaccharides and their applications. Trends Food Sci. Technol. 144, 104317. https://doi.org/10.1016/j.tifs.2023.104317.
Chen, J., Xu, Q., He, F., Yue, W., Hu, G., Gan, J., Xie, H., 2022. Pretreatment of corn stover by levulinic acid-based protic ionic liquids for enhanced enzymatic hydrolysis. ACS Sustain. Chem. Eng. 10 (21), 7134–7148. https://doi.org/10.1021/acssuschemeng.2c01339.
Cheng, M., Qin, Z., Chen, Y., Hu, S., Ren, Z., Zhu, M., 2017. Efficient extraction of cellulose nanocrystals through hydrochloric acid hydrolysis catalyzed by inorganic chlorides under hydrothermal conditions. ACS Sustain. Chem. Eng. 5 (6), 4656–4664. https://doi.org/10.1021/acssuschemeng.6b03194.
Chin, S.F., Jimmy, F.B., Pang, S.C., 2018. Size controlled fabrication of cellulose nanoparticles for drug delivery applications. J. Drug Deliv. Sci. Technol. 43, 262–266. https://doi.org/10.1016/j.jddst.2017.10.021.
Chin, D.W.K., Lim, S., Pang, Y.L., Lim, C.H., Shuit, S.H., Lee, K.M., Chong, C.T., 2021. Effects of organic solvents on the organosolv pretreatment of degraded empty fruit bunch for fractionation and lignin removal. Sustainability 13 (12), 6757. https://doi.org/10.3390/su13126757.
Chorkendorff, I., Niemantsverdriet, J.W., 2003. Concepts of Modern Catalysis and Kinetics. Wiley. https://doi.org/10.1002/3527602658.
Chutia, H., Mahanta, C.L., 2021. Properties of starch nanoparticle obtained by ultrasonication and high pressure homogenization for developing carotenoids-enriched powder and pickering nanoemulsion. Innov. Food Sci. Emerg. Technol. 74, 102822. https://doi.org/10.1016/j.ifset.2021.102822.
Cielecka, I., Ryngajłło, M., Maniukiewicz, W., Bielecki, S., 2021. Highly stretchable bacterial cellulose produced by Komagataeibacter hansenii SI1. Polymers 13 (24), 4455. https://doi.org/10.3390/polym13244455.
Collazo-Bigliardi, S., Ortega-Toro, R., Chiralt Boix, A., 2018. Reinforcement of thermoplastic starch films with cellulose fibres obtained from rice and coffee husks. Journal of Renewable Materials 6 (7), 599–610. https://doi.org/10.32604/JRM.2018.00127.
Collazo-Bigliardi, S., Ortega-Toro, R., Chiralt, A., 2019. Using lignocellulosic fractions of coffee husk to improve properties of compatibilised starch-PLA blend films. Food Packag. Shelf Life 22, 100423. https://doi.org/10.1016/j.fpsl.2019.100423.
Cordt, C., Meckel, T., Geissler, A., Biesalski, M., 2020. Entrapment of hydrophobic biocides into cellulose acetate nanoparticles by nanoprecipitation. Nanomaterials 10 (12), 2447. https://doi.org/10.3390/nano10122447.
Corrêa, A.C., Teodoro, K.B.R., Simão, J.A., Claro, P.I.C., de Morais Teixeira, E., Mattoso, L.H.C., Marconcini, J.M., 2020. Cellulose nanocrystals from curaua fibers and poly[ethylene- <scp> *co* </scp> -(vinyl acetate)] nanocomposites: effect of drying process of CNCs on thermal and mechanical properties. Polym. Compos. 41 (5), 1736–1748. https://doi.org/10.1002/pc.25493.
Crespo, J., Majano-Majano, A., Lara-Bocanegra, A.J., Guaita, M., 2020. Mechanical properties of small clear specimens of Eucalyptus globulus labill. Materials 13 (4), 906. https://doi.org/10.3390/ma13040906.
Cudjoe, E., Hunsen, M., Xue, Z., Way, A.E., Barrios, E., Olson, R.A., Hore, M.J.A., Rowan, S.J., 2017. Miscanthus Giganteus: a commercially viable sustainable source of cellulose nanocrystals. Carbohydr. Polym. 155, 230–241. https://doi.org/10.1016/j.carbpol.2016.08.049.
Culsum, N.T.U., Melinda, C., Leman, I., Wibowo, A., Budhi, Y.W., 2021. Isolation and characterization of cellulose nanocrystals (CNCs) from industrial denim waste using ammonium persulfate. Mater. Today Commun. 26, 101817. https://doi.org/10.1016/j.mtcomm.2020.101817.
Czaikoski, A., da Cunha, R.L., Menegalli, F.C., 2020. Rheological behavior of cellulose nanofibers from cassava peel obtained by combination of chemical and physical processes. Carbohydr. Polym. 248, 116744. https://doi.org/10.1016/j.carbpol.2020.116744.
Dai, Y., van Spronsen, J., Witkamp, G.-J., Verpoorte, R., Choi, Y.H., 2013. Natural deep eutectic solvents as new potential media for green technology. Anal. Chim. Acta 766, 61–68. https://doi.org/10.1016/j.aca.2012.12.019.
Dai, H., Ou, S., Huang, Y., Huang, H., 2018. Utilization of pineapple peel for production of nanocellulose and film application. Cellulose 25 (3), 1743–1756. https://doi.org/10.1007/s10570-018-1671-0.
Dai, J., Xiao, Z., Li, J., Ge, Q., Wang, H., Sha, R., Mao, J., 2023. The structural characteristic of bamboo shoot shell polysaccharides extracted using ultrasound-assisted phosphotungstic acid hydrolysis and its protection against cell oxidative injury. Int. J. Food Sci. Technol. 58 (4), 2115–2129. https://doi.org/10.1111/ijfs.16009.
Das, R., Lindström, T., Sharma, P.R., Chi, K., Hsiao, B.S., 2022. Nanocellulose for sustainable water purification. Chem. Rev. 122 (9), 8936–9031. https://doi.org/10.1021/acs.chemrev.1c00683.
Debnath, B., Duarah, P., Purkait, M.K., 2023. Microwave-assisted quick synthesis of microcrystalline cellulose from black tea waste (Camellia sinensis) and characterization. Int. J. Biol. Macromol. 244, 125354. https://doi.org/10.1016/j.ijbiomac.2023.125354.
Delicano, J.A., 2018. A review on abaca fiber reinforced composites. Compos. Interfaces 25 (12), 1039–1066. https://doi.org/10.1080/09276440.2018.1464856.
Destandau, E., Michel, T., 2022. Chapter 4. Microwave-assisted extraction. In: Prado, J., Rostagno, M. (Eds.), Natural Ppoduction Extraction. Royal Society of Chemistry, pp. 144–201. https://doi.org/10.1039/9781839165894-00144.
Dey, N., Kumar, G., Vickram, A.S., Mohan, M., Singhania, R.R., Patel, A.K., Dong, C.-D., Anbarasu, K., Thanigaivel, S., Ponnusamy, V.K., 2022. Nanotechnology-assisted production of value-added biopotent energy-yielding products from lignocellulosic biomass refinery – a review. Bioresour. Technol. 344, 126171. https://doi.org/10.1016/j.biortech.2021.126171.
Dhali, K., Ghasemlou, M., Daver, F., Cass, P., Adhikari, B., 2021. A review of nanocellulose as a new material towards environmental sustainability. Sci. Total Environ. 775, 145871. https://doi.org/10.1016/j.scitotenv.2021.145871.
Dilamian, M., Noroozi, B., 2021. Rice straw agri-waste for water pollutant adsorption: relevant mesoporous super hydrophobic cellulose aerogel. Carbohydr. Polym. 251, 117016. https://doi.org/10.1016/j.carbpol.2020.117016.
Djafari Petroudy, S.R., Chabot, B., Loranger, E., Naebe, M., Shojaeiarani, J., Gharehkhani, S., Ahvazi, B., Hu, J., Thomas, S., 2021. Recent advances in cellulose nanofibers preparation through energy-efficient approaches: a review. Energies 14 (20), 6792. https://doi.org/10.3390/en14206792.
Druetta, P., Picchioni, F., 2019. Polymer and nanoparticles flooding as a new method for enhanced oil recovery. J. Petrol. Sci. Eng. 177, 479–495. https://doi.org/10.1016/j.petrol.2019.02.070.
Du, H., Liu, C., Mu, X., Gong, W., Lv, D., Hong, Y., Si, C., Li, B., 2016. Preparation and characterization of thermally stable cellulose nanocrystals via a sustainable approach of FeCl3-catalyzed formic acid hydrolysis. Cellulose 23 (4), 2389–2407. https://doi.org/10.1007/s10570-016-0963-5.
Dungani, R., Owolabi, A.F., Saurabh, C.K., Khalil, H.P.S.A., Tahir, P.M., Hazwan, C.I.C.M., Ajijolakewu, K.A., Masri, M.M., Rosamah, E., Aditiawati, P., 2017. Preparation and fundamental characterization of cellulose nanocrystal from oil palm fronds biomass. J. Polym. Environ. 25 (3), 692–700. https://doi.org/10.1007/s10924-016-0854-8.
Durán-Valencia, C., Bai, B., Reyes, H., Fajardo-López, R., Barragán-Aroche, F., López-Ramírez, S., 2014. Development of enhanced nanocomposite preformed particle gels for conformance control in high-temperature and high-salinity oil reservoirs. Polym. J. 46 (5), 277–284. https://doi.org/10.1038/pj.2013.99.
Dwivedi, M., Dwivedi, J., Shen, S., Dwivedi, P., Guangli, L., Xiarong, X., 2022. Emerging application of nanocelluloses for microneedle devices. In: Handbook of Nanocelluloses. Springer International Publishing, pp. 335–359. https://doi.org/10.1007/978-3-030-89621-8_33.
Ebrahimi, R., Fathi, M., Ghoddusi, H.B., 2024. Pickering emulsions stabilized by cellulose nanocrystals extracted from hazelnut shells: production and stability under different harsh conditions. Int. J. Biol. Macromol. 258, 128982. https://doi.org/10.1016/j.ijbiomac.2023.128982.
El Amri, A., Ouass, A., bensalah, jaouad, Wardighi, Z., Zahra Bouhassane, F., Zarrouk, A., Habsaoui, A., Rifi, E.-H., Lebkiri, A., 2023. Extraction and characterization of cellulosic nanocrystals from stems of the reed plant large-leaved cattail (Typha latifolia). Mater. Today Proc. 72, 3609–3616. https://doi.org/10.1016/j.matpr.2022.08.408.
Emenike, E.C., Iwuozor, K.O., Saliu, O.D., Ramontja, J., Adeniyi, A.G., 2023. Advances in the extraction, classification, modification, emerging and advanced applications of crystalline cellulose: a review. Carbohydrate Polymer Technologies and Applications 6, 100337. https://doi.org/10.1016/j.carpta.2023.100337.
Emmanuel, M., 2024. Unveiling the revolutionary role of nanoparticles in the oil and gas field: unleashing new avenues for enhanced efficiency and productivity. Heliyon 10 (13), e33957. https://doi.org/10.1016/j.heliyon.2024.e33957.
Espino-Pérez, E., Domenek, S., Belgacem, N., Sillard, C., Bras, J., 2014. Green process for chemical functionalization of nanocellulose with carboxylic acids. Biomacromolecules 15 (12), 4551–4560. https://doi.org/10.1021/bm5013458.
Espinosa, S.C., Kuhnt, T., Foster, E.J., Weder, C., 2013. Isolation of thermally stable cellulose nanocrystals by phosphoric acid hydrolysis. Biomacromolecules 14 (4), 1223–1230. https://doi.org/10.1021/bm400219u.
Etale, A., Onyianta, A.J., Turner, S.R., Eichhorn, S.J., 2023. Cellulose: a review of water interactions, applications in composites, and water treatment. Chem. Rev. 123 (5), 2016–2048. https://doi.org/10.1021/acs.chemrev.2c00477.
Evans, S.K., Wesley, O.N., Nathan, O., Moloto, M.J., 2019. Chemically purified cellulose and its nanocrystals from sugarcane baggase: isolation and characterization. Heliyon 5 (10), e02635. https://doi.org/10.1016/j.heliyon.2019.e02635.
Eyley, S., Thielemans, W., 2014. Surface modification of cellulose nanocrystals. Nanoscale 6 (14), 7764–7779. https://doi.org/10.1039/C4NR01756K.
Fakher, S., Ahdaya, M., Elturki, M., Imqam, A., Elgahawy, Y., 2019. The effect of unconventional oil reservoirs' nano pore size on the stability of asphaltene during carbon dioxide injection. Day. https://doi.org/10.7122/CMTC-558486-MS.
Ferreira, J.A., Taherzadeh, M.J., 2020. Improving the economy of lignocellulose-based biorefineries with organosolv pretreatment. Bioresour. Technol. 299, 122695. https://doi.org/10.1016/j.biortech.2019.122695.
Filipova, I., Serra, F., Tarrés, Q., Mutjé, P., Delgado-Aguilar, M., 2020. Oxidative treatments for cellulose nanofibers production: a comparative study between TEMPO-Mediated and ammonium persulfate oxidation. Cellulose 27 (18), 10671–10688. https://doi.org/10.1007/s10570-020-03089-7.
Filpponen, I., Argyropoulos, D.S., 2010. Regular linking of cellulose nanocrystals via click chemistry: synthesis and formation of cellulose nanoplatelet gels. Biomacromolecules 11 (4), 1060–1066. https://doi.org/10.1021/bm1000247.
Fisher, K.E., Hellmich, R.L., Bradbury, S.P., 2020. Estimates of common milkweed (Asclepias syriaca) utilization by monarch larvae (Danaus plexippus) and the

significance of larval movement. J. Insect Conserv. 24 (2), 297–307. https://doi.org/10.1007/s10841-019-00213-2.
Florea, M., Hagemann, H., Santosa, G., Abbott, J., Micklem, C.N., Spencer-Milnes, X., de Arroyo Garcia, L., Paschou, D., Lazenbatt, C., Kong, D., Chughtai, H., Jensen, K., Freemont, P.S., Kitney, R., Reeve, B., Ellis, T., 2016. Engineering control of bacterial cellulose production using a genetic toolkit and a new cellulose-producing strain. Proc. Natl. Acad. Sci. 113 (24). https://doi.org/10.1073/pnas.1522985113.
Foo, M.L., Tan, C.R., Lim, P.D., Ooi, C.W., Tan, K.W., Chew, I.M.L., 2019. Surface-modified nanocrystalline cellulose from oil palm empty fruit bunch for effective binding of curcumin. Int. J. Biol. Macromol. 138, 1064–1071. https://doi.org/10.1016/j.ijbiomac.2019.07.035.
Gan, P.G., Sam, S.T., Abdullah, M.F., Omar, M.F., Tan, L.S., 2020. An alkaline deep eutectic solvent based on potassium carbonate and glycerol as pretreatment for the isolation of cellulose nanocrystals from empty fruit bunch. Bioresources 15 (1), 1154–1170. https://doi.org/10.15376/biores.15.1.1154-1170.
Ganapathy, T., Sathiskumar, R., Senthamaraikannan, P., Saravanakumar, S.S., Khan, A., 2019. Characterization of raw and alkali treated new natural cellulosic fibres extracted from the aerial roots of banyan tree. Int. J. Biol. Macromol. 138, 573–581. https://doi.org/10.1016/j.ijbiomac.2019.07.136.
García, A., Labidi, J., Belgacem, M.N., Bras, J., 2017. The nanocellulose biorefinery: woody versus herbaceous agricultural wastes for NCC production. Cellulose 24 (2), 693–704. https://doi.org/10.1007/s10570-016-1144-2.
Garcia-Garcia, D., Lopez-Martinez, J., Balart, R., Strömberg, E., Moriana, R., 2018. Reinforcing capability of cellulose nanocrystals obtained from pine cones in a biodegradable poly(3-hydroxybutyrate)/poly(ε-caprolactone) (PHB/PCL) thermoplastic blend. Eur. Polym. J. 104, 10–18. https://doi.org/10.1016/j.eurpolymj.2018.04.036.
Gbadamosi, A.O., Kiwalabye, J., Junin, R., Augustine, A., 2018. A review of gas enhanced oil recovery schemes used in the North Sea. J. Pet. Explor. Prod. Technol. 8 (4), 1373–1387. https://doi.org/10.1007/s13202-018-0451-6.
Gbadamosi, A.O., Junin, R., Manan, M.A., Agi, A., Oseh, J.O., Usman, J., 2019. Synergistic application of aluminium oxide nanoparticles and oilfield polyacrylamide for enhanced oil recovery. J. Petrol. Sci. Eng. 182, 106345. https://doi.org/10.1016/j.petrol.2019.106345.
Gbadamosi, A., Yusuff, A., Agi, A., Muruga, P., Junin, R., Jeffrey, O., 2022. Mechanistic study of nanoparticles-assisted xanthan gum polymer flooding for enhanced oil recovery: a comparative study. J. Pet. Explor. Prod. Technol. 12 (1), 207–213. https://doi.org/10.1007/s13202-021-01334-8.
Gbonhinbor, J.R., Yelebe, Z.R., Obuebite, A.A., Agi, A., 2023. Variations in formation resistivity and geometric tortuosity factors for consolidated Niger Delta formations. Nat. Resour. Res. 32 (3), 1093–1109. https://doi.org/10.1007/s11053-023-10181-9.
Gbonhinbor, J.R., Yelebe, Z.R., Yousuo, D., Agi, A., 2025. Rheological evaluation of natural polysaccharide-based biopolymers through porous media. Colloid Polym. Sci. 303 (7), 1155–1169. https://doi.org/10.1007/s00396-025-05412-9.
Ge, W., Shuai, J., Wang, Y., Zhou, Y., Wang, X., 2022. Progress on chemical modification of cellulose in "green" solvents. Polym. Chem. 13 (3), 359–372. https://doi.org/10.1039/D1PY00879J.
George, J., Sabapathi, S.N., 2015. Cellulose nanocrystals: synthesis, functional properties, and applications. Nanotechnol. Sci. Appl. 45. https://doi.org/10.2147/NSA.S64386.
George, S., Thomas, S., Nandanan Nedumpillil, N., Jose, S., 2023. Extraction and characterization of fibers from water hyacinth stem using a custom-made decorticator. J. Nat. Fibers 20 (2). https://doi.org/10.1080/15440478.2023.2212927.
Gholinezhad, S., Kantzas, A., Bryant, S.L., 2022. Effect of surface functionalized silica nanoparticles on interfacial behavior: wettability, interfacial tension and emulsification characteristics. J. Mol. Liq. 349, 118220. https://doi.org/10.1016/j.molliq.2021.118220.
Gicquel, E., Bras, J., Rey, C., Putaux, J.-L., Pignon, F., Jean, B., Martin, C., 2019. Impact of sonication on the rheological and colloidal properties of highly concentrated cellulose nanocrystal suspensions. Cellulose 26 (13–14), 7619–7634. https://doi.org/10.1007/s10570-019-02622-7.
Glińska, K., Gitalt, J., Torrens, E., Plechkova, N., Bengoa, C., 2021. Extraction of cellulose from corn stover using designed ionic liquids with improved reusing capabilities. Process Saf. Environ. Prot. 147, 181–191. https://doi.org/10.1016/j.psep.2020.09.035.
Gomri, C., Cretin, M., Semsarilar, M., 2022. Recent progress on chemical modification of cellulose nanocrystal (CNC) and its application in nanocomposite films and membranes-A comprehensive review. Carbohydr. Polym. 294, 119790. https://doi.org/10.1016/j.carbpol.2022.119790.
Gopinath, R., Billigraham, P., Sathishkumar, T.P., Sanjay, M.R., Siengchin, S., 2022. Characterization of *Sida acuta* fiber and its polymer composites with effect of fly ash. J. Nat. Fibers 19 (14), 8811–8829. https://doi.org/10.1080/15440478.2021.1967833.
Gunathilake, T.M.S.U., Ching, Y.C., Uyama, H., Nguyen, D.H., Chuah, C.H., 2021. Investigations on the interactions of proteins with nanocellulose produced via sulphuric acid hydrolysis. Int. J. Biol. Macromol. 193, 1522–1531. https://doi.org/10.1016/j.ijbiomac.2021.10.215.
Gungoren, C., Ozkan, S.G., Ozdemir, O., 2024. Use of ultrasound in physical and chemical mineral processing operations. In: Ikhmayies, S.J. (Ed.), Advances in Minerals Research. Springer, pp. 25–54. https://doi.org/10.1007/978-3-031-49175-7_2.
Gunjan, C., Manikanika, L., 2023. Extraction of cellulose from agro waste – a short review. Mater. Today Proc. 92, 233–239. https://doi.org/10.1016/j.matpr.2023.04.378.
Guo, S., Kumar Awasthi, M., Wang, Y., Xu, P., 2021. Current understanding in conversion and application of tea waste biomass: a review. Bioresour. Technol. 338, 125530. https://doi.org/10.1016/j.biortech.2021.125530.
Gupta, U.S., Tiwari, S., 2024. Mechanical and surface characterization of sisal fibers after cold glow discharge argon plasma treatment. Biomass Convers. Biorefinery 14 (8), 9163–9177. https://doi.org/10.1007/s13399-022-03247-w.
Habibi, Y., 2014. Key advances in the chemical modification of nanocelluloses. Chem. Soc. Rev. 43 (5), 1519–1542. https://doi.org/10.1039/C3CS60204D.
Habibi, Y., Lucia, L.A., Rojas, O.J., 2010. Cellulose nanocrystals: chemistry, Self-assembly, and applications. Chem. Rev. 110 (6), 3479–3500. https://doi.org/10.1021/cr900339w.
Hadou, A., Belaadi, A., Alshahrani, H., Khan, M.K.A., 2024. Extraction and characterization of novel cellulose fibers from dracaena draco plant. Mater. Chem. Phys. 313, 128790. https://doi.org/10.1016/j.matchemphys.2023.128790.
Haji Badri, K., 2016. Thermal behaviors of oil palm empty fruit BUNCH fiber upon exposure to acid-base aqueous solutions. Malays. J. Anal. Sci. 20 (5), 1095–1103. https://doi.org/10.17576/mjas-2016-2005-15.
Hajiali, F., Jin, T., Yang, G., Santos, M., Lam, E., Moores, A., 2022. Mechanochemical transformations of biomass into functional materials. ChemSusChem 15 (7). https://doi.org/10.1002/cssc.202102535.
Haldar, D., Dey, P., Thomas, J., Singhania, R.R., Patel, A.K., 2022. One pot bioprocessing in lignocellulosic biorefinery: a review. Bioresour. Technol. 365, 128180. https://doi.org/10.1016/j.biortech.2022.128180.
Hardiningtyas, S.D., Putra, B.U., Anggara, K.B., Yuniasani, I., Ramadhan, W., Pari, R.F., Uju, Hastuti, N., Indrawan, D.A., Wakabayashi, R., Goto, M., Kamiya, N., 2024. Sustainable synthesis of cellulose nanofibers from industrial agar seaweed waste biomass using hydrated deep eutectic solvents. Waste Biomass Valoriz. 15 (8), 4899–4913. https://doi.org/10.1007/s12649-024-02499-z.
Harini, U., Harish, S., Harishankar, A., Buvaneswaran, M., Sinija, V.R., 2024. Extraction and characterization of microcrystalline cellulose from wine waste. Food Bioprod. Process. 144, 92–101. https://doi.org/10.1016/j.fbp.2024.01.001.
Hastuti, N., Kanomata, K., Kitaoka, T., 2018. Hydrochloric acid hydrolysis of pulps from oil palm empty fruit bunches to produce cellulose nanocrystals. J. Polym. Environ. 26 (9), 3698–3709. https://doi.org/10.1007/s10924-018-1248-x.
Haunreiter, K.J., Dichiara, A.B., Gustafson, R., 2022. Nanocellulose by ammonium persulfate oxidation: an alternative to TEMPO-mediated oxidation. ACS Sustain. Chem. Eng. 10 (12), 3882–3891. https://doi.org/10.1021/acssuschemeng.1c07814.
Haunreiter, K.J., Dichiara, A.B., Gustafson, R., 2024. Ammonium persulfate oxidized nanofibrillated cellulose as a sustainable wet-end paper reinforcement additive. Sustain. Mater. Technol. 41, e01007. https://doi.org/10.1016/j.susmat.2024.e01007.
Heggset, E.B., Chinga-Carrasco, G., Syverud, K., 2017. Temperature stability of nanocellulose dispersions. Carbohydr. Polym. 157, 114–121. https://doi.org/10.1016/j.carbpol.2016.09.077Heinze.
Heinze, T., El Seoud, O.A., Koschella, A., 2018. Production and Characteristics of Cellulose from Different Sources. In: Heinze, T., El, Seoud, Koschella, A. (Eds.), Springer Series on Polymer and Composite Materials. Springer, pp. 1–38. https://doi.org/10.1007/978-3-319-73168-1_1.
Hemida, M.H., Moustafa, H., Mehanny, S., Morsy, M., Dufresne, A., Rahman, E.N.A.E.L., Ibrahim, M.M., 2023. Cellulose nanocrystals from agricultural residues (Eichhornia crassipes): extraction and characterization. Heliyon 9 (6), e16436. https://doi.org/10.1016/j.heliyon.2023.e16436.
Hermsdorff, G.B., Escobar, E.L.N., da Silva, T.A., Filho, A.Z., Corazza, M.L., Ramos, L.P., 2023. Ethanol organosolv pretreatment of sugarcane bagasse assisted by organic acids and supercritical carbon dioxide. Carbohydr. Polym. 300, 120263. https://doi.org/10.1016/j.carbpol.2022.120263.
Hernández, J.A., Romero, V.H., Escalante, A., Toriz, G., Rojas, O.J., Sulbarán, B.C., 2018. Agave tequilana bagasse as source of cellulose nanocrystals via organosolv treatment. Bioresources 13 (2). https://doi.org/10.15376/biores.13.2.3603-3614.
Hernández, E., Valero, E., Rodríguez, I., Guerra, E., Espinoza, J., Briceño, R., Veliz, A., 2020. Enhancing the Recovery of an Extra Heavy Oil Reservoir by Using Low Salinity Polymer Flooding. https://doi.org/10.2118/199014-MS. Day 1 Mon, July 27, 2020.
Ho, B.-K., Chin, S.-F., Pang, S.-C., 2020. pH-responsive carboxylic cellulose acetate nanoparticles for controlled release of penicillin G. J. Sci. Adv. Mater. Devices 5 (2), 224–232. https://doi.org/10.1016/j.jsamd.2020.04.002.
Hongrattanavichit, I., Aht-Ong, D., 2020. Nanofibrillation and characterization of sugarcane bagasse agro-waste using water-based steam explosion and high-pressure homogenization. J. Clean. Prod. 277, 123471. https://doi.org/10.1016/j.jclepro.2020.123471.
Houfani, A.A., Anders, N., Spiess, A.C., Baldrian, P., Benallaoua, S., 2020. Insights from enzymatic degradation of cellulose and hemicellulose to fermentable sugars– a review. Biomass Bioenergy 134, 105481. https://doi.org/10.1016/j.biombioe.2020.105481.
Hu, R., Tang, S., Mpelwa, M., Jiang, Z., Feng, S., 2021. Research progress of viscoelastic surfactants for enhanced oil recovery. Energy Explor. Exploit. 39 (4), 1324–1348. https://doi.org/10.1177/0144598720980209.

Hu, X., Ma, T., Lu, S., Song, Y., 2022. Studies into interactions and interfacial characteristics between cellulose nanocrystals and bovine serum albumin. Food Chem. X 13, 100194. https://doi.org/10.1016/j.fochx.2021.100194.

Huang, W., 2018. Cellulose nanopapers. In: Huang, W.Y. (Ed.), Nanopapers. Elsevier, pp. 121–173. https://doi.org/10.1016/B978-0-323-48019-2.00005-0.

Ibrahim, N.I., Sultan, M.T.H., Łukaszewicz, A., Shah, A.U.M., Shahar, F.S., Józwik, J., Najeeb, M.I., Grzejda, R., 2024. Characterization and isolation method of Gigantochloa scortechinii (Buluh Semantan) cellulose nanocrystals. Int. J. Biol. Macromol. 272, 132847. https://doi.org/10.1016/j.ijbiomac.2024.132847.

Imuetinyan, H., Agi, A., Gbadamosi, A., Junin, R., Oseh, J., 2022. Oil-water interfacial tension, wettability alteration and foaming studies of natural surfactant extracted from Vernonia Amygdalina. Pet. Res. 7 (3), 350–356. https://doi.org/10.1016/j.ptlrs.2021.12.006.

Indirasetyo, N.L., Kusmono, 2022. Isolation and properties of cellulose nanocrystals fabricated by ammonium persulfate oxidation from Sansevieria trifasciata fibers. Fibers 10 (7), 61. https://doi.org/10.3390/fib10070061.

Ishak, W.W., Ahmad, I., Ramli, S., Amin, M.M., 2018. Gamma irradiation-assisted synthesis of cellulose nanocrystal-reinforced gelatin hydrogels. Nanomaterials 8 (10), 749. https://doi.org/10.3390/nano8100749.

Islam, T., Peng, C., Ali, I., Li, J., Khan, Z.M., Sultan, M., Naz, I., 2021. Synthesis of rice husk-derived magnetic biochar through liquefaction to adsorb anionic and cationic dyes from aqueous solutions. Arabian J. Sci. Eng. 46 (1), 233–246. https://doi.org/10.1007/s13369-020-04537-z.

Jakobsen, T.D., Simon, S., Heggset, E.B., Syverud, K., Paso, K., 2018. Interactions between surfactants and cellulose nanofibrils for enhanced oil recovery. Ind. Eng. Chem. Res. 57 (46), 15749–15758. https://doi.org/10.1021/acs.iecr.8b04206.

Jaouahar, M., Ablouh, E.-H., Hanani, Z., Jaklič, B., Spreitzer, M., Semlali, F.-Z., Ait Benhamou, A., Samih, Y., El Achaby, M., Sehaqui, H., 2024. Preparation and characterization of sulfated nanocellulose: from hydrogels to highly transparent films. Int. J. Biol. Macromol. 260, 129464. https://doi.org/10.1016/j.ijbiomac.2024.129464.

Ji, H., Xiang, Z., Qi, H., Han, T., Pranovich, A., Song, T., 2019. Strategy towards one-step preparation of carboxylic cellulose nanocrystals and nanofibrils with high yield, carboxylation and highly stable dispersibility using innocuous citric acid. Green Chem. 21 (8), 1956–1964. https://doi.org/10.1039/C8GC03493A.

Jiang, J., Zhu, Y., Jiang, F., 2021. Sustainable isolation of nanocellulose from cellulose and lignocellulosic feedstocks: recent progress and perspectives. Carbohydr. Polym. 267, 118188. https://doi.org/10.1016/j.carbpol.2021.118188.

Jiang, K., Xiong, C., Ding, B., Geng, X., Liu, W., Chen, W., Huang, T., Xu, H., Xu, Q., Liang, B., 2023. Nanomaterials in EOR: a review and future perspectives in unconventional reservoirs. Energy Fuels 37 (14), 10045–10060. https://doi.org/10.1021/acs.energyfuels.3c01146.

Jing, L., Shi, T., Chang, Y., Meng, X., He, S., Xu, H., Yang, S., Liu, J., 2024. Cellulose-based materials in environmental protection: a scientometric and visual analysis review. Sci. Total Environ. 929, 172576. https://doi.org/10.1016/j.scitotenv.2024.172576.

Judith, R.-B.D., Pámanes-Carrasco, G.A., Delgado, E., Rodríguez-Rosales, M.D.J., Medrano-Roldán, H., Reyes-Jáquez, D., 2022. Extraction optimization and molecular dynamic simulation of cellulose nanocrystals obtained from bean forage. Biocatal. Agric. Biotechnol. 43, 102443. https://doi.org/10.1016/j.bcab.2022.102443.

Junior de Menezes, A., Siqueira, G., Curvelo, A.A.S., Dufresne, A., 2009. Extrusion and characterization of functionalized cellulose whiskers reinforced polyethylene nanocomposites. Polymer 50 (19), 4552–4563. https://doi.org/10.1016/j.polymer.2009.07.038.

Kalia, S., Boufi, S., Celli, A., Kango, S., 2014. Nanofibrillated cellulose: surface modification Judithand potential applications. Colloid Polym. Sci. 292 (1), 5–31. https://doi.org/10.1007/s00396-013-3112-9.

Kallel, F., Bettaieb, F., Khiari, R., García, A., Bras, J., Chaabouni, S.E., 2016. Isolation and structural characterization of cellulose nanocrystals extracted from garlic straw residues. Ind. Crop. Prod. 87, 287–296. https://doi.org/10.1016/j.indcrop.2016.04.060.

Kamelnia, E., Divsalar, A., Darroudi, M., Yaghmaei, P., Sadri, K., 2019. Production of new cellulose nanocrystals from Ferula gummosa and their use in medical applications via investigation of their biodistribution. Ind. Crop. Prod. 139, 111538. https://doi.org/10.1016/j.indcrop.2019.111538.

Kameshwar, A.K.S., Qin, W., 2018. Comparative study of genome-wide plant biomass-degrading CAZymes in white rot, brown rot and soft rot fungi. Mycology 9 (2), 93–105. https://doi.org/10.1080/21501203.2017.1419296.

Kandhola, G., Djioleu, A., Rajan, K., Labbé, N., Sakon, J., Carrier, D.J., Kim, J.-W., 2020. Maximizing production of cellulose nanocrystals and nanofibers from pre-extracted loblolly pine kraft pulp: a response surface approach. Bioresources and Bioprocessing 7 (1), 19. https://doi.org/10.1186/s40643-020-00302-0.

Kassab, Z., Abdellaoui, Y., Salim, M.H., Bouhfid, R., Qaiss, A.E.K., El Achaby, M., 2020. Micro- and nano-celluloses derived from hemp stalks and their effect as polymer reinforcing materials. Carbohydr. Polym. 245, 116506. https://doi.org/10.1016/j.carbpol.2020.116506.

Kedzior, S.A., Gabriel, V.A., Dubé, M.A., Cranston, E.D., 2021. Nanocellulose in emulsions and heterogeneous water-based polymer systems: a review. Adv. Mater. 33 (28). https://doi.org/10.1002/adma.202002404.

Keshu, Rani, M., Yadav, Meenu, J., Chaudhary, S., Shanker, U., 2021. An updated review on synthetic approaches of green nanomaterials and their application for removal of water pollutants: current challenges, assessment and future perspectives. J. Environ. Chem. Eng. 9 (6), 106763. https://doi.org/10.1016/j.jece.2021.106763.

Khan, P., Ali, S., Jan, R., Kim, K.-M., 2024. Lignin nanoparticles: transforming environmental remediation. Nanomaterials 14 (18), 1541. https://doi.org/10.3390/nano14181541.

Kian, L.K., Saba, N., Jawaid, M., Fouad, H., 2020. Characterization of microcrystalline cellulose extracted from olive fiber. Int. J. Biol. Macromol. 156, 347–353. https://doi.org/10.1016/j.ijbiomac.2020.04.015.

Klochko, N.P., Barbash, V.A., Klepikova, K.S., Kopach, V.R., Tyukhov, I.I., Yashchenko, O.V., Zhadan, D.O., Petrushenko, S.I., Dukarov, S.V., Lyubov, V.M., Khrypunova, A.L., 2020. Use of biomass for a development of nanocellulose-based biodegradable flexible thin film thermoelectric material. Sol. Energy 201, 21–27. https://doi.org/10.1016/j.solener.2020.02.091.

Korolovych, V.F., Cherpak, V., Nepal, D., Ng, A., Shaikh, N.R., Grant, A., Xiong, R., Bunning, T.J., Tsukruk, V.V., 2018. Cellulose nanocrystals with different morphologies and chiral properties. Polymer 145, 334–347. https://doi.org/10.1016/j.polymer.2018.04.064.

Kumar, R., Dao, E., Mohanty, K.K., 2010. Emulsion Flooding of Heavy Oil. All Days. https://doi.org/10.2118/129914-MS.

Kumar, A., Kumar, P., Manoharan, N., 2014. Launch of new cement brand in existing market. Biosci. Biotechnol. Res. Asia 11 (SE). https://doi.org/10.13005/bbra/1384, 01–08.

Kumar, R., Sharma, R. Kr, Singh, A.P., 2017. Cellulose based grafted biosorbents - journey from lignocellulose biomass to toxic metal ions sorption applications - a review. J. Mol. Liq. 232, 62–93. https://doi.org/10.1016/j.molliq.2017.02.050.

Kumar, N., Ali, S., Kumar, A., Mandal, A., 2020. Design and formulation of surfactant stabilized O/W emulsion for application in enhanced oil recovery: effect of pH, salinity and temperature. Oil & Gas Science and Technology – Revue d'IFP Energies Nouvelles 75, 72. https://doi.org/10.2516/ogst/2020066.

Kumar, G., Upadhyay, S., Yadav, D.K., Malakar, S., Dhurve, P., Suri, S., 2023. Application of ultrasound technology for extraction of color pigments from plant sources and their potential bio-functional properties: a review. J. Food Process. Eng. 46 (6). https://doi.org/10.1111/jfpe.14238.

Kumar, A., Dutta, D., Kalita, D., Majumdar, B., Saikia, S.P., Banik, D., 2024. Extraction, physicochemical and structural characterisation of palm grass leaf fibres for sustainable and cleaner production of textile and allied cellulosic applications. J. Clean. Prod. 448, 141733. https://doi.org/10.1016/j.jclepro.2024.141733.

Kumari, P., Seth, R., Meena, A., Sharma, D., 2023. Enzymatic synthesis of cellulose nanocrystals from lemongrass and its application in improving anti-cancer drug release, uptake and efficacy. Ind. Crop. Prod. 192, 115933. https://doi.org/10.1016/j.indcrop.2022.115933.

Kusmono, Listyanda, R.F., Wildan, M.W., Ilman, M.N., 2020. Preparation and characterization of cellulose nanocrystal extracted from ramie fibers by sulfuric acid hydrolysis. Heliyon 6 (11), e05486. https://doi.org/10.1016/j.heliyon.2020.e05486.

Lani, N.S., Ngadi, N., 2014. Extraction and characterization of cellulose from empty fruit bunch (EFB) fiber. Jurnal Teknologi 68 (5).

Lanjewar, S., Mukherjee, A., Khandewal, P., Ghosh, A.K., Mullick, A., Moulik, S., Roy, A., 2021. Thermodynamics of synthesis and separation performance of interfacially polymerized ªlooseº reverse osmosis membrane: benchmarking for greywater treatment. Chem. Eng. J. 417, 127929. https://doi.org/10.1016/j.cej.2020.127929.

Lashari, N., Hussain, T., Ganat, T., Kalam, S., Hussain, K., Aslam, S., Ahmed, S., 2024. Synergistic effect of graphene oxide and partially hydrolyzed polyacrylamide for enhanced oil recovery: merging coreflood experimental and CFD modeling approaches. J. Mol. Liq. 394, 123733. https://doi.org/10.1016/j.molliq.2023.123733.

Lasseuguette, E., 2008. Grafting onto microfibrils of native cellulose. Cellulose 15 (4), 571–580. https://doi.org/10.1007/s10570-008-9200-1.

Leboucher, J., Bazin, P., Goux, D., El Siblani, H., Travert, A., Barbulée, A., Bréard, J., Duchemin, B., 2020. High-yield cellulose hydrolysis by HCl vapor: co-crystallization, deuterium accessibility and high-temperature thermal stability. Cellulose 27 (6), 3085–3105. https://doi.org/10.1007/s10570-020-03002-2.

Ledyastuti, M., Jason, J., Aditama, R., 2021. Effect of nanocellulose on water-oil interfacial tension. Key Eng. Mater. 874, 13–19. https://doi.org/10.4028/www.scientific.net/KEM.874.13.

Lee, H.V., Hamid, S.B.A., Zain, S.K., 2014. Conversion of lignocellulosic biomass to nanocellulose: structure and chemical process. Sci. World J. 1–20. https://doi.org/10.1155/2014/631013. 2014.

Lee, M., Heo, M.H., Lee, H., Lee, H.-H., Jeong, H., Kim, Y.-W., Shin, J., 2018. Facile and eco-friendly extraction of cellulose nanocrystals *via* electron beam irradiation followed by high-pressure homogenization. Green Chem. 20 (11), 2596–2610. https://doi.org/10.1039/C8GC00577J.

Lee, K.M., Quek, J.D., Tey, W.Y., Lim, S., Kang, H.-S., Quen, L.K., Mahmood, W.A.W., Jamaludin, S.I.S., Teng, K.H., Khoo, K.S., 2022. Biomass valorization by integrating ultrasonication and deep eutectic solvents: delignification, cellulose digestibility and solvent reuse. Biochem. Eng. J. 187, 108587. https://doi.org/10.1016/j.bej.2022.108587.

Lee, H.V., Yazid, N.A., Bin Johan, M.R., 2024. Cellulose and hemicellulose: types, cleavage, and depolymerization. In: Rahimpour, M.R., Bakhtyari, A., Makarem, M.A. (Eds.), Advances in Hydrotreating for Integrated Biofuel Production. Elsevier, pp. 51–75. https://doi.org/10.1016/B978-0-443-19076-6.00003-0.

Leszczyńska, A., Radzik, P., Szefer, E., Mičušík, M., Omastová, M., Pielichowski, K., 2019. Surface modification of cellulose nanocrystals with succinic anhydride. Polymers 11 (5), 866. https://doi.org/10.3390/polym11050866.

Levitt, D.B., Pope, G.A., 2008. Selection and Screening of Polymers for Enhanced-Oil Recovery. *All Days*. https://doi.org/10.2118/113845-MS.
Li, B., Xu, W., Kronlund, D., Määttänen, A., Liu, J., Smått, J.-H., Peltonen, J., Willför, S., Mu, X., Xu, C., 2015. Cellulose nanocrystals prepared via formic acid hydrolysis followed by TEMPO-mediated oxidation. Carbohydr. Polym. 133, 605–612. https://doi.org/10.1016/j.carbpol.2015.07.033.
Li, M.-C., Mei, C., Xu, X., Lee, S., Wu, Q., 2016. Cationic surface modification of cellulose nanocrystals: toward tailoring dispersion and interface in carboxymethyl cellulose films. Polymer 107, 200–210. https://doi.org/10.1016/j.polymer.2016.11.022.
Li, Q., Wei, B., Lu, L., Li, Y., Wen, Y., Pu, W., Li, H., Wang, C., 2017. Investigation of physical properties and displacement mechanisms of surface-grafted nanocellulose fluids for enhanced oil recovery. Fuel 207, 352–364. https://doi.org/10.1016/j.fuel.2017.06.103.
Li, X., Liu, Y., Hao, J., Wang, W., 2018. Study of almond shell characteristics. Materials 11 (9), 1782. https://doi.org/10.3390/ma11091782.
Li, H., Ge, W., Zhang, J., Kasomo, R.M., Leng, J., Weng, X., Chen, Q., Gao, Q., Song, S., Xiao, L., Tian, C., 2020. Control foaming performance of phosphate rocks used for wet-process of phosphoric acid production by phosphoric acid. Hydrometallurgy 195, 105364. https://doi.org/10.1016/j.hydromet.2020.105364.
Li, P., Wang, Y., Hou, Q., Liu, H., Lei, H., Jian, B., Li, X., 2020. Preparation of cellulose nanofibrils from okara by high pressure homogenization method using deep eutectic solvents. Cellulose 27 (5), 2511–2520. https://doi.org/10.1007/s10570-019-02929-5.
Li, M., Wu, Q., Moon, R.J., Hubbe, M.A., Bortner, M.J., 2021. Rheological aspects of cellulose nanomaterials: governing factors and emerging applications. Adv. Mater. 33 (21). https://doi.org/10.1002/adma.202006052.
Li, Z., Kang, W.-L., Li, M.-L., Yang, H.-B., Zhu, T.-Y., He, Y.-Q., Jiang, H.-Z., Zhou, B.-B., Hao, J.-T., 2023. Surface-functionalized cellulose nanocrystals (CNC) and synergisms with surfactant for enhanced oil recovery in low-permeability reservoirs. Pet. Sci. 20 (3), 1572–1583. https://doi.org/10.1016/j.petsci.2022.11.010.
Lim, W.-L., Gunny, A.A.N., Kasim, F.H., AlNashef, I.M., Arbain, D., 2019. Alkaline deep eutectic solvent: a novel green solvent for lignocellulose pulping. Cellulose 26 (6), 4085–4098. https://doi.org/10.1007/s10570-019-02346-8.
Lima, A.R., Cristofoli, N.L., da Costa, A.M.R., Saraiva, J.A., Vieira, M.C., 2023. Comparative study of the production of cellulose nanofibers from agro-industrial waste streams of Salicornia ramosissima by acid and enzymatic treatment. Food Bioprod. Process. 137, 214–225. https://doi.org/10.1016/j.fbp.2022.11.012.
Lin, D., Fu, Y., Li, X., Wang, L., Hou, M., Hu, D., Li, Q., Zhang, Z., Xu, C., Qiu, S., Wang, Z., Boczkaj, G., 2022. Application of persulfate-based oxidation processes to address diverse sustainability challenges: a critical review. J. Hazard Mater. 440, 129722. https://doi.org/10.1016/j.jhazmat.2022.129722.
Littunen, K., Snoei de Castro, J., Samoylenko, A., Xu, Q., Quaggin, S., Vainio, S., Seppälä, J., 2016. Synthesis of cationized nanofibrillated cellulose and its antimicrobial properties. Eur. Polym. J. 75, 116–124. https://doi.org/10.1016/j.eurpolymj.2015.12.008.
Liu, P., Zhang, X., Wu, Y., Li, X., 2017. Enhanced oil recovery by air-foam flooding system in tight oil reservoirs: study on the profile-controlling mechanisms. J. Petrol. Sci. Eng. 150, 208–216. https://doi.org/10.1016/j.petrol.2016.12.001.
Liu, H., Jin, P., Zhu, F., Nie, L., Qiu, H., 2021a. A review on the use of ionic liquids in preparation of molecularly imprinted polymers for applications in solid-phase extraction. TrAC, Trends Anal. Chem. 134, 116132. https://doi.org/10.1016/j.trac.2020.116132.
Liu, Q., He, W.-Q., Aguedo, M., Xia, X., Bai, W.-B., Dong, Y.-Y., Song, J.-Q., Richel, A., Goffin, D., 2021b. Microwave-assisted alkali hydrolysis for cellulose isolation from wheat straw: influence of reaction conditions and non-thermal effects of microwave. Carbohydr. Polym. 253, 117170. https://doi.org/10.1016/j.carbpol.2020.117170.
Liu, X.-L., Zhu, C.-F., Liu, H.-C., Zhu, J.-M., 2022. Quantitative analysis of degree of substitution/molar substitution of etherified polysaccharide derivatives. Des. Monomers Polym. 25 (1), 75–88. https://doi.org/10.1080/15685551.2022.2054118.
Liu, Y., Gao, L., Chen, L., Zhou, W., Wang, C., Ma, L., 2023. Exploring carbohydrate extraction from biomass using deep eutectic solvents: factors and mechanisms. iScience 26 (9), 107671. https://doi.org/10.1016/j.isci.2023.107671.
Long, K., Liu, J., Zhang, S., Luo, H., Zhang, P., Yu, L., Liu, R., Duan, L., Li, Q., Cha, R., 2024. Production of highly substituted cationic cellulose nanofibrils through disk milling/high-pressure homogenization. Cellulose 31 (7), 4217–4230. https://doi.org/10.1007/s10570-024-05861-5.
Lou, R., Zhang, X., 2022. Evaluation of pretreatment effect on lignin extraction from wheat straw by deep eutectic solvent. Bioresour. Technol. 344, 126174. https://doi.org/10.1016/j.biortech.2021.126174.
Louis, A.C.F., Venkatachalam, S., Gupta, S., 2022. Innovative strategy for rice straw valorization into nanocellulose and nanohemicellulose and its application. Ind. Crop. Prod. 179, 114695. https://doi.org/10.1016/j.indcrop.2022.114695.
Lv, D., Du, H., Che, X., Wu, M., Zhang, Y., Liu, C., Nie, S., Zhang, X., Li, B., 2019a. Tailored and integrated production of functional cellulose nanocrystals and cellulose nanofibrils via sustainable formic acid hydrolysis: Kinetic study and characterization. ACS Sustain. Chem. Eng. 7 (10), 9449–9463. https://doi.org/10.1021/acssuschemeng.9b00714.
Lv, M., Luo, C., Yang, J., Zhou, Y., Liu, C., Xu, B., 2019b. Effect of number of oxypropylene on dynamic interfacial tensions of extended surfactants. Colloids Surf. A Physicochem. Eng. Asp. 570, 429–437. https://doi.org/10.1016/j.colsurfa.2019.03.054.
Ma, J., Shen, J., Wang, C., Wei, Y., 2018. Preparation of dual-function chelating resin with high capacity and adjustable adsorption selectivity to variety of heavy metal ions. J. Taiwan Inst. Chem. Eng. 91, 532–538. https://doi.org/10.1016/j.jtice.2018.05.038.
Ma, H., Cheng, Z., Li, X., Li, B., Fu, Y., Jiang, J., 2023. Advances and challenges of cellulose functional materials in sensors. J. Bioresour. Bioprod. 8 (1), 15–32. https://doi.org/10.1016/j.jobab.2022.11.001.
Madani, H., Wibowo, A., Judawisastra, H., Nishiyama, N., Budhi, Y.W., 2022. One-step extraction of cellulose nanocrystals from high lignin biomass through ammonium persulfate oxidation method. Adv. Nat. Sci. Nanosci. Nanotechnol. 13 (1), 015007. https://doi.org/10.1088/2043-6262/ac549a.
Mahur, B.K., Ahuja, A., Singh, S., Maji, P.K., Rastogi, V.K., 2023. Different nanocellulose morphologies (cellulose nanofibers, nanocrystals and nanospheres) extracted from Sunn hemp (Crotalaria Juncea). Int. J. Biol. Macromol. 253, 126657. https://doi.org/10.1016/j.ijbiomac.2023.126657.
Manikumar, Y., Panis, N.I., Ridzuan, N., Gbonhinbor, J., Umunnawuike, C., Agi, A., 2024. Ultrasound assisted surfactant nanofluid oil recovery from contaminated oily sludge. In: SPE Nigeria Annual International Conference and Exhibition. https://doi.org/10.2118/221601-MS.
Manimaran, P., Senthamaraikannan, P., Sanjay, M.R., Marichelvam, M.K., Jawaid, M., 2018. Study on characterization of Furcraea foetida new natural fiber as composite reinforcement for lightweight applications. Carbohydr. Polym. 181, 650–658. https://doi.org/10.1016/j.carbpol.2017.11.099.
Mankar, A.R., Pandey, A., Modak, A., Pant, K.K., 2021. Pretreatment of lignocellulosic biomass: a review on recent advances. Bioresour. Technol. 334, 125235. https://doi.org/10.1016/j.biortech.2021.125235.
Marakana, P.G., Dey, A., Saini, B., 2021. Isolation of nanocellulose from lignocellulosic biomass: synthesis, characterization, modification, and potential applications. J. Environ. Chem. Eng. 9 (6), 106606. https://doi.org/10.1016/j.jece.2021.106606.
Mariano, M., El Kissi, N., Dufresne, A., 2014. Cellulose nanocrystals and related nanocomposites: review of some properties and challenges. J. Polym. Sci. B Polym. Phys. 52 (12), 791–806. https://doi.org/10.1002/polb.23490.
Mariyate, J., Bera, A., 2023. Paradigm shift towards the sustainability in upstream oil industry for enhanced recovery - a state-of-art review. J. Clean. Prod. 386, 135784. https://doi.org/10.1016/j.jclepro.2022.135784.
Martins, J.R., Abe, M.M., Brienzo, M., 2022. Chemical modification strategies for developing functionalized hemicellulose: advanced applications of modified hemicellulose. In: Brienzo, M. (Ed.), Hemicellulose Biorefinery: a Sustainable Solution for Value Addition to Bio-based Products and Bioenergy. Springer, pp. 171–205. https://doi.org/10.1007/978-981-16-3682-0_6.
Masek, A., Kosmalska, A., 2022. Technological limitations in obtaining and using cellulose biocomposites. Front. Bioeng. Biotechnol. 10. https://doi.org/10.3389/fbioe.2022.912052.
Massarweh, O., Abushaikha, A.S., 2020. The use of surfactants in enhanced oil recovery: a review of recent advances. Energy Rep. 6, 3150–3178. https://doi.org/10.1016/j.egyr.2020.11.009.
Mboowa, D., 2024. A review of the traditional pulping methods and the recent improvements in the pulping processes. Biomass Convers. Biorefinery 14 (1), 1–12. https://doi.org/10.1007/s13399-020-01243-6.
Meda, R.S., Jain, S., Singh, S., Verma, C., Nandi, U., Maji, P.K., 2022. Novel Lagenaria siceraria peel waste based cellulose nanocrystals: isolation and rationalizing H-bonding interactions. Ind. Crop. Prod. 186, 115197. https://doi.org/10.1016/j.indcrop.2022.115197.
Melikoğlu, A.Y., Bilek, S.E., Cesur, S., 2019. Optimum alkaline treatment parameters for the extraction of cellulose and production of cellulose nanocrystals from Apple pomace. Carbohydr. Polym. 215, 330–337. https://doi.org/10.1016/j.carbpol.2019.03.103.
Meng, X., Yoo, C.G., Pu, Y., Ragauskas, A.J., 2022. Opportunities and challenges for flow-through hydrothermal pretreatment in advanced biorefineries. Bioresour. Technol. 343, 126061. https://doi.org/10.1016/j.biortech.2021.126061.
Meraj, A., Jawaid, M., Singh, S.P., Nasef, M.M., Ariffin, H., Haafiz, M.K.M., 2023. Effect of natural deep eutectic solvents on properties of micro crystalline cellulose isolated from kenaf fibre. Ind. Crop. Prod. 203, 117129. https://doi.org/10.1016/j.indcrop.2023.117129.
Meryemoglu, B., 2021. Biomass hydrolysis with phosphotungstic acid. Catal. Commun. 149, 106248. https://doi.org/10.1016/j.catcom.2020.106248.
Meulendijks, N., Burghoorn, M., van Ee, R., Mourad, M., Mann, D., Keul, H., Bex, G., van Veldhoven, E., Verheijen, M., Buskens, P., 2017. Electrically conductive coatings consisting of Ag-decorated cellulose nanocrystals. Cellulose 24 (5), 2191–2204. https://doi.org/10.1007/s10570-017-1240-y.
Midhun Dominic, C.D., Raj, V., Neenu, K.V., Begum, P.M.S., Formela, K., Saeb, M.R., Prabhu, D.D., Poornima Vijayan, P., Ajithkumar, T.G., Parameswaranpillai, J., 2022. Chlorine-free extraction and structural characterization of cellulose nanofibers from waste husk of millet (Pennisetum glaucum). Int. J. Biol. Macromol. 206, 92–104. https://doi.org/10.1016/j.ijbiomac.2022.02.078.
Mikulcová, V., Urbánková, L., Kašpárková, V., Bordes, R., 2023. On the stabilization of emulsions by cellulose nanocrystals and nanofibrils: interfacial behavior and synergism. Colloids Surf. A Physicochem. Eng. Asp. 675, 131975. https://doi.org/10.1016/j.colsurfa.2023.131975.
Mishra, R.K., Mentha, S.S., Misra, Y., Dwivedi, N., 2023. Emerging pollutants of severe environmental concern in water and wastewater: a comprehensive review on current developments and future research. Water-Energy Nexus 6, 74–95. https://doi.org/10.1016/j.wen.2023.08.002.

Mishra, R.K., Yadav, A., Mishra, V., Mishra, S.N., Singh, D.S., Verma, D.K., 2024. Fundamental theory of electromagnetic spectrum, dielectric and magnetic properties, molecular rotation, and the green chemistry of microwave heating equipment. In: Verma, D.K., Verma, C., Fuertes, P.O. (Eds.), Green Chemical Synthesis with Microwaves and Ultrasound. Wiley, pp. 21–67. https://doi.org/10.1002/9783527844494.ch2.
Missoum, K., Belgacem, M., Bras, J., 2013. Nanofibrillated cellulose surface modification: a review. Materials 6 (5), 1745–1766. https://doi.org/10.3390/ma6051745.
Moghaddam, M.K., Gheshlagh, F.G., Moezzi, M., 2024. Extraction and characterization of cellulose microfibers from cornhusk for application as reinforcing agent in biocomposite. Int. J. Biol. Macromol. 264, 130669. https://doi.org/10.1016/j.ijbiomac.2024.130669.
Mohamed, A.H., Yahaya, N., Mohamad, S., Kamaruzaman, S., Osman, H., Nishiyama, N., Hirota, Y., 2022. Synthesis of oil palm empty fruit bunch-based magnetic-carboxymethyl cellulose nanofiber composite for magnetic solid-phase extraction of organophosphorus pesticides in environmental water samples. Microchem. J. 183, 108045. https://doi.org/10.1016/j.microc.2022.108045.
Mohanta, V., Madras, G., Patil, S., 2014. Layer-by-Layer assembled thin films and microcapsules of nanocrystalline cellulose for hydrophobic drug delivery. ACS Appl. Mater. Interfaces 6 (22), 20093–20101. https://doi.org/10.1021/am505681e.
Mohsenatabar Firozjaii, A., Saghafi, H.R., 2020. Review on chemical enhanced oil recovery using polymer flooding: fundamentals, experimental and numerical simulation. Petroleum 6 (2), 115–122. https://doi.org/10.1016/j.petlm.2019.09.003.
Mokhena, T.C., John, M.J., 2020. Esterified cellulose nanofibres from saw dust using vegetable oil. Int. J. Biol. Macromol. 148, 1109–1117. https://doi.org/10.1016/j.ijbiomac.2020.01.278.
Molnes, S.N., Paso, K.G., Strand, S., Syverud, K., 2017. The effects of pH, time and temperature on the stability and viscosity of cellulose nanocrystal (CNC) dispersions: implications for use in enhanced oil recovery. Cellulose 24 (10), 4479–4491. https://doi.org/10.1007/s10570-017-1437-0.
Molnes, S.N., Mamonov, A., Paso, K.G., Strand, S., Syverud, K., 2018. Investigation of a new application for cellulose nanocrystals: a study of the enhanced oil recovery potential by use of a green additive. Cellulose 25 (4), 2289–2301. https://doi.org/10.1007/s10570-018-1715-5.
Money, B., Modather, R.H., Abutu, D., Ismail, N., Agi, A., Nyah, F., Mahat, S.Q.B., 2025. A review on advancing clay-based geopolymers for high-temperature oil well cements: mechanisms, durability, and applications. Petroleum Research. https://doi.org/10.1016/j.ptlrs.2025.08.005.
Montesantos, N., Maschietti, M., 2020. Supercritical carbon dioxide extraction of lignocellulosic bio-oils: the potential of fuel upgrading and chemical recovery. Energies 13 (7), 1600. https://doi.org/10.3390/en13071600.
Moon, R.J., Martini, A., Nairn, J., Simonsen, J., Youngblood, J., 2011. Cellulose nanomaterials review: structure, properties and nanocomposites. Chem. Soc. Rev. 40 (7), 3941. https://doi.org/10.1039/c0cs00108b.
Moradi, E., Fathi, M., 2023. Production of cellulose nanocrystals from tomato pomace as a food waste and their application for stabilizing of pickering emulsions. Bioactive Carbohydrates and Dietary Fibre 30, 100378. https://doi.org/10.1016/j.bcdf.2023.100378.
Morais, E.S., da Costa Lopes, A.M., Freire, M.G., Freire, C.S.R., Coutinho, J.A.P., Silvestre, A.J.D., 2020. Use of ionic liquids and deep eutectic solvents in polysaccharides dissolution and extraction processes towards sustainable biomass valorization. Molecules 25 (16), 3652. https://doi.org/10.3390/molecules25163652.
Morán-Aguilar, M.G., Calderón-Santoyo, M., de Souza Oliveira, R.P., Aguilar-Uscanga, M.G., Domínguez, J.M., 2022. Deconstructing sugarcane bagasse lignocellulose by acid-based deep eutectic solvents to enhance enzymatic digestibility. Carbohydr. Polym. 298, 120097. https://doi.org/10.1016/j.carbpol.2022.120097.
Moran-Miraba, J.M., 2013. Advanced-microscopy techniques for the characterization of cellulose structure and cellulose-cellulase interactions. In: van de Ven, T., Godbout, L. (Eds.), Cellulose - Fundamental Aspects. InTech. https://doi.org/10.5772/56584.
Mu, X., Gray, D.G., 2014. Formation of chiral nematic films from cellulose nanocrystal suspensions is a two-stage process. Langmuir 30 (31), 9256–9260. https://doi.org/10.1021/la501741r.
Nair, L.G., Agrawal, K., Verma, P., 2023. Organosolv pretreatment: an in-depth purview of mechanics of the system. Bioresources and Bioprocessing 10 (1), 50. https://doi.org/10.1186/s40643-023-00673-0.
Nam, N.N., Do, H.D.K., Trinh, K.T.L., Lee, N.Y., 2023. Design strategy and application of deep eutectic solvents for green synthesis of nanomaterials. Nanomaterials 13 (7), 1164. https://doi.org/10.3390/nano13071164.
Nang Vu, A., Hoang Nguyen, L., Yoshimura, K., Duy Tran, T., Van Le, H., 2024. Cellulose nanocrystals isolated from sugarcane bagasse using the formic/peroxyformic acid process: structural, chemical, and thermal properties. Arab. J. Chem. 17 (8), 105841. https://doi.org/10.1016/j.arabjc.2024.105841.
Naseem, S., Rizwan, M., Durrani, A.I., Munawar, A., Siddique, S., Habib, F., 2024. Green and efficient synthesis of cellulose nanocrystals from Hamelia patens leftover via hydrolysis of microwave assisted-ionic liquid (MWAIL) pretreated microcrystalline cellulose. Int. J. Biol. Macromol. 271, 132791. https://doi.org/10.1016/j.ijbiomac.2024.132791.
Natalya, S.A.C., Kadja, G.T.M., Azhari, N.J., Khalil, M., Fajar, A.T.N., 2022. Two-dimensional (2D) nanomaterials for enhanced oil recovery (EOR): a review. FlatChem 34, 100383. https://doi.org/10.1016/j.flatc.2022.100383.
Nechyporchuk, O., Pignon, F., Belgacem, M.N., 2015. Morphological properties of nanofibrillated cellulose produced using wet grinding as an ultimate fibrillation process. J. Mater. Sci. 50 (2), 531–541. https://doi.org/10.1007/s10853-014-8609-1.
Neenu, K.V., Dominic, C.D.M., Begum, P.M.S., Parameswaranpillai, J., Kanoth, B.P., David, D.A., Sajadi, S.M., Dhanyasree, P., Ajithkumar, T.G., Badawi, M., 2022. Effect of oxalic acid and sulphuric acid hydrolysis on the preparation and properties of pineapple pomace derived cellulose nanofibers and nanopapers. Int. J. Biol. Macromol. 209, 1745–1759. https://doi.org/10.1016/j.ijbiomac.2022.04.138.
Negi, G.S., Anirbid, S., Sivakumar, P., 2021. Applications of silica and titanium dioxide nanoparticles in enhanced oil recovery: Promises and challenges. Pet. Res. 6 (3), 224–246. https://doi.org/10.1016/j.ptlrs.2021.03.001.
Ng, L.Y., Wong, T.J., Ng, C.Y., Amelia, C.K.M., 2021. A review on cellulose nanocrystals production and characterization methods from Elaeis guineensis empty fruit bunches. Arab. J. Chem. 14 (9), 103339. https://doi.org/10.1016/j.arabjc.2021.103339.
Ngouangna, E.N., Jaafar, M.Z., Norddin, M., Agi, A., Yakasai, F., Oseh, J.O., Mamah, S.C., Yahya, M.N., Al-Ani, M., 2023. Effect of salinity on hydroxyapatite nanoparticles flooding in enhanced oil recovery: a mechanistic study. ACS Omega 8 (20), 17819–17833. https://doi.org/10.1021/acsomega.3c00695.
Ngouangna, E.N., Manan, M.A., Oseh, J.O., Norddin, M.N.A.M., Agi, A., Gbadamosi, A.O., 2020. Influence of (3–Aminopropyl) triethoxysilane on silica nanoparticle for enhanced oil recovery. J. Mol. Liq. 315, 113740. https://doi.org/10.1016/j.molliq.2020.113740.
Ngouangna, E.N., Jaafar, M.Z., Norddin, M.N.A.M., Agi, A., Risal, A.R., Mamah, S.C., Oseh, J.O., 2022. The effect of hydroxyapatite nanoparticles on wettability and brine-oil interfacial tension as enhance oil recovery mechanisms. J. Petrol. Sci. Eng. 218, 110941. https://doi.org/10.1016/j.petrol.2022.110941.
Nguyen Thi, B.T., Ong, L.K., Nguyen Thi, D.T., Ju, Y.-H., 2017. Effect of subcritical water pretreatment on cellulose recovery of water hyacinth (Eichhornia crassipe). J. Taiwan Inst. Chem. Eng. 71, 55–61. https://doi.org/10.1016/j.jtice.2016.12.028.
Ni, Y., Li, J., Fan, L., 2021. Effects of ultrasonic conditions on the interfacial property and emulsifying property of cellulose nanoparticles from ginkgo seed shells. Ultrason. Sonochem. 70, 105335. https://doi.org/10.1016/j.ultsonch.2020.105335.
Nitzsche, R., Gröngröft, A., Köchermann, J., Meisel, K., Etzold, H., Verges, M., Leschinsky, M., Bachmann, J., Saake, B., Torkler, S., Patzsch, K., Rößiger, B., Pufky-Heinrich, D., Unkelbach, G., 2021. Platform and fine chemicals from woody biomass: demonstration and assessment of a novel biorefinery. Biomass Convers. Biorefinery 11 (6), 2369–2385. https://doi.org/10.1007/s13399-020-00769-z.
Noremylia, M.B., Hassan, M.Z., Ismail, Z., 2022. Recent advancement in isolation, processing, characterization and applications of emerging nanocellulose: a review. Int. J. Biol. Macromol. 206, 954–976. https://doi.org/10.1016/j.ijbiomac.2022.03.064.
Nóvak, I.C., Segat, B., Garcia, M.C.F., Pezzin, A.P.T., Schneider, A.L., dos Santos Schneider, A.L., 2024. Alternative production of bacterial cellulose by Komagataeibacter hansenii and microbial consortium. Polímeros 34 (2). https://doi.org/10.1590/0104-1428.20230080.
Novo, L.P., Bras, J., García, A., Belgacem, N., da Silva Curvelo, A.A., 2016. A study of the production of cellulose nanocrystals through subcritical water hydrolysis. Ind. Crop. Prod. 93, 88–95. https://doi.org/10.1016/j.indcrop.2016.01.012.
Nowrouzi, I., Manshad, A.K., Mohammadi, A.H., 2022. Effects of MgO, γ-Al_2O_3, and TiO_2 nanoparticles at low concentrations on interfacial tension (IFT), rock wettability, and oil recovery by spontaneous imbibition in the process of smart nanofluid injection into carbonate reservoirs. ACS Omega 7 (26), 22161–22172. https://doi.org/10.1021/acsomega.1c07134.
Musa, M.S.M., Agi, A., Nwaichi, P.I., Ridzuan, N., Mahat, S.Q.A.B., 2023. Simulation study of polymer flooding performance: Effect of salinity, polymer concentration in the Malay Basin. Geoenergy Sci. Eng. 228, 211986. https://doi.org/10.1016/j.geoen.2023.211986.
Nugroho, R.W.N., Tardy, B.L., Eldin, S.M., Ilyas, R.A., Mahardika, M., Masruchin, N., 2023. Controlling the critical parameters of ultrasonication to affect the dispersion state, isolation, and chiral nematic assembly of cellulose nanocrystals. Ultrason. Sonochem. 99, 106581. https://doi.org/10.1016/j.ultsonch.2023.106581.
Nyah, F., Ridzuan, N., Ikechukwu Nwaichi, P., Umunnawuike, C., Agi, A., 2024. Comprehensive review on the role of salinity on oil recovery mechanisms during chemical flooding. J. Mol. Liq. 415, 126308. https://doi.org/10.1016/j.molliq.2024.126308.
Nyah, F., Ridzuan, N., Aziz, M.A.B., Gbonhinbor, J., Money, B., Nwaichi, P.I., Ummuawuike, C., David, A., Agi, A., 2025. Bibliometric insights into cellulose nanoparticles: advancing sustainable enhanced oil recovery in HTHP reservoirs. In: SPE Nigeria Annual International Conference and Exhibition. https://doi.org/10.2118/228643-MS.
Nyoo Putro, J., Soetaredjo, F.E., Santoso, S.P., Irawaty, W., Yuliana, M., Wijaya, C.J., Saptoro, A., Sunarso, J., Ismadji, S., 2024. Jackfruit peel cellulose nanocrystal – alginate hydrogel for doripenem adsorption and release study. Int. J. Biol. Macromol. 257, 128502. https://doi.org/10.1016/j.ijbiomac.2023.128502.
Oberlintner, A., Likozar, B., Novak, U., 2021. Hydrophobic functionalization reactions of structured cellulose nanomaterials: mechanisms, kinetics and in silico multi-scale models. Carbohydr. Polym. 259, 117742. https://doi.org/10.1016/j.carbpol.2021.117742.

Odejobi, O.J., Ajala, O.O., Osuolale, F.N., 2024. Review on potential of using agricultural, municipal solid and industrial wastes as substrates for biogas production in Nigeria. Biomass Convers. Biorefinery 14 (2), 1567–1579. https://doi.org/10.1007/s13399-022-02613-y.

Ogunjobi, J.K., Adewale, A.I., Adeyemi, S.A., 2023. Cellulose nanocrystals from siam weed: synthesis and physicochemical characterization. Heliyon 9 (1), e13104. https://doi.org/10.1016/j.heliyon.2023.e13104.

Ojala, J., Visanko, M., Laitinen, O., Österberg, M., Sirviö, J.A., Liimatainen, H., 2018. Emulsion stabilization with functionalized cellulose nanoparticles fabricated using deep eutectic solvents. Molecules 23 (11), 2765. https://doi.org/10.3390/molecules23112765.

Omidi, A., Manshad, A.K., Moradi, S., Ali, J.A., Sajadi, S.M., Keshavarz, A., 2020. Smart- and nano-hybrid chemical EOR flooding using Fe3O4/eggshell nanocomposites. J. Mol. Liq. 316, 113880. https://doi.org/10.1016/j.molliq.2020.113880.

Ovejero, J.G., Gallo-Cordova, A., Roca, A.G., Morales, M.P., Veintemillas-Verdaguer, S., 2021. Reproducibility and scalability of magnetic nanoheater synthesis. Nanomaterials 11 (8), 2059. https://doi.org/10.3390/nano11082059.

Pacheco-Fernández, I., Pino, V., 2019. Green solvents in analytical chemistry. Curr. Opin. Green Sustainable Chem. 18, 42–50. https://doi.org/10.1016/j.cogsc.2018.12.010.

Painuli, S., Semwal, P., Bachheti, A., Bachheti, R.K., Husen, A., 2020. Nanomaterials from non-wood forest products and their applications. In: Husen, A., Jawaid, m. (Eds.), Nanomaterials for Agriculture and Forestry Applications. Elsevier, pp. 15–40. https://doi.org/10.1016/B978-0-12-817852-2.00002-0.

Pandey, A., Telmadarreie, A., Trifkovic, M., Bryant, S., 2018. Cellulose nanocrystal stabilized emulsions for conformance control and fluid diversion in porous media. In: SPE Annual Technical Conference and Exhibition. https://doi.org/10.2118/191609-MS.

Pandi, N., Sonawane, S.H., Kishore, K.A., 2021. Synthesis of cellulose nanocrystals (CNCs) from cotton using ultrasound-assisted acid hydrolysis. Ultrason. Sonochem. 70, 105353. https://doi.org/10.1016/j.ultsonch.2020.105353.

Pangsang, N., Rattanapan, U., Thanapimmetha, A., Srinopphakhun, P., Liu, C.-G., Zhao, X.-Q., Bai, F.-W., Sakdaronnarong, C., 2019. Chemical-free fractionation of palm empty fruit bunch and palm fiber by hot-compressed water technique for ethanol production. Energy Rep. 5, 337–348. https://doi.org/10.1016/j.egyr.2019.02.008.

Parihar, D., Kumar, M., Gehlot, P.S., Surolia, P.K., Prasad, G., 2022. Extraction and characterization of fractionated cellulose from *Acacia Senegal*. J. Nat. Fibers 19 (15), 10499–10512. https://doi.org/10.1080/15440478.2021.1994092.

Park, H.-W., Jang, N.-G., Seo, H.-S., Kwon, K., Shin, S., 2023. Facile synthesis of self-adhesion and ion-conducting 2-Acrylamido-2-Methylpropane sulfonic acid/tannic acid hydrogels using electron beam irradiation. Polymers 15 (18), 3836. https://doi.org/10.3390/polym15183836.

Patel, B., Guo, M., Izadpanah, A., Shah, N., Hellgardt, K., 2016. A review on hydrothermal pre-treatment technologies and environmental profiles of algal biomass processing. Bioresour. Technol. 199, 288–299. https://doi.org/10.1016/j.biortech.2015.09.064.

Patel, D.K., Dutta, S.D., Lim, K.-T., 2019. Nanocellulose-based polymer hybrids and their emerging applications in biomedical engineering and water purification. RSC Adv. 9 (33), 19143–19162. https://doi.org/10.1039/C9RA03261D.

Pattnaik, F., Nanda, S., Kumar, V., Naik, S., Dalai, A.K., 2021. Subcritical water hydrolysis of phragmites for sugar extraction and catalytic conversion to platform chemicals. Biomass Bioenergy 145, 105965. https://doi.org/10.1016/j.biombioe.2021.105965.

Pereira, M.L. de O., Maia, K.C.B., Silva, W.C., Leite, A.C., Francisco, A.D., dos, S., Vasconcelos, T.L., Nascimento, R.S.V., Grasseschi, D., 2020. Fe_3O_4 nanoparticles as surfactant carriers for enhanced oil recovery and scale prevention. ACS Appl. Nano Mater. 3 (6), 5762–5772. https://doi.org/10.1021/acsanm.0c00939.

Pereira, J.E., Moita, A.S., Moreira, A.L.N., 2022. The pressing need for green nanofluids: a review. J. Environ. Chem. Eng. 10 (3), 107940. https://doi.org/10.1016/j.jece.2022.107940.

Perez-Palacios, T., Ruiz-Carrascal, J., Solomando, J.C., de-la-Haba, F., Pajuelo, A., Antequera, T., 2022. Recent developments in the microencapsulation of fish oil and natural extracts: procedure, quality evaluation and food enrichment. Foods 11 (20), 3291. https://doi.org/10.3390/foods11203291.

Perumal, A.B., Nambiar, R.B., Sellamuthu, P.S., Sadiku, E.R., Li, X., He, Y., 2022. Extraction of cellulose nanocrystals from areca waste and its application in eco-friendly biocomposite film. Chemosphere 287, 132084. https://doi.org/10.1016/j.chemosphere.2021.132084.

Peter, Z., 2021. Order in cellulosics: historical review of crystal structure research on cellulose. Carbohydr. Polym. 254, 117417. https://doi.org/10.1016/j.carbpol.2020.117417.

Pinto, E., Aggrey, W.N., Boakye, P., Amenuvor, G., Sokama-Neuyam, Y.A., Fokuo, M.K., Karimaie, H., Sarkodie, K., Adenutsi, C.D., Erzuah, S., Rockson, M.A.D., 2022. Cellulose processing from biomass and its derivatization into carboxymethylcellulose: a review. Sci. Afr. 15, e01078. https://doi.org/10.1016/j.sciaf.2021.e01078.

Pires, J.R.A., Souza, V.G.L., Fernando, A.L., 2019. Valorization of energy crops as a source for nanocellulose production – current knowledge and future prospects. Ind. Crop. Prod. 140, 111642. https://doi.org/10.1016/j.indcrop.2019.111642.

Podoprigora, D.G., Byazrov, R.R., Lagutina, M.A., Arabov, D.V., Galimov, V.V., Ermolin, D.,S., 2024. A novel integrated methodology for screening, assessment and ranking of promising oilfields for polymer floods. Advances in Geo-Energy Research 12 (1), 8–21. https://doi.org/10.46690/ager.2024.04.02.

Pradhan, D., Jaiswal, A.K., Jaiswal, S., 2022. Emerging technologies for the production of nanocellulose from lignocellulosic biomass. Carbohydr. Polym. 285, 119258. https://doi.org/10.1016/j.carbpol.2022.119258.

Pramasari, D.A., Sondari, D., Rachmawati, S.A., Ningrum, R.S., Sufiandi, S., 2021. The effect of alkaline-autoclaving delignification on chemical component changes of sugarcane trash. IOP Conf. Ser. Earth Environ. Sci. 759 (1), 012010. https://doi.org/10.1088/1755-1315/759/1/012010.

Pratama, A.W., Mahardika, M., Widiastuti, N., Piluharto, B., Ilyas, R.A., Sapuan, S.M., Amelia, D., Firmanda, A., 2024. Isolation and characterization of highly thermal stable microcrystalline cellulose derived from belulang grass (Eleusine indica). Case Stud. Chem. Environ. Eng. 9, 100743. https://doi.org/10.1016/j.cscee.2024.100743.

Pulido-Barragán, E.U., Morales-Cepeda, A.B., Castro-Guerrero, C.F., Koschella, A., Heinze, T., 2021. Upgrading Euphorbia antisyphilitica fiber compost: a waste material turned into nanocrystalline cellulose. Ind. Crop. Prod. 160, 113111. https://doi.org/10.1016/j.indcrop.2020.113111.

Purkayastha, S., Saha, S., Ghosh, A.K., 2021. Influence of green extraction process of nano fibrillated cellulose using subcritical water/<scp> CO_2 </scp> on its properties and development of its bio composite. Polym. Eng. Sci. 61 (5), 1310–1323. https://doi.org/10.1002/pen.25644.

Putra, D.F., Temizel, C., 2018. The optimization and analysis of hydrocarbon recovery under injection of biopolymer, synthetic polymer and gels in a heterogeneous reservoir. Journal of Earth Energy Engineering 7 (1), 19–41. https://doi.org/10.25299/jeee.2018 vol7 (1).1301.

Qiao, C., Chen, G., Zhang, J., Yao, J., 2016. Structure and rheological properties of cellulose nanocrystals suspension. Food Hydrocoll. 55, 19–25. https://doi.org/10.1016/j.foodhyd.2015.11.005.

Qu, H., Liu, B., Li, L., Zhou, Y., 2020. A bifunctional recoverable catalyst based on phosphotungstic acid for cellulose hydrolysis to fermentable sugars. Fuel Process. Technol. 199, 106272. https://doi.org/10.1016/j.fuproc.2019.106272.

Rajput, A., Raj, S.K., Sharma, J., Rathod, N.H., Maru, P.D., Kulshrestha, V., 2021. Sulfonated poly ether ether ketone (SPEEK) based composite cation exchange membranes for salt removal from brackish water. Colloids Surf. A Physicochem. Eng. Asp. 614, 126157. https://doi.org/10.1016/j.colsurfa.2021.126157.

Ramesh, V.K., Chintala, V., Kumar, S., 2021. Recent developments, challenges and opportunities for harnessing solar renewable energy for thermal enhanced oil recovery (EOR). Energy Sources, Part A Recovery, Util. Environ. Eff. 43 (22), 2878–2895. https://doi.org/10.1080/15567036.2019.1639850.

Rana, A.K., Frollini, E., Thakur, V.K., 2021. Cellulose nanocrystals: pretreatments, preparation strategies, and surface functionalization. Int. J. Biol. Macromol. 182, 1554–1581. https://doi.org/10.1016/j.ijbiomac.2021.05.119.

Rana, A.K., Thakur, M.K., Gupta, V.K., Thakur, V.K., 2024. Exploring the role of nanocellulose as potential sustainable material for enhanced oil recovery: new paradigm for a circular economy. Process Saf. Environ. Prot. 183, 1198–1222. https://doi.org/10.1016/j.psep.2024.01.085.

Randis, R., Darmadi, D.B., Gapsari, F., Sonief, A.A., 2024. Isolation and characterization of microcrystalline cellulose from oil palm fronds biomass using consecutive chemical treatments. Case Stud. Chem. Environ. Eng. 9, 100616. https://doi.org/10.1016/j.cscee.2024.100616.

Ravindran, R., Jaiswal, A.K., 2016. A comprehensive review on pre-treatment strategy for lignocellulosic food industry waste: challenges and opportunities. Bioresour. Technol. 199, 92–102. https://doi.org/10.1016/j.biortech.2015.07.106.

Raza, M., Abu-Jdayil, B., 2022. Cellulose nanocrystals from lignocellulosic feedstock: a review of production technology and surface chemistry modification. Cellulose 29 (2), 685–722. https://doi.org/10.1007/s10570-021-04371-y.

Raza, S., Gates, I.D., 2021. Effect of cellulose nanocrystal nanofluid on displacement of oil in a Hele-Shaw cell. J. Petrol. Sci. Eng. 196, 108068. https://doi.org/10.1016/j.petrol.2020.108068.

Raza, M., Abu-Jdayil, B., Banat, F., Al-Marzouqi, A.H., 2022. Isolation and characterization of cellulose nanocrystals from date palm waste. ACS Omega 7 (29), 25366–25379. https://doi.org/10.1021/acsomega.2c02333.

Razali, N.A.M., Mohd Sohaimi, R., Othman, R.N.I.R., Abdullah, N., Demon, S.Z.N., Jasmani, L., Yunus, W.M.Z.W., Ya'acob, W.M.H.W., Salleh, E.M., Norizan, M.N., Halim, N.A., 2022. Comparative study on extraction of cellulose fiber from rice straw waste from chemo-mechanical and pulping method. Polymers 14 (3), 387. https://doi.org/10.3390/polym14030387.

Reddy, N., Yang, Y., 2009. Properties and potential applications of natural cellulose fibers from the bark of cotton stalks. Bioresour. Technol. 100 (14), 3563–3569. https://doi.org/10.1016/j.biortech.2009.02.047.

Reimer, M., Eckel, F., Rothammer, M., Van Opdenbosch, D., Zollfrank, C., 2023. Manufacturing of cellulose-based nano- and submicronparticles via different precipitation methods. Cellulose 30 (14), 8861–8881. https://doi.org/10.1007/s10570-023-05397-0.

Ren, H., Xu, Z., Du, C., Ling, Z., Yang, W., Pan, L., Tian, Y., Fan, W., Zheng, Y., 2023. Preparation and characterization of starch-based composite films reinforced by quinoa (Chenopodium quinoa Willd.) straw cellulose nanocrystals. Int. J. Biol. Macromol. 242, 124938. https://doi.org/10.1016/j.ijbiomac.2023.124938.

Rodríguez-Fabià, S., Torstensen, J., Johansson, L., Syverud, K., 2022. Hydrophobization of lignocellulosic materials part II: chemical modification. Cellulose 29 (17), 8957–8995. https://doi.org/10.1007/s10570-022-04824-y.

Rohaizu, R., Wanrosli, W.D., 2017. Sono-assisted TEMPO oxidation of oil palm lignocellulosic biomass for isolation of nanocrystalline cellulose. Ultrason. Sonochem. 34, 631–639. https://doi.org/10.1016/j.ultsonch.2016.06.040.

Rossi, B.R., Pellegrini, V.O.A., Cortez, A.A., Chiromito, E.M.S., Carvalho, A.J.F., Pinto, L.O., Rezende, C.A., Mastelaro, V.R., Polikarpov, I., 2021. Cellulose nanofibers production using a set of recombinant enzymes. Carbohydr. Polym. 256, 117510. https://doi.org/10.1016/j.carbpol.2020.117510.

Rovera, C., Carullo, D., Bellesia, T., Büyüktaş, D., Ghaani, M., Caneva, E., Farris, S., 2023. Extraction of high-quality grade cellulose and cellulose nanocrystals from different lignocellulosic agri-food wastes. Front. Sustain. Food Syst. 6. https://doi.org/10.3389/fsufs.2022.1087867.

Rubiyah, M.H., Melethil, K., Varghese, S., Kurian, M., Babu, S., Jojo, L., Thomas, B., 2023. Isolation and characterization of cellulose nanofibrils from agro-biomass of Jackfruit (Artocarpus heterophyllus) rind, using a soft and benign acid hydrolysis. Carbohydrate Polymer Technologies and Applications 6, 100374. https://doi.org/10.1016/j.carpta.2023.100374.

Saha, S., Ghosh, R., 2019. Cellulose Nanocrystals from lignocellulosic agro-waste: a comparative study on conventional and ultrasonic assisted preparation methods. Mater. Today Proc. 11, 628–636. https://doi.org/10.1016/j.matpr.2019.03.020.

Saini, S., Kardam, S.K., Kadam, A.A., Kumar, V., Gaikwad, K.K., 2022. Green and energy-efficient extraction of cellulose nano-fibrils from rice straw and its coating to improve functional properties of rice straw paperboard made via refiner mechanical pulping. Prog. Org. Coating 165, 106747. https://doi.org/10.1016/j.porgcoat.2022.106747.

Sakthipriya, N., Doble, M., Sangwai, J.S., 2017. Enhanced microbial degradation of waxy crude oil: a review on current status and future perspective. Int. J. Oil Gas Coal Technol. 16 (2), 130. https://doi.org/10.1504/IJOGCT.2017.086315.

Salem, K.G., Tantawy, M.A., Gawish, A.A., Salem, A.M., Gomaa, S., El-hoshoudy, A.N., 2024. Key aspects of polymeric nanofluids as a new enhanced oil recovery approach: a comprehensive review. Fuel 368, 131515. https://doi.org/10.1016/j.fuel.2024.131515.

Samsudin, N.A., Low, F.W., Yusoff, Y., Shakeri, M., Tan, X.Y., Lai, C.W., Asim, N., Oon, C.S., Newaz, K.S., Tiong, S.K., Amin, N., 2020. Effect of temperature on synthesis of cellulose nanoparticles via ionic liquid hydrolysis process. J. Mol. Liq. 308, 113030. https://doi.org/10.1016/j.molliq.2020.113030.

Sankhla, S., Sardar, H.H., Neogi, S., 2021. Greener extraction of highly crystalline and thermally stable cellulose micro-fibers from sugarcane bagasse for cellulose nano-fibrils preparation. Carbohydr. Polym. 251, 117030. https://doi.org/10.1016/j.carbpol.2020.117030.

Saravana Kumaar, A., Senthilkumar, A., Sornakumar, T., Saravanakumar, S.S., Arthanariesewaran, V.P., 2019. Physicochemical properties of new cellulosic fiber extracted from *Carica papaya* bark. J. Nat. Fibers 16 (2), 175–184. https://doi.org/10.1080/15440478.2017.1410514.

Sarker, T.R., Pattnaik, F., Nanda, S., Dalai, A.K., Meda, V., Naik, S., 2021. Hydrothermal pretreatment technologies for lignocellulosic biomass: a review of steam explosion and subcritical water hydrolysis. Chemosphere 284, 131372. https://doi.org/10.1016/j.chemosphere.2021.131372.

Scelsi, E., Angelini, A., Pastore, C., 2021. Deep eutectic solvents for the valorisation of lignocellulosic biomasses towards fine chemicals. Biomass 1 (1), 29–59. https://doi.org/10.3390/biomass1010003.

Selvaraj, S., Chauhan, A., Dutta, V., Verma, R., Rao, S.K., Radhakrishnan, A., Ghotekar, S., 2024. A state-of-the-art review on plant-derived cellulose-based green hydrogels and their multifunctional role in advanced biomedical applications. Int. J. Biol. Macromol. 265, 130991. https://doi.org/10.1016/j.ijbiomac.2024.130991.

Shahzad, A., Ullah, M.W., Ali, J., Aziz, K., Javed, M.A., Shi, Z., Manan, S., Ul-Islam, M., Nazar, M., Yang, G., 2023. The versatility of nanocellulose, modification strategies, and its current progress in wastewater treatment and environmental remediation. Sci. Total Environ. 858, 159937. https://doi.org/10.1016/j.scitotenv.2022.159937.

Shaikh, H.M., Anis, A., Poulose, A.M., Al-Zahrani, S.M., Madhar, N.A., Alhamidi, A., Aldeligan, S.H., Alsubaie, F.S., 2022. Synthesis and characterization of cellulose triacetate obtained from date palm (Phoenix dactylifera L.) trunk mesh-derived cellulose. Molecules 27 (4), 1434. https://doi.org/10.3390/molecules27041434.

Sheferaw, L., Gideon, R.K., Ejegu, H., Gatew, Y., 2023. Extraction and characterization of fiber from the stem of *Cyperus papyrus* plant. J. Nat. Fibers 20 (1). https://doi.org/10.1080/15440478.2022.2149661.

Shen, Z., Sheng, J.J., 2018. Experimental and numerical study of permeability reduction caused by asphaltene precipitation and deposition during CO2 huff and puff injection in eagle ford shale. Fuel 211, 432–445. https://doi.org/10.1016/j.fuel.2017.09.047.

Shen, P., Tang, Q., Chen, X., Li, Z., 2022. Nanocrystalline cellulose extracted from bast fibers: Preparation, characterization, and application. Carbohydr. Polym. 290, 119462. https://doi.org/10.1016/j.carbpol.2022.119462.

Sheng, J.J., Leonhardt, B., Azri, N., 2015. Status of polymer-flooding technology. J. Can. Petrol. Technol. 54 (2), 116–126. https://doi.org/10.2118/174541-PA.

Shi, Z., Yang, Q., Cai, J., Kuga, S., Matsumoto, Y., 2014. Effects of lignin and hemicellulose contents on dissolution of wood pulp in aqueous NaOH/urea solution. Cellulose 21 (3), 1205–1215. https://doi.org/10.1007/s10570-014-0226-2.

Shibly, M.A.H., Islam, Md I., Rahat, Md N.H., Billah, M.M., Rahman, M.M., Bashar, M.S., Abdul, B., Alorfi, H.S., 2024. Extraction and characterization of a novel cellulosic fiber derived from the bark of Rosa hybrida plant. Int. J. Biol. Macromol. 257, 128446. https://doi.org/10.1016/j.ijbiomac.2023.128446.

Sikder, M.B.H., Rashid, S.S., Ab Rahim, M.H., Mazila Ramli, A.N., Roslan, R., 2023. Enzymatic pretreatment of palm oil empty fruit bunch. Mater. Today Proc. 75, 193–196. https://doi.org/10.1016/j.matpr.2022.12.241.

Sikder, Md B.H., Rashid, S.S., Rahim, M.H.A., Ramli, A.N.M., Roslan, R., Sasi, A.A., Mustafa, A.H., 2023. Enzymatic cellulose nanocrystal production from pretreated palm oil empty fruit bunch fibers. Mater. Today Proc. https://doi.org/10.1016/j.matpr.2023.10.115.

Singh, H.K., Patil, T., Vineeth, S.K., Das, S., Pramanik, A., Mhaske, S.T., 2020a. Isolation of microcrystalline cellulose from corn stover with emphasis on its constituents: corn cover and corn cob. Mater. Today Proc. 27, 589–594. https://doi.org/10.1016/j.matpr.2019.12.065.

Singh, S.S., Lim, L.-T., Manickavasagan, A., 2020b. Ultrasound-assisted alkali-urea pre-treatment of miscanthus × giganteus for enhanced extraction of cellulose fiber. Carbohydr. Polym. 247, 116758. https://doi.org/10.1016/j.carbpol.2020.116758.

Singh, S., Bhardwaj, S., Meda, R.S., Verma, C., Chhajed, M., Ghosh, K., Maji, P.K., 2023. Insights into thermal degradation kinetics and liquid crystalline behavior of cellulose nanocrystals from the waste of Cajanus cajan (pigeon pea). Int. J. Biol. Macromol. 242, 124507. https://doi.org/10.1016/j.ijbiomac.2023.124507.

Skiba, E.A., Budaeva, V.V., Ovchinnikova, E.V., Gladysheva, E.K., Kashcheyeva, E.I., Pavlov, I.N., Sakovich, G.V., 2020. A technology for pilot production of bacterial cellulose from oat hulls. Chem. Eng. J. 383, 123128. https://doi.org/10.1016/j.cej.2019.123128.

Skiba, E.A., Gladysheva, E.K., Budaeva, V.V., Aleshina, L.A., Sakovich, G.V., 2022. Yield and quality of bacterial cellulose from agricultural waste. Cellulose 29 (3), 1543–1555. https://doi.org/10.1007/s10570-021-04372-x.

Smith, E.L., Abbott, A.P., Ryder, K.S., 2014. Deep eutectic solvents (DESs) and their applications. Chem. Rev. 114 (21), 11060–11082. https://doi.org/10.1021/cr300162p.

Smriti, S.A., Haque, A.N.M.A., Khadem, A.H., Siddiqa, F., Rahman, A.N.M.M., Himu, H.A., Farzana, N., Islam, Md A., Naebe, M., 2023. Recent developments of the nanocellulose extraction from water hyacinth: a review. Cellulose 30 (14), 8617–8641. https://doi.org/10.1007/s10570-023-05374-7.

Smyth, M., García, A., Rader, C., Foster, E.J., Bras, J., 2017. Extraction and process analysis of high aspect ratio cellulose nanocrystals from corn (Zea mays) agricultural residue. Ind. Crop. Prod. 108, 257–266. https://doi.org/10.1016/j.indcrop.2017.06.006.

Sofla, M.R.K., Brown, R.J., Tsuzuki, T., Rainey, T.J., 2016. A comparison of cellulose nanocrystals and cellulose nanofibres extracted from bagasse using acid and ball milling methods. Adv. Nat. Sci. Nanosci. Nanotechnol. 7 (3), 035004. https://doi.org/10.1088/2043-6262/7/3/035004.

Sohni, S., Begum, S., Hashim, R., Khan, S.B., Mazhar, F., Syed, F., Khan, S.A., 2024. Physicochemical characterization of microcrystalline cellulose derived from underutilized orange peel waste as a sustainable resource under biorefinery concept. Bioresour. Technol. Rep. 25, 101731. https://doi.org/10.1016/j.biteb.2023.101731.

Song, Y., Jiang, W., Zhang, Y., Wang, H., Zou, F., Yu, K., Han, G., 2018. A novel process of nanocellulose extraction from kenaf bast. Mater. Res. Express 5 (8), 85032. https://doi.org/10.1088/2053-1591/aac80d.

Song, K., Zhu, X., Zhu, W., Li, X., 2019. Preparation and characterization of cellulose nanocrystal extracted from Calotropis procera biomass. Bioresources and Bioprocessing 6 (1), 45. https://doi.org/10.1186/s40643-019-0279-z.

Soppie, A.G., Betené, A.D.O., Anicet Noah, P.M., Njom, A.E., Betené Ebanda, F., Ateba, A., Mewoli, A., Efeze, D.N., Moukené, R., 2023. Chemical extraction and its effect on the properties of cordleaf burbark (Triumfetta cordifolia A. rich) fibres for the manufacture of textile yarns. Heliyon 9 (6), e17581. https://doi.org/10.1016/j.heliyon.2023.e17581.

Su, W., Hou, J., Lv, C., Liu, J., 2018. Experimental study on a combined profile modification system for EOR by starch graft copolymer gel and N< SUB align="right">2 foam. Int. J. Oil Gas Coal Technol. 17 (2), 189. https://doi.org/10.1504/IJOGCT.2018.089957.

Sumini, M., Andrade, G.J.S., Tischer, C.A., Kobayashi, R.K.T., Nakazato, G., 2024. Production of bacterial cellulose by Komagataeibacter xylinus: biochemistry, synthesis and applications. Cellulose. https://doi.org/10.1007/s10570-024-06179-y.

Sun, B., Hou, Q., Liu, Z., He, Z., Ni, Y., 2014. Stability and efficiency improvement of ASA in internal sizing of cellulosic paper by using cationically modified cellulose nanocrystals. Cellulose 21 (4), 2879–2887. https://doi.org/10.1007/s10570-014-0283-6.

Sun, Y., Zhang, W., Li, J., Han, R., Lu, C., 2023. Mechanism and performance analysis of nanoparticle-polymer fluid for enhanced oil recovery: a review. Molecules 28 (11), 4331. https://doi.org/10.3390/molecules28114331.

Sunasee, R., Hemraz, U., 2018. Synthetic strategies for the fabrication of cationic surface-modified cellulose nanocrystals. Fibers 6 (1), 15. https://doi.org/10.3390/fib6010015.

Supian, M.A.F., Amin, K.N.M., Jamari, S.S., Mohamad, S., 2020. Production of cellulose nanofiber (CNF) from empty fruit bunch (EFB) via mechanical method. J. Environ. Chem. Eng. 8 (1), 103024. https://doi.org/10.1016/j.jece.2019.103024.

Suyambulingam, I., Sudherson, D.P.S., Perumal, S.N., Perumal, S.N., 2024. Comprehensive characterization of microcrystalline cellulose from lemon grass (Cymbopogan citratus) oil extraction agro-industrial waste for cementitious composites applications. Int. J. Biol. Macromol., 132644 https://doi.org/10.1016/j.ijbiomac.2024.132644.

Szymańska-Chargot, M., Cieśla, J., Pękala, P., Pieczywek, P.M., Oleszek, W., Żyła, M., Szkopek, Z., Zdunek, A., 2022. The influence of high-intensity ultrasonication

on properties of cellulose produced from the hop stems, the byproduct of the hop cones production. Molecules 27 (9), 2624. https://doi.org/10.3390/molecules27092624.
Taflick, T., Schwendler, L.A., Rosa, S.M.L., Bica, C.I.D., Nachtigall, S.M.B., 2017. Cellulose nanocrystals from acacia bark–Influence of solvent extraction. Int. J. Biol. Macromol. 101, 553–561. https://doi.org/10.1016/j.ijbiomac.2017.03.076.
Tang, S., Yu, Y., Tan, X., Sheng, Y., Dong, Q., Liu, R., Li, Y., Yuan, S., Wang, Y., Zhang, Q., 2024. Impact of surfactants on the pretreatment of rice straw with tetrahydro-2-furanmethanol and aluminum chloride to enhance enzymatic saccharification. Ind. Crop. Prod. 210, 118139. https://doi.org/10.1016/j.indcrop.2024.118139.
Tashiro, K., Gakhutishvili, M., 2019. Crystal structure of cellulose-iodine complex. Polymer 171, 140–148. https://doi.org/10.1016/j.polymer.2019.03.034.
Taylor, M., Alabdrabalameer, H., Skoulou, V., 2019. Choosing physical, physicochemical and chemical methods of pre-treating lignocellulosic wastes to repurpose into solid fuels. Sustainability 11 (13), 3604. https://doi.org/10.3390/su11133604.
Tengsuthiwat, J., A, V., R, V., G, Y.G.T., Rangappa, S.M., Siengchin, S., 2024. Characterization of novel natural cellulose fiber from Ficus macrocarpa bark for lightweight structural composite application and its effect on chemical treatment. Heliyon 10 (9), e30442. https://doi.org/10.1016/j.heliyon.2024.e30442.
Thakur, M., Pathania, D., Sharma, G., Naushad, Mu, Bhatnagar, A., Khan, M.R., 2018. Synthesis, characterization and environmental applications of a new biocomposite Gelatin-Zr(IV) phosphate. J. Polym. Environ. 26 (4), 1415–1424. https://doi.org/10.1007/s10924-017-1043-0.
Thakur, V., Guleria, A., Kumar, S., Sharma, S., Singh, K., 2021. Recent advances in nanocellulose processing, functionalization and applications: a review. Mater. Adv. 2 (6), 1872–1895. https://doi.org/10.1039/D1MA00049G.
Thapa, S., Mishra, J., Arora, N., Mishra, P., Li, H., O'Hair, J., Bhatti, S., Zhou, S., 2020. Microbial cellulolytic enzymes: diversity and biotechnology with reference to lignocellulosic biomass degradation. Rev. Environ. Sci. Biotechnol. 19 (3), 621–648. https://doi.org/10.1007/s11157-020-09536-y.
Theivasanthi, T., Anne Christma, F.L., Toyin, A.J., Gopinath, S.C.B., Ravichandran, R., 2018. Synthesis and characterization of cotton fiber-based nanocellulose. Int. J. Biol. Macromol. 109, 832–836. https://doi.org/10.1016/j.ijbiomac.2017.11.054.
Thomas, B., Raj, M.C., Athira, K.B., Joy, J., Moores, A., Drisko, G.L., Sanchez, C., 2018. Nanocellulose, a versatile green platform: from biosources to materials and their applications. Chem. Rev. 118 (24), 11575–11625. https://doi.org/10.1021/acs.chemrev.7b00627.
Thompson, L., Azadmanjiri, J., Nikzad, M., Sbarski, I., Wang, J., Yu, A., 2019. Cellulose nanocrystals: production, functionalization and advanced applications. Rev. Adv. Mater. Sci. 58 (1), 1–16. https://doi.org/10.1515/rams-2019-0001.
Tian, D., Guo, Y., Hu, J., Yang, G., Zhang, J., Luo, L., Xiao, Y., Deng, S., Deng, O., Zhou, W., Shen, F., 2020. Acidic deep eutectic solvents pretreatment for selective lignocellulosic biomass fractionation with enhanced cellulose reactivity. Int. J. Biol. Macromol. 142, 288–297. https://doi.org/10.1016/j.ijbiomac.2019.09.100.
Tian, K., Pu, W., Li, S., Wang, Q., Liu, S., 2023. An amphiphilic nano titanium dioxide based nanofluid: preparation, dispersion, emulsion, interface properties, wettability and application in enhanced oil recovery. Chem. Eng. Res. Des. 197, 685–696. https://doi.org/10.1016/j.cherd.2023.08.011.
Tiong, A.C.Y., Tan, I.S., Foo, H.C.Y., Lam, M.K., Mahmud, H. Ben, Lee, K.T., 2020. Macroalgae-derived regenerated cellulose in the stabilization of oil-in-water pickering emulsions. Carbohydr. Polym. 249, 116875. https://doi.org/10.1016/j.carbpol.2020.116875.
Tiong, A.C.Y., Tan, I.S., Foo, H.C.Y., Lam, M.K., Mahmud, H. Ben, Lee, K.T., Show, P.L., 2023. Study on the synergism of cellulose nanocrystals and janus graphene oxide for enhanced oil recovery. Geoenergy Sci. Eng. 221, 111242. https://doi.org/10.1016/j.petrol.2022.111242.
Tong, X., Shen, W., Chen, X., Jia, M., Roux, J., 2020. Preparation and mechanism analysis of morphology-controlled cellulose nanocrystals via compound enzymatic hydrolysis of eucalyptus pulp. J. Appl. Polym. Sci. 137 (9). https://doi.org/10.1002/app.48407.
Tong, X., He, Z., Zheng, L., Pande, H., Ni, Y., 2023. Enzymatic treatment processes for the production of cellulose nanomaterials: a review. Carbohydr. Polym. 299, 120199. https://doi.org/10.1016/j.carbpol.2022.120199.
Trache, D., Hussin, M.H., Hui Chuin, C.T., Sabar, S., Fazita, M.R.N., Taiwo, O.F.A., Hassan, T.M., Haafiz, M.K.M., 2016. Microcrystalline cellulose: isolation, characterization and bio-composites application—A review. Int. J. Biol. Macromol. 93, 789–804. https://doi.org/10.1016/j.ijbiomac.2016.09.056.
Trilokesh, C., Uppuluri, K.B., 2019. Isolation and characterization of cellulose nanocrystals from jackfruit peel. Sci. Rep. 9 (1), 16709. https://doi.org/10.1038/s41598-019-53412-x.
Tuerxun, D., Pulingam, T., Nordin, N.I., Chen, Y.W., Kamaldin, J. Bin, Julkapli, N.B.M., Lee, H.V., Leo, B.F., Johan, M.R., 2019. Synthesis, characterization and cytotoxicity studies of nanocrystalline cellulose from the production waste of rubberwood and kenaf-bast fibers. Eur. Polym. J. 116, 352–360. https://doi.org/10.1016/j.eurpolymj.2019.04.021.
Umar, A.A., Saaid, I.B.M., Sulaimon, A.A., Pilus, R.B.M., 2018. A review of petroleum emulsions and recent progress on water-in-crude oil emulsions stabilized by natural surfactants and solids. J. Petrol. Sci. Eng. 165, 673–690. https://doi.org/10.1016/j.petrol.2018.03.014.
Umunnawuike, C., Mahat, S.Q.A., Ridzuan, N., Gbonhinbor, J., Agi, A., 2024. Biohydrogen production: a review of Current trends and future prospects. In: SPE Nigeria Annual International Conference and Exhibition. https://doi.org/10.2118/221600-MS.
Valencia, L., Handa, R., Monti, S., Jasso-Salcedo, A.B., Georgouvelas, D., Magaña, I., Díaz de León, R., Velikov, K.P., Mathew, A.P., Kumar, S., 2022. On the mineralization of nanocellulose to produce functional hybrid materials. J. Mater. Chem. A 10 (17), 9248–9276. https://doi.org/10.1039/D2TA00457G.
Van-Pham, D.-T., Pham, T.Y.N., Tran, M.C., Nguyen, C.-N., Tran-Cong-Miyata, Q., 2020. Extraction of thermally stable cellulose nanocrystals in short processing time from waste newspaper by conventional acid hydrolysis. Mater. Res. Express 7 (6), 65004. https://doi.org/10.1088/2053-1591/ab9668.
Vaz, F.L., da Rocha Lins, J., Alves Alencar, B.R., Silva de Abreu, Í.B., Vidal, E.E., Ribeiro, E., Valadares de Sá Barretto Sampaio, E., Cezar Menezes, R.S., Dutra, E.D., 2021. Chemical pretreatment of sugarcane bagasse with liquid fraction recycling. Renew. Energy 174, 666–673. https://doi.org/10.1016/j.renene.2021.04.087.
Ventura-Cruz, S., Tecante, A., 2021. Nanocellulose and microcrystalline cellulose from agricultural waste: review on isolation and application as reinforcement in polymeric matrices. Food Hydrocoll. 118, 106771. https://doi.org/10.1016/j.foodhyd.2021.106771.
Vergara, P., Ladero, M., García-Ochoa, F., Villar, J.C., 2018. Pre-treatment of corn stover, Cynara cardunculus L. stems and wheat straw by ethanol-water and diluted sulfuric acid: comparison under different energy input conditions. Bioresour. Technol. 270, 449–456. https://doi.org/10.1016/j.biortech.2018.09.058.
Vicente-Flores, M., Hernández-Varela, J.D., Chanona-Pérez, J.J., Perea-Flores, M.J., Méndez-Méndez, J.V., Mendoza-León, H.F., 2024. Nanomechanical characterization of isolated cellulose fibers from cuajilote fruit (parmentiera edulis): an alternative crop for extracting cellulosic materials. Bioresour. Technol. Rep. 25, 101764. https://doi.org/10.1016/j.biteb.2024.101764.
Vijayakkannan, K., Rajendran, I., 2024. Extraction and characterization of a new natural cellulosic fiber from the Habara Plant Stem (HF) as potential reinforcement for polymer composites. Int. J. Biol. Macromol. 269, 131818. https://doi.org/10.1016/j.ijbiomac.2024.131818.
Vinatoru, M., Mason, T.J., Calinescu, I., 2017. Ultrasonically assisted extraction (UAE) and microwave assisted extraction (MAE) of functional compounds from plant materials. TrAC, Trends Anal. Chem. 97, 159–178. https://doi.org/10.1016/j.trac.2017.09.002.
Vincent, S., Kandasubramanian, B., 2021. Cellulose nanocrystals from agricultural resources: extraction and functionalisation. Eur. Polym. J. 160, 110789. https://doi.org/10.1016/j.eurpolymj.2021.110789.
Vu, A.N., Nguyen, L.H., Tran, H.-C.V., Yoshimura, K., Tran, T.D., Van Le, H., Nguyen, N.-U.T., 2024. Cellulose nanocrystals extracted from rice husk using the formic/peroxyformic acid process: isolation and structural characterization. RSC Adv. 14 (3), 2048–2060. https://doi.org/10.1039/D3RA06724F.
Wahib, S.A., Da'na, D.A., Al-Ghouti, M.A., 2022. Insight into the extraction and characterization of cellulose nanocrystals from date pits. Arab. J. Chem. 15 (3), 103650. https://doi.org/10.1016/j.arabjc.2021.103650.
Wang, Y., Wang, X., Xie, Y., Zhang, K., 2018. Functional nanomaterials through esterification of cellulose: a review of chemistry and application. Cellulose 25 (7), 3703–3731. https://doi.org/10.1007/s10570-018-1830-3.
Wang, H., Li, J., Zeng, X., Tang, X., Sun, Y., Lei, T., Lin, L., 2020a. Extraction of cellulose nanocrystals using a recyclable deep eutectic solvent. Cellulose 27 (3), 1301–1314. https://doi.org/10.1007/s10570-019-02867-2.
Wang, H., Pudukudy, M., Ni, Y., Zhi, Y., Zhang, H., Wang, Z., Jia, Q., Shan, S., 2020b. Synthesis of nanocrystalline cellulose via ammonium persulfate-assisted swelling followed by oxidation and their chiral self-assembly. Cellulose 27 (2), 657–676. https://doi.org/10.1007/s10570-019-02789-z.
Wang, J., Wang, Y., Ma, Z., Yan, L., 2020c. Dissolution of highly molecular weight cellulose isolated from wheat straw in deep eutectic solvent of Choline/l-Lysine hydrochloride. Green Energy Environ. 5 (2), 232–239. https://doi.org/10.1016/j.gee.2020.03.010.
Wang, H., Huang, H., Bi, W., Ji, G., Zhou, B., Zhuo, L., 2022. Deep and ultra-deep oil and gas well drilling technologies: progress and prospect. Nat. Gas. Ind. B 9 (2), 141–157. https://doi.org/10.1016/j.ngib.2021.08.019.
Wang, B., Wang, S., Yan, H., Bai, Y., She, Y., Zhang, F., 2023. Synthesis and enhanced oil recovery potential of the bio-nano-oil displacement system. ACS Omega 8 (19), 17122–17133. https://doi.org/10.1021/acsomega.3c01447.
Wang, Y., Liu, H., Ji, X., Wang, Q., Tian, Z., Fatehi, P., 2023a. Production of nanocellulose using acidic deep eutectic solvents based on choline chloride and carboxylic acids: a review. Int. J. Biol. Macromol. 245, 125227. https://doi.org/10.1016/j.ijbiomac.2023.125227.
Wang, Y., Liu, H., Wang, Q., An, X., Ji, X., Tian, Z., Liu, S., Yang, G., 2023b. Recent advances in sustainable preparation of cellulose nanocrystals via solid acid hydrolysis: a mini-review. Int. J. Biol. Macromol. 253, 127353. https://doi.org/10.1016/j.ijbiomac.2023.127353.
Wang, L., Li, G., Chen, X., Yang, Y., Liew, R.K., Abo-Dief, H.M., Lam, S.S., Sellami, R., Peng, W., Li, H., 2024a. Extraction strategies for lignin, cellulose, and hemicellulose to obtain valuable products from biomass. Adv. Compos. Hybrid Mater. 7 (6), 219. https://doi.org/10.1007/s42114-024-01009-y.
Wang, L., Li, Y., Ye, L., Zhi, C., Zhang, T., Miao, M., 2024b. Unveiling structure and performance of tea-derived cellulose nanocrystals. Int. J. Biol. Macromol. 270, 132117. https://doi.org/10.1016/j.ijbiomac.2024.132117.
Wei, B., Wu, R., Lu, L., Ning, X., Xu, X., Wood, C., Yang, Y., 2017. Influence of individual ions on oil/brine/rock interfacial interactions and oil–water flow behaviors in porous media. Energy Fuels 31 (11), 12035–12045. https://doi.org/10.1021/acs.energyfuels.7b02458.
Wei, B., Wang, Y., Mao, R., Xu, X., Wood, C., Wen, Y., 2019. Design of nanocellulose fibrils containing lignin segment (L-NCF) for producing stable liquid foams as

"green" flooding agents for oil recovery. ACS Sustain. Chem. Eng. 7 (13), 11426–11437. https://doi.org/10.1021/acssuschemeng.9b01249.

Wei, W., Wang, B., Wang, X., Ling, R., Jin, Y., 2021. Comparison of acid and alkali catalyzed ethylene glycol organosolv pretreatment for sugar production from bagasse. Bioresour. Technol. 320, 124293. https://doi.org/10.1016/j.biortech.2020.124293.

Weligama Thuppahige, V.T., Moghaddam, L., Welsh, Z.G., Wang, T., Karim, A., 2023. Investigation of critical properties of cassava (Manihot esculenta) peel and bagasse as starch-rich fibrous agro-industrial wastes for biodegradable food packaging. Food Chem. 422, 136200. https://doi.org/10.1016/j.foodchem.2023.136200.

Wong, Y.H., Chew, E.M.T.-Z., Toh, P.Y., Chng, L.M., 2021. Evaluation of oil palm empty fruit bunch for cellulose production. IOP Conf. Ser. Earth Environ. Sci. 945 (1), 012021. https://doi.org/10.1088/1755-1315/945/1/012021.

Wu, S., Zhao, D., Li, Z., Zhu, Q., 2016. New evaluation function for the oil recovery and carbon sequestration of CO<SUB align="right">2-EOR project. Int. J. Comput. Appl. Technol. 54 (1), 14. https://doi.org/10.1504/IJCAT.2016.077794.

Xie, H., Zou, Z., Du, H., Zhang, X., Wang, X., Yang, X., Wang, H., Li, G., Li, L., Si, C., 2019. Preparation of thermally stable and surface-functionalized cellulose nanocrystals via mixed H2SO4/Oxalic acid hydrolysis. Carbohydr. Polym. 223, 115116. https://doi.org/10.1016/j.carbpol.2019.115116.

Xiong, R., Zhang, X., Tian, D., Zhou, Z., Lu, C., 2012. Comparing microcrystalline with spherical nanocrystalline cellulose from waste cotton fabrics. Cellulose 19 (4), 1189–1198. https://doi.org/10.1007/s10570-012-9730-4.

Xu, J., Dai, L., Zhang, C., Gui, Y., Yuan, L., Lei, Y., Fan, B., 2020. Ionic liquid-aided hydrothermal treatment of lignocellulose for the synergistic outputs of carbon dots and enhanced enzymatic hydrolysis. Bioresour. Technol. 305, 123043. https://doi.org/10.1016/j.biortech.2020.123043.

Xu, Z., Zhang, X., Yang, X., Yu, Y., Lin, H., Sheng, K., 2021. Synthesis of Fe/N Co-doped porous carbon spheres derived from corncob for supercapacitors with high performances. Energy Fuels 35 (17), 14157–14168. https://doi.org/10.1021/acs.energyfuels.1c01922.

Yadav, C., Saini, A., Zhang, W., You, X., Chauhan, I., Mohanty, P., Li, X., 2021. Plant-based nanocellulose: a review of routine and recent preparation methods with current progress in its applications as rheology modifier and 3D bioprinting. Int. J. Biol. Macromol. 166, 1586–1616. https://doi.org/10.1016/j.ijbiomac.2020.11.038.

Yakasai, F., Jaafar, M.Z., Bandyopadhyay, S., Agi, A., 2021. Current developments and future outlook in nanofluid flooding: a comprehensive review of various parameters influencing oil recovery mechanisms. J. Ind. Eng. Chem. 93, 138–162. https://doi.org/10.1016/j.jiec.2020.10.017.

Yakasai, F., Jaafar, M.Z., Sidek, M.A., Bandyopadhyay, S., Agi, A., Ngouangna, E.N., 2023. Co-precipitation and grafting of (3-Aminopropyl) triethoxysilane on Ferro nanoparticles to enhance oil recovery mechanisms at reservoir conditions. J. Mol. Liq. 371, 121007. https://doi.org/10.1016/j.molliq.2022.121007.

Yan, Y., Wang, L., Sang, G., Han, X., 2022. Influence of polymer viscoelasticity on microscopic remaining oil production. Polymers 14 (5), 940. https://doi.org/10.3390/polym14050940.

Yang, D., Peng, X.-W., Zhong, L.-X., Cao, X.-F., Chen, W., Sun, R.-C., 2013. Effects of pretreatments on crystalline properties and morphology of cellulose nanocrystals. Cellulose 20 (5), 2427–2437. https://doi.org/10.1007/s10570-013-9997-0.

Yang, J., Ching, Y., Chuah, C., 2019a. Applications of lignocellulosic fibers and lignin in bioplastics: a review. Polymers 11 (5), 751. https://doi.org/10.3390/polym11050751.

Yang, H., Zhang, Y., Kato, R., Rowan, S.J., 2019b. Preparation of cellulose nanofibers from miscanthus x. Giganteus by ammonium persulfate oxidation. Carbohydr. Polym. 212, 30–39. https://doi.org/10.1016/j.carbpol.2019.02.008.

Yang, X., Xie, H., Du, H., Zhang, X., Zou, Z., Zou, Y., Liu, W., Lan, H., Zhang, X., Si, C., 2019c. Facile extraction of thermally stable and dispersible cellulose nanocrystals with high yield via a green and recyclable $FeCl_3$ -Catalyzed deep eutectic solvent system. ACS Sustain. Chem. Eng. 7 (7), 7200–7208. https://doi.org/10.1021/acssuschemeng.9b00209.

Yang, X., Zheng, A., Zhao, Z., Xia, S., Wang, Q., Wei, G., Huang, Z., Jiang, L., Wang, S., Li, H., 2020. Maximizing production of sugar and ultrafine lignin particles from recalcitrant softwood by different acids-assisted organosolvolysis and fast pyrolysis. J. Clean. Prod. 276, 122827. https://doi.org/10.1016/j.jclepro.2020.122827.

Yang, S., Yan, C., Cai, J., Pan, Y., Han, Q., 2024. Research progress in nanoparticle inhibitors for crude oil asphaltene deposition. Molecules 29 (5), 1135. https://doi.org/10.3390/molecules29051135.

Yao, Y., Wei, M., Kang, W., 2021. A review of wettability alteration using surfactants in carbonate reservoirs. Adv. Colloid Interface Sci. 294, 102477. https://doi.org/10.1016/j.cis.2021.102477.

Ye, G., Zeng, D., Zhang, S., Fan, M., Zhang, H., Xie, J., 2018. Ethanol production from mixtures of sugarcane bagasse and dioscorea composita extracted residue with high solid loading. Bioresour. Technol. 257, 23–29. https://doi.org/10.1016/j.biortech.2018.02.008.

Ye, W., Yokota, S., Fan, Y., Kondo, T., 2021. A combination of aqueous counter collision and TEMPO-mediated oxidation for doubled carboxyl contents of α-chitin nanofibers. Cellulose 28 (4), 2167–2181. https://doi.org/10.1007/s10570-021-03676-2.

Yee, S.N., Zhong, X.O., Yi, P.T., Mei, L.O., Peng, Y.H., 2024. Optimization of purified cellulose extraction from corn cob and characterization of the isolated product. Cellul. Chem. Technol. 102, 125–142. https://doi.org/10.1016/j.cct.2024.1130-3.

Yu, Y., Wu, J., Ren, X., Lau, A., Rezaei, H., Takada, M., Bi, X., Sokhansanj, S., 2022. Steam explosion of lignocellulosic biomass for multiple advanced bioenergy processes: a review. Renew. Sustain. Energy Rev. 154, 111871. https://doi.org/10.1016/j.rser.2021.111871.

Zadeh, Z.E., Abdulkhani, A., Aboelazayem, O., Saha, B., 2020. Recent insights into lignocellulosic biomass pyrolysis: a critical review on pretreatment, characterization, and products upgrading. Processes 8 (7), 799. https://doi.org/10.3390/pr8070799.

Zeng, J., Hu, F., Cheng, Z., Wang, B., Chen, K., 2021. Isolation and rheological characterization of cellulose nanofibrils (CNFs) produced by microfluidic homogenization, ball-milling, grinding and refining. Cellulose 28 (6), 3389–3408. https://doi.org/10.1007/s10570-021-03702-3.

Zeynalli, M., Mushtaq, M., Al-Shalabi, E.W., Alfazazi, U., Hassan, A.M., AlAmeri, W., 2023. A comprehensive review of viscoelastic polymer flooding in sandstone and carbonate rocks. Sci. Rep. 13 (1), 17679. https://doi.org/10.1038/s41598-023-44896-9.

Zhang, N., Li, S., Xiong, L., Hong, Y., Chen, Y., 2015. Cellulose-hemicellulose interaction in wood secondary cell-wall. Model. Simulat. Mater. Sci. Eng. 23 (8), 085010. https://doi.org/10.1088/0965-0393/23/8/085010.

Zhang, K., Pei, Z., Wang, D., 2016. Organic solvent pretreatment of lignocellulosic biomass for biofuels and biochemicals: a review. Bioresour. Technol. 199, 21–33. https://doi.org/10.1016/j.biortech.2015.08.102.

Zhang, S., Zhang, F., Jin, L., Liu, B., Mao, Y., Liu, Y., Huang, J., 2019. Preparation of spherical nanocellulose from waste paper by aqueous NaOH/thiourea. Cellulose 26 (8), 5177–5185. https://doi.org/10.1007/s10570-019-02434-9.

Zhang, H., Chen, Y., Wang, S., Ma, L., Yu, Y., Dai, H., Zhang, Y., 2020. Extraction and comparison of cellulose nanocrystals from lemon (Citrus limon) seeds using sulfuric acid hydrolysis and oxidation methods. Carbohydr. Polym. 238, 116180. https://doi.org/10.1016/j.carbpol.2020.116180.

Zhang, J., Li, K., Liu, S., Huang, S., Xu, C., 2022. Alkaline hydrogen peroxide pretreatment combined with bio-additives to boost high-solids enzymatic hydrolysis of sugarcane bagasse for succinic acid processing. Bioresour. Technol. 345, 126550. https://doi.org/10.1016/j.biortech.2021.126550.

Zhang, Y., Deng, W., Wu, M., Rahmaninia, M., Xu, C., Li, B., 2023. Tailoring functionality of nanocellulose: current status and critical challenges. Nanomaterials 13 (9), 1489. https://doi.org/10.3390/nano13091489.

Zhang, A., Quan, H., Yu, J., Chen, X., Huang, Z., 2024a. Hydroxyl-functionalized carbon nanoparticles alter the asphaltene aggregate structure and reduce the viscosity of heavy oil. ACS Appl. Nano Mater. 7 (18), 21925–21935. https://doi.org/10.1021/acsanm.4c03920.

Zhang, X., Fang, C., Cheng, Y., Li, M., Liu, J., 2024b. Fine extraction of cellulose from corn straw and the application for eco-friendly packaging films enhanced with polyvinyl alcohol. Int. J. Biol. Macromol. 268, 131984. https://doi.org/10.1016/j.ijbiomac.2024.131984.

Zhang, X., Ni, H., Xu, X., Li, L., Kang, H., Li, D., 2024c. Recent advancements in the synthesis, functionalization, and utilization of cellulose nanocrystals. Resour. Chem. Mater. https://doi.org/10.1016/j.recm.2024.05.003.

Zhao, H., Song, Q., Wu, X., Yao, Q., 2015. Study on the transformation of inherent potassium during the fast-pyrolysis process of rice straw. Energy Fuels 29 (10), 6404–6411. https://doi.org/10.1021/acs.energyfuels.5b00851.

Zheng, D., Zhang, Y., Guo, Y., Yue, J., 2019. Isolation and characterization of nanocellulose with a novel shape from walnut (Juglans Regia L.) shell agricultural waste. Polymers 11 (7), 1130. https://doi.org/10.3390/polym11071130.

Zheng, Y., Wang, Z., Huang, Y., Wang, H., Xiao, Q., Ye, H., Huang, X., 2024. Extraction and preparation of cellulose nanocrystal from Brewer's spent grain and application in pickering emulsions. Bioactive Carbohydrates and Dietary Fibre 31, 100418. https://doi.org/10.1016/j.bcdf.2024.100418.

Zhong, H., He, Y., Yang, E., Bi, Y., Yang, T., 2022. Modeling of microflow during viscoelastic polymer flooding in heterogenous reservoirs of daqing oilfield. J. Petrol. Sci. Eng. 210, 110091. https://doi.org/10.1016/j.petrol.2021.110091.

Zhong, H., Shi, B., Bi, Y., Cao, X., Zhang, H., Yu, C., Tang, H., 2025. Interaction of elasticity and wettability on enhanced oil recovery in viscoelastic polymer flooding: a case study on oil droplet. Geoenergy Sci. Eng. 250, 213827. https://doi.org/10.1016/j.geoen.2025.213827.

Zhou, Z., Ouyang, D., Liu, D., Zhao, X., 2023. Oxidative pretreatment of lignocellulosic biomass for enzymatic hydrolysis: progress and challenges. Bioresour. Technol. 367, 128208. https://doi.org/10.1016/j.biortech.2022.128208.

Zhu, N., Ji, H., Yu, P., Niu, J., Farooq, M.U., Akram, M.W., Udego, I.O., Li, H., Niu, X., 2018. Surface modification of magnetic iron oxide nanoparticles. Nanomaterials 8 (10), 810. https://doi.org/10.3390/nano8100810.

Zhu, L., Liang, K., Wang, M., Xing, T., Chen, C., Wang, Q., 2023. Microwave-assisted formic acid/cold caustic extraction for separation of cellulose and hemicellulose from biomass. Bioresources 18 (4), 6896–6912. https://doi.org/10.15376/biores.18.4.6896-6912.

Zoppe, J.O., Österberg, M., Venditti, R.A., Laine, J., Rojas, O.J., 2011. Surface interaction forces of cellulose nanocrystals grafted with thermoresponsive polymer brushes. Biomacromolecules 12 (7), 2788–2796. https://doi.org/10.1021/bm200551p.

Zoppe, J.O., Larsson, P.A., Cusola, O., 2020. Surface modification of nanocellulosics and functionalities. In: Filpponen, I., Peresin, M.S., Nypelo, T. (Eds.), Lignocellulosics. Elsevier, pp. 17–63. https://doi.org/10.1016/B978-0-12-804077-5.00003-8.

Zuo, P., Qu, S., Shen, W., 2019. Asphaltenes: separations, structural analysis and applications. J. Energy Chem. 34, 186–207. https://doi.org/10.1016/j.jechem.2018.10.004.

Yarbrough, J.M., Zhang, R., Mittal, A., Vander, Wall., Bomble, Y.J., Decker, S.R., Himmel, M.E., Ciesielski, P.N., 2017. Multifunctional cellulolytic enzymes outperform processive fungal cellulases for coproduction of nanocellulose and biofuels. ACS Nano 11 (3), 3101–3109. https://doi.org/10.1021/acsnano.7b00086.